Physiological Costs of Altered Hydrothermal Conditions in Harvested Forests

A thesis presented to
The Faculty of Graduate Studies
of
Lakehead University
By
Melissa Henderson

In partial fulfillment of requirements for the degree of
Master of Science in Biology

August 2025

ABSTRACT

Amphibians are among the most rapidly declining vertebrate groups worldwide, with habitat modification and climate change driving widespread population declines. Much work on amphibian vulnerability focuses on gradual shifts of climate change. While in many landscapes, habitat-altering disturbances such as clearcutting introduce sudden shifts in thermal and hydric environments on timescales far shorter than those of potential local adaptation and potentially removing critical microhabitat refugia. Such changes may be particularly relevant for amphibians, whose behaviour and ecological performance is linked to both body temperature and dehydration status. However, predicting the impacts of harvesting on amphibian hydrothermal physiology is not straightforward as higher temperatures (up to thermal optima) may increase performance, while dehydration will decrease it. To untangle these effects, I compared hydrothermal performance curves for *Dryophytes versicolor* with water loss rates and operative temperatures of replica frogs in harvested, edge, and unharvested boreal forest across four time-since-cut stages. Replica frog water loss was significantly correlated with real frog water loss ($R^2 = 0.86$). I found performance declines past 15-20% dehydration and that baseline performance was lower at cooler temperatures and higher dehydrations. Clearcut environments reduced performance for gray treefrogs during overnight activity periods, particularly in uncovered microhabitats, across all time-since-cut groups, indicating that the increased hydrothermal vulnerability from harvesting is maintained through succession. By examining the relationship between performance, hydration, and temperature, we can begin to understand how removal or alteration of key microhabitats may impact individual fitness and population persistence within disturbed landscapes.

LAND ACKNOWLEDGEMENT

I respectfully acknowledge that the research for this project took place on the traditional territory of multiple Indigenous Nations. Lakehead University and many of the field sites used in this work are located on the traditional lands of the Anishinabek Nation and the territory of Fort William First Nation, signatory to the Robinson-Superior Treaty of 1850.

This research has benefited from my presence on these lands, which are deeply shaped by ongoing histories of colonization. I am grateful and honoured to have had the opportunity to learn and work here, and I recognize that gratitude is not a substitute for action. Land acknowledgement is only a small part of building and maintaining meaningful relationships with the First Peoples of Canada. I am committed to continuing the work of learning from, supporting, and fostering equitable collaborations with Indigenous communities whose lands and knowledge systems continue to be vital to this work.

With this acknowledgement, I seek to honour the Indigenous peoples of the many places where I conducted fieldwork.

ACKNOWLEDGEMENTS

I don't know if I could have made it through this thesis in the state I am in without the help and support of numerous wonderful people.

To my supervisor Dr. Adam Algar, for your support, guidance, and patience throughout this project. I especially appreciate your ability to offer mentorship while pushing me to explore ideas independently. Also, thank you for bearing with me through the frustrations of fieldwork and data analysis. Your trust and encouragement were instrumental in my growth as a researcher. I am grateful to have worked with you in your lab.

I would also like to thank my committee members Dr. Carissa Brown and Dr. Stephen Mayor for both your expertise and advice throughout this project, particularly your knowledge of Boreal Forest dynamics.

To all the folks in the Ectotherm Ecology Lab, who all together created a wonderful community and supportive environment. Almost everyone has come out to help me with fieldwork. Special thanks to Olivia Leach and Scarlett Hanley for spending most of their summer away from their families to fight off mosquitos, ticks, and blackflies while manoeuvring tricky terrain, and spend long days outside in all kinds of unfavourable weather.

Also, a special thanks to folks who offered up their homes to us during the summer season. To Cam and Marg, for hosting Scarlett and I (special thanks to Marg for giving me a second pair of hiking boots, and to Cal for coping with me disrupting your morning peace by waking up at 5 am to prepare for the day). To Mark and Christine Bode for letting Ryley and I camp out at your home for a week. You all have lovely homes/camps, and I am grateful to have been given a place to stay at them.

To my friends back in Ottawa and family around the world who have supported me throughout some of the most difficult moments in my life (so far) while trying to navigate completing a thesis and personal hardships. Especially to Jake, John, Emily, and Gil for your understanding and support and willingness to listen to me vent. Also, to my aunt, for welcoming me into Thunder Bay and supporting me throughout these last two years.

I would not be where I am today without the endless support from both of my parents. Mum, for encouraging me in every decision I've made up to this point and lending your support even when you didn't agree with my decisions (thank you especially for driving me from Ottawa to Thunder Bay and back). Last, and never least, to my dad, whose passing during this degree has been a significant loss. Dad, thank you for sharing your love of the natural world with me—through catching frogs with me and teaching me about plants and flowers as a kid, you sparked the curiosity that led me to where I am today. I have taken about 1000 photos of flowers, mushrooms, and frogs for you. The thought of laughing with you about my most hilariously miserable days in the field kept me going more times than I can count. I miss you every day, and I'll never stop pausing to admire a flower or mushroom in your honour.

TABLE OF CONTENTS

List of Figures

List of Tables

1 INTRODUCTION

Amphibians are among the most rapidly declining vertebrate groups worldwide, with habitat modification and climate change driving widespread population declines (Hof et al., 2011; Luedtke et al., 2023; Stuart et al., 2004). Most work on anuran climate sensitivity assumes gradual change under shifting climate regimes (see Scheffers et al., 2013). However, in many landscapes, habitat-altering disturbances such as clearcutting introduce sudden and often extreme shifts in thermal and hydric environments (Franklin et al., 2002; Gardner et al., 2007; R. D. Semlitsch et al., 2009) on timescales far shorter than those of potential local adaptation (De Frenne et al., 2019), and potentially removing critical microhabitat refugia (Tuff et al., 2016). These rapid, localized, changes can fundamentally alter habitat quality by degrading or removing the microhabitats used for thermoregulation, hydration, and refuge.

Among the most critical factors influencing amphibian survival and performance are temperature and water availability, which together shape their metabolic processes, behavior, and overall fitness (Anderson & Andrade, 2017; Greenberg & Palen, 2021; Lertzman-Lepofsky et al., 2020; Rozen-Rechels et al., 2019). Ectothermic organisms, such as amphibians, are especially vulnerable to shifting climate because they rely on external environmental conditions to regulate their body temperature and hydration and maintain physiological function (Hillman et al., 2008; Huey et al., 2012; Wells, 2010). While the effects of temperature on amphibian function have been well studied (Cossins, 2012; Deutsch, 2008; Huey & Kingsolver, 1989; Pottier et al., 2025; Rollins-Smith & Le Sage, 2023; Sunday et al., 2014), dehydration also imposes considerable physiological costs, influencing locomotor capacity, metabolic efficiency, predator escape, and foraging success (Anderson & Andrade, 2017; Gatten, 1987; Rogowitz et al., 1999; Shoemaker et al., 1992).

To navigate the potential challenges of extreme hydrothermal habitat conditions, many ectotherms depend on specific microhabitats—such as shaded refuges, moist substrates, or hydrothermally preferable retreats—that offer opportunities for thermoregulation and hydration (Klinges et al., 2024). Microclimatic refuges may thus be essential for daily and seasonal survival and for long-term persistence. However, the availability and quality of these spaces are increasingly threatened by the rapid pace of habitat disturbance, land-use change, and the accelerating impacts of climate change, including rising temperatures and intensified drought (Luedtke et al., 2023; Zhang et al., 2021). Moreover, long-term dependence on retreats under increased thermal and hydric vulnerability comes with a cost as it can reduce available activity hours (Huey & Stevenson, 1979). Reduced activity time constrains essential behaviors such as foraging, mating, and dispersal, ultimately limiting energy acquisition and reproductive output (Rittenhouse et al., 2008; Spotila et al., 1992). Over time, these limitations can lead to reduced recruitment and population growth, and reliance on retreat sites has been shown to predict population-level declines under warming scenarios (Duarte et al., 2012; Sinervo et al., 2010).

While the effects of both temperature and hydration have been considered separately, few studies have jointly considered temperature and hydration in the context of real-world environmental conditions, despite evidence that these factors interact to shape behavior, distribution, and fitness (Anderson & Andrade, 2017; Greenberg & Palen, 2021; Lertzman-Lepofsky et al., 2020; Rozen-Rechels et al., 2019; Shoemaker & Nagy, 1977). Further, many microclimate studies rely on sampling at a single location and point in time or presence/absence data (Janin et al., 2011; Robinson et al., 2023) which fail to capture the effects of prolonged exposure or the consequences of chronic thermal stress, especially under fluctuating environmental conditions. Moreover, most eco-physiological models are diurnally biased,

underrepresenting the nocturnal activity patterns of amphibians (Kearney & Porter, 2004; Kearney & Predavec, 2000; Klinges et al., 2024; Rutschmann et al., 2024) and potentially resulting in misleading conclusions about species abilities to cope with environmental change.

In this thesis, I assess how rapid changes in microhabitats post-clearcutting affect the physiological capacities that are attainable for Eastern Gray Treefrogs (*Dryophytes versicolor,* Hylidae) within regenerating habitats. By examining these conditions across different stages of forest succession, I estimate how habitat quality shifts throughout 20-years of forest regrowth post-clearcut and evaluate the potential for forest-dwelling amphibians to persist under altered hydrothermal regimes.

1.1 Background

Forest harvesting reconfigures the ecological structure and function of North American forest ecosystems (Weber & Flannigan, 1997; Wolf et al., 2021). Many plant species possess adaptive mechanisms (e.g. shade tolerant birch and aspen) either to survive or to quickly recolonise cleared areas, and differences in recolonisation regimes amongst species post-disturbance results in a diversity of vegetational composition trajectories (Dawe et al., 2022; Grandpré et al., 1993). Over the past 50 years, forest harvesting has rapidly altered the structure and composition of the boreal forest primarily through removal of canopy, mid story, and understory vegetation cover (Bergeron & Fenton, 2012; Dupuch & Fortin, 2013; Keenan & Kimmins, 1993). Combined with favourable temperature conditions due to global climate warming, clearcutting regimes are expected to shift Boreal Forest composition towards forests dominated by broadleaf deciduous tree species, which regenerate quickly in full sunlight (Anyomi et al., 2022; Carleton & Maclellan, 1994; Dawe et al., 2022; Larocque et al., 2024).

Forest harvesting has both positive and negative effects on forest dwelling species, depending partially on vegetational composition during post-cut forest succession (Harper et al., 2015; Hocking & Semlitsch, 2008; Popescu & Hunter, 2011; Semlitsch et al., 2009; Todd et al., 2014). The effects of harvesting vary depending on pre-harvest stand composition and topography, the extent of canopy, debris, and vegetation removal, post-harvest management, and pre- and post-harvest climate and topography (Keenan & Kimmins, 1993; Carleton & Maclellan, 1994). More intensive cutting regimes that undergo multiple disturbance are more prone to overall forest composition shifts than single less intensive disturbances (Larocque et al., 2024). Forestry companies in Northwestern Ontario currently implement removal strategies that (cl)aim to simulate the effects of natural disturbances on forest composition (Natural Resources & Forestry, 2001). The dominant approach in this region is intensive even-aged management which leaves some retention trees or small patches of forest upon the landscape (Natural Resources & Forestry, 2023). However, clearcut cycles are relatively short compared to cycles of natural disturbance (Jõgiste et al., 2017; Kuuluvainen et al., 2021; Larocque et al., 2024), resulting in multiple overlapping disturbances over shorter-time periods, shifts in forest composition, and altered ecosystem stability (Jõgiste et al., 2017).

Clearcutting significantly alters forest macrohabitat structure by removing canopy cover and fragmenting continuous forest into smaller, disconnected, patches. This fragmentation increases the density of forest edges and open-canopy areas with limited shade, thereby reducing connectivity between remnant forest patches (Tuff et al., 2016). The resulting landscape is a mosaic of forest interior, edge, and open (cut) areas, each exhibiting distinct environmental characteristics (Bergeron & Fenton, 2012; Boucher et al., 2011; Remmel et al., 2023). Forest interiors generally exhibit greater heat storage capacity than open or edge environments due to

their dense vegetation, enclosed air space, and higher humidity levels, which result from reduced direct solar radiation (Geiger et al., 1965). In contrast, clearcuts and forest edges are subject to more extreme climatic fluctuations, often experiencing higher temperatures, lower humidity, and increased wind exposure (Chen et al., 1993; Murcia, 1995). Even-aged management practices, commonly associated with clearcutting, also influence long-term forest regeneration and structural complexity by simplifying age and species composition across regenerating stands (Bergeron et al., 1999; Fenton et al., 2009).

1.2 Modifications of microclimate from forestry practices

Macrohabitat modifications often lead to pronounced shifts in forest microclimates. Microclimates refer to localized variations in physical conditions—such as temperature, humidity, light, and wind—that occur at small spatial scales within a larger habitat (Chen, 1999; Chen et al., 1993; Geiger et al., 1965). These fine-scale environmental conditions are shaped by structural features like vegetation density, canopy cover, and species composition, and they play a critical role in influencing species distributions and ecosystem dynamics under habitat change (Chen, 1999; De Frenne et al., 2019; Dobrowski, 2011; Keppel et al., 2017; Máliš et al., 2023).

Within forests, microhabitat variability occurs along both horizontal (edge-to-interior) and vertical (canopy-to-ground) gradients. Wind speed decreases with height due to surface friction; the ground absorbs solar radiation during the day and emits infrared radiation at night, contributing to daily microclimatic variation (Geiger et al., 1965). Canopy and ground vegetation play essential roles in moderating temperature and humidity through shading, evaporative cooling, and insulating ground heat at night (Burrow et al., 2023; Wolf et al., 2021). As one moves toward the forest floor, air temperature typically decreases while relative humidity

increases (Geiger et al., 1965). Together, canopy and ground vegetation help create more thermally stable forest microclimates (Burrow et al., 2023).

Microhabitat conditions may differ substantially between clear, partially cleared, edge, and forested plots (Chen et al., 1993; Geiger et al., 1965). Changes to ground level vegetation and woody debris (providing damp and shaded spaces), as well as mid-story foliage and canopy cover can modify the conditions of various microclimates by simultaneously altering incident solar radiation, albedo (surface reflectance), wind speed, decreased humidity, and resulting vapor pressure deficits (Campbell & Norman, 1998; Geiger et al., 1965; Lindenmayer et al., 2020; Murcia, 1995; Wolf et al., 2021). Canopy and understory layers regulate solar exposure by direct interception and through reflection from leaf surfaces, helping buffer extreme temperatures and reduce moisture loss through evaporative cooling (Wolf et al., 2021). Ground level vegetation further stabilizes temperatures by reducing evening temperature declines through insolation of ground radiation and retaining radiant heat (Geiger et al., 1965). Clearcuts are more spatially homogenous than unharvested areas due to the absence of layered vegetation and canopy structure (Lundmark et al., 2017; Rittenhouse et al., 2008). Yet, these open environments may experience greater diurnal variation, with sharper temperature drops at night and higher thermal extremes during the day compared to forested areas (Geiger et al., 1965).

1.3 Hydrothermal impacts on organismal performance

To successfully occupy a habitat and obtain energy needed for growth, maintenance, and reproduction, organisms must maintain a positive energy balance between themselves and their environment (Spotila et al., 1992; Tracy et al., 2010). Organisms exchange energy between themselves and their environments in the form of heat and water in multiple ways, including absorbed and emitted radiation, convection (through the surrounding air), conduction (through

surfaces), evaporation (Spotila et al., 1992). In ectotherms, where metabolic heat is minimal, the outcome of these exchanges determines body temperature and hydration status, both of which have high ecological relevance as individuals cannot maintain long-term activity in habitats where their body temperature surpasses critical limits or their daily water loss exceeds their daily water uptake (Spotila et al., 1992). Thus, the suitability of an environment for an organism is, in part, determined by the time in which it can remain active before reaching its maximum tolerable body temperature and dehydration level (Campbell & Norman, 1998). Altered microclimatic conditions can impact heat and water exchange processes and subsequent energy balances, thereby influencing the physiological suitability of the given environment for a particular organism.

Among ectotherms, amphibians may be particularly sensitive to microclimate modifications because they have permeable skin. The easy movement of water across their skin means that amphibians can substantially lower their body temperatures through evaporative cooling in environments where thermal conditions approach thermal limits, however this mechanism comes with a trade-off via increased vulnerability to desiccation (Spotila et al., 1992; Tracy, 1976). Vegetation loss, particularly of canopy and ground cover, exposes amphibians to increased solar radiation and higher vapor pressure deficits, which accelerate water loss and reduce soil and atmospheric moisture availability (Geiger et al., 1965; Wolf et al., 2021). Elevated wind speeds in disturbed forests can further dehydrate microhabitats by thinning boundary layers and displacing humid air, compounding stress on moisture-dependent species (Spotila et al., 1992).

Amphibian physiological performance is strongly shaped by body temperature and hydration state (Huey et al., 2012). Many key functions, including locomotion, respiration, and

163 growth, are sensitive to changes in temperature (Deutsch, 2008; Huey & Kingsolver, 1989), and
164 dehydration can further constrain performance across these systems (Anderson & Andrade,
165 2017; Gatten, 1987; Greenberg & Palen, 2021; Preest & Pough, 1989; Rogowitz et al., 1999).
166 Among these, locomotion provides an especially informative measure of performance because it
167 integrates neuromuscular, metabolic, and behavioral responses to environmental stressors and is
168 affected by organisms' hydrothermal state (Navas et al., 2008). Locomotion is necessary for
169 processes affecting amphibian survival including reproductive efforts, predator avoidance,
170 predation, and dispersal between habitats (Gatten et al., 1992). The relationship between
171 performance and temperature is commonly represented as a thermal performance curve (TPC).
172 TPCs generally show performance initially increasing slowly a maximum at the thermal
173 optimum, then rapidly declining (Angilletta, 2009) (Figure 1.1.1). TPCs are not fixed and can be
174 modified by an individual's acclimatization to previous or current environmental experiences
175 (Schulte et al., 2011).

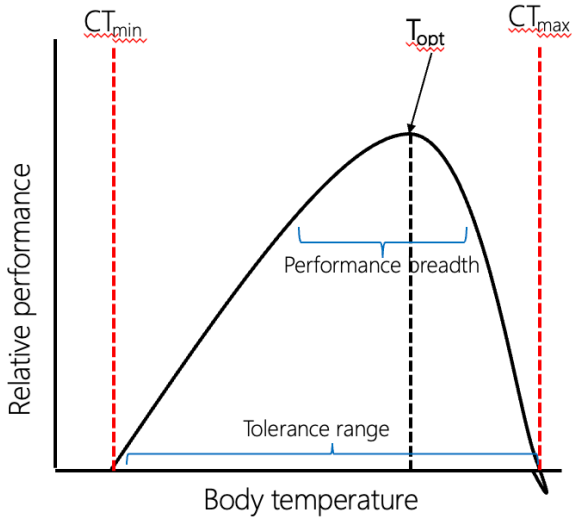

Figure 1.1.1 Hypothetical thermal performance curve including critical thermal minimum (CT_{min}), critical thermal maximum (CT_{max}), thermal optimum (T_{opt}), performance breadth, and tolerance range.

Dehydration can also alter thermal performance curves by shifting thermal optima downward (Anderson & Andrade, 2017; A. Mitchell & Bergmann, 2016; Preest & Pough, 1989), and narrowing the temperature range over which amphibians maintain high physiological function (i.e. performance breadth). While mild dehydration may have limited effects, performance declines sharply beyond this threshold, with frogs exhibiting reduced peak capacities and narrower thermal windows under moderate to severe dehydration (Anderson & Andrade, 2017; A. Mitchell & Bergmann, 2016). Therefore, thermal and hydric effects on performance are not independent and impacts of temperature on performance tend to be greater when animals are dehydrated (Greenberg & Palen, 2021). The combined effects of temperature and hydration state can be represented by a hydrothermal performance curve (HTPC). Multiple hydrothermal performance curves can be combined into a hydrothermal performance surface (HTPS).

Hydrothermal stress impairs amphibian performance by disrupting key physiological systems involved in locomotion, muscle function, and energy production (Anderson & Andrade, 2017; Greenberg & Palen, 2021; Moore & Gatten Jr, 1989; Rome et al., 1992). Amphibians can move in a variety of different ways for various tasks (e.g. reproduction, foraging, predator avoidance) through different types of muscle contractions, muscle fiber recruitment, and aerobic and anaerobic activity pathways (Rome et al., 1992). Aerobic capacity determines muscular endurance and controls activation and relaxation of muscles during sustained movement, while ATP and phosphocreatine stores are used for short-burst locomotion and maximal mechanical power output (Moore & Gatten Jr, 1989; Rome et al., 1992). Hydrothermal stress and desiccation impair aerobic function and deplete ATP stores, increasing reliance on less efficient anaerobic metabolism (Gatten et al., 1992; Preest & Pough, 1989). Cardiovascular performance declines with reduced heart rate, blood flow, and oxygen transport (Gatten, 1987; Gatten et al., 1992; Hillman, 1978). Dehydration-induced hyperosmolality draws water from muscles and the brain, accelerating fatigue (Hillman, 1978; Moore & Gatten Jr, 1989; Pough et al., 1983; Rogowitz et al., 1999; Senzano & Andrade, 2018). Reduced oxygen and hydration impair muscle fiber recruitment and timing of contractions (Rome et al., 1992), shifting metabolic activity towards less efficient anaerobic pathways. Although anaerobic pathways may sustain brief locomotion under stress, they yield less ATP and cause lactate buildup, accelerating time to fatigue (Gatten, 1987; Moore & Gatten Jr, 1989). In amphibians, intracellular ATP stores are sufficient to sustain maximal muscular effort for only 1–3 seconds**,** after which energy must be supplied by phosphocreatine and anaerobic glycolysis (Bennett, 1978). Consequently, anaerobic capacity can typically support intense activity for 30–60 seconds before fatigue sets in. Anaerobic capacity may be unaffected by small amounts of short-term dehydration and may allow individuals to

sustain brief periods of locomotion under hydrothermally stressful conditions. However, it remains unclear how ATP use and anaerobic locomotor capacities will be affected in amphibians experiencing frequent hydrothermally stressful conditions. The short-term limitations on anaerobic activity and the effects on aerobic metabolic pathways may be partially responsible for the reduction in locomotor capacities of dehydrated frogs (Gatten, 1987; Moore & Gatten Jr, 1989; Rogowitz et al., 1999).

1.4 Interspecific variations in hydrothermal tolerance

Individuals in different habitats experiencing changing hydrothermal conditions must balance their physiological tolerance margins with resource habitat preferences (Köhler et al., 2011). Because amphibians are often exposed to fluctuating microclimates, they routinely operate under varying hydration states and temperatures (Anderson & Andrade, 2017; Greenberg & Palen, 2021; Lertzman-Lepofsky et al., 2020; A. Mitchell & Bergmann, 2016; Navas et al., 2008). Environmental trade-offs can thus arise, where selecting optimal temperatures may increase desiccation risk and vice-a-versa. The nature and severity of these trade-offs vary across species and habitats, and the degree to which individuals can buffer hydrothermal microhabitat fluctuations depends partially on physiological traits like cutaneous resistance, body size, skin secretions, and oxygen uptake pathways (Gunderson & Stillman, 2015; Navas, 1996; Rogowitz et al., 1999; Spotila et al., 1992). Behavioural buffering strategies, such as seeking out refugia, adjusting posture, reducing activity, or altering movement patterns can also help minimize exposure to hydrothermal conditions near or above individual limits (Gunderson & Stillman, 2015; Spotila et al., 1992).

Species vary in their capacity to buffer hydrothermal stressors, and these differences are often shaped by both physiological tolerance limits and behavioral plasticity (Nowakowski et al.,

2018; Prates & Navas, 2009; Toledo & Jared, 1993; Wilson, 2001). High temperatures may be favourable and benefit performance for terrestrial and arboreal amphibians who possess physiological and behavioural adaptations that lower their desiccation risk (Hossack et al., 2009; Tracy et al., 2010). For instance, arboreal frogs with higher resistance to cutaneous water loss (Rc) than more aquatic species, aided by thicker skin and mucus secretions, can tolerate greater hydrothermal extremes and may engage more readily in behavioral thermoregulation (Roznik et al., 2018; Young et al., 2005). Arboreal species can also maintain favourable hydrothermal body conditions by moving vertically along trees and seeking out refuges located along trunks or branches to avoid increased temperatures at ground level (Biazzo & Quintana-Ascencio, 2022; J. R. Johnson et al., 2008). Terrestrial species may access standing water or moist refuges on the ground (e.g. under leaf litter along soil, in understory vegetation) if available (Hossack et al., 2013; Tracy et al., 2007). In contrast, species with lower dehydration tolerance are more restricted to favorable microhabitats and microclimates to maintain water balance (Navas et al., 2021).

The effectiveness and availability of behavioural modification strategies also depend on local habitat structure and quality and environmental context (Greenberg & Palen, 2021; A. Mitchell & Bergmann, 2016; Navas et al., 2008). The effects of altered temperatures or moisture availability are also context-dependent, such that changes in temperature and hydration may be positive or negative depending on whether they push organisms toward or away from their hydrothermal optima (Huey et al., 2012). High quality habitats (hydrothermally) allow organisms to operate close to their optimum for longer periods than low quality habitats with hydrothermal conditions near or above individual's tolerable limits. Activity in low quality habitats may be more energetically costly and impair an individual's ability to perform essential functions

required for survival, particularly if microhabitats offer limited buffering (Neel & McBrayer, 2018). Greater occurrence of low quality habitat requires animals to spend more time and energy behaviourally hydro-thermo-regulating by seeking refugia or maintaining water conservation poses during forced inactivity (Biazzo & Quintana-Ascencio, 2022; Navas et al., 2008; Sears et al., 2016; Sears & Angilletta, 2015), potentially impacting ecological functioning, fitness and even population dynamics. Improving our understanding of how environmental change and human activities affect hydrothermal physiological quality of habitats, and the shifting distribution of high- and low-quality habitat across the landscape is thus a key step in determining the vulnerability of species to ongoing habitat loss and modification.

1.5 Hypotheses

In this thesis, I determine how forest harvesting reconfigures the physiological quality of boreal landscapes for an arboreal amphibian. I examine microhabitat conditions between harvested and un-harvested forests at different stages of forest succession to determine if microhabitat conditions in clearcut environments reduce gray treefrog performance. These conditions are then compared with the species' hydrothermal niche determined from HTPS using jump performance. I propose the following hypotheses:

Hypothesis 1a: Initial impacts of harvesting on hydrothermal vulnerability are maintained during succession.

Rationale: Canopy removal in recent cuts is expected to increase exposure to temperature extremes both overnight and during the day and increases desiccation risk, limiting amphibian activity capacity. These differences may be maintained because of differences between clearcut regrowth and unharvested forest structure, since the former is shaped by intensive management

and develops high stand density with minimal canopy gaps, reduced sunlight penetration, and limited air movement, resulting in microclimates distinct from relatively unmanaged forests. These clearcut conditions that can persist for decades, with full recovery potentially taking a minimum of 60 years (Brassard & and Chen, 2006; Cyr et al., 2009).

- Predictions:
    1) Performance will be lower in recent clearcuts than adjacent forest.
    2) Performance will be significantly different between forest and clearcuts regardless of the time that has elapsed since cutting.

Alternative hypothesis 1b: Impacts of harvesting on hydrothermal vulnerability are rapidly erased by succession.

Rationale: This could be because rapid vegetation regrowth increases lower-level vegetation cover and shading, while reducing air movement due to stand density. These changes can enhance local humidity and create more favourable microhabitats for amphibians, leading to conditions in older clearcuts that are similar to those in adjacent forests

- Prediction: Differences in performance between clearcuts and adjacent forest will only be present in recent clearcuts.

Hypothesis 2: Clearcutting has a greater effect on hydrothermal vulnerability during nighttime activity than during daytime inactivity in disturbed environments.

Rationale: I expect this because during the day, frogs may make use of covered refuges to buffer against temperature variations and desiccation risk from exposure. However, overnight during peak activity hours, frogs may occur more frequently in uncovered microhabitats, which could expose them to rapidly cooling temperatures that approach their critical thermal minimums

- Prediction: Performance reductions between clearcuts and forests will be more pronounced overnight in exposed microhabitats than during the day in covered microhabitats.

2 METHODS

To understand how temperature and hydration jointly shape performance capacities in clearcut habitats, I first fit separate temperature-dependent and hydration-dependent performance curves, then combined them to generate a predictive hydrothermal performance surface across the full combination of laboratory-tested temperatures and hydration combinations. I then applied this predictive surface to infer potential performance of critical microhabitats in clearcut environments across forest recovery stages.

2.1 Hydrothermal Performance Tests

2.1.1 Animal collection and housing

We collected twelve adult male Eastern gray treefrogs (*Dryophytes versicolor*; Hylidae) on May 30 and 31, 2024, from three ponds. Four were collected on the evening of May 30 from a pond located at the northern end of Dog Lake Road, ON. Eight were collected on May 31 from two breeding ponds at the Kamview Nordic Centre, ON. I only used males because of the difficulty in finding enough females to achieve an adequate sample size. Animals were brought to Lakehead University's Biology Aquatics Facility (BAF) and housed in individual glass terraria and acclimated for one week at 20°C ± 3°C and >70% humidity in a 12:12 light-dark cycle. Each tank was lined with damp paper towels and contained two PVC pipe perches, a refuge and plastic aquarium vegetation for enrichment, and a water dish. Paper towel substrate was regularly dampened with de-chlorinated water and was changed during daily cleaning or

when soiled. Water dishes were changed daily. Frogs were fed 6 crickets every 3 days, along with a dietary supplement of either multivitamin, calcium, or calcium +D3.

2.1.2 Performance testing schedule

I separated frogs into three groups of four individuals and randomly selected one frog from each group as a control throughout each of the trials. For all trials and groups, the control was kept at the experimental temperature but was not dehydrated and jumped on the same schedule as test animals to account for potential performance losses due to cumulative physiological fatigue over the course of each trial (Greenberg & Palen, 2021). Prior to testing, individuals were fasted for 24 hours to avoid digestion-induced thermal variation (Preest & Pough, 1989;). They then partook in one trial and were given a two-day recovery period before the next trial. One group was tested each day and the order of test temperatures was randomized across groups. At the start of each trial day, I randomized the order in which animals underwent trials. Start times were staggered every 30 minutes between animals to avoid having multiple individuals reach the target dehydration levels simultaneously. If, at any point during the trials, an animal was deemed unfit to continue, they were immediately removed from trials for the day and placed in a recovery water bath for at least an hour or until they had returned to their pre-trial weight and were returned to their enclosure. Veterinary approval was obtained before using these animals in subsequent trials (this occurred only once across all trials).

2.1.3 Hydration and temperature manipulations

Jumping ability was tested at four hydration levels (100%, 92%, 84 %, 75%, 70%) and five temperatures (37°C, 33°C, 24°C, 15°C, 8°C). Frogs were only taken to 37°C at 100% hydration. Body temperature and hydration status were varied by placing animals in a

dehydration tunnel (transparent acrylic tube with screened ends and a fan; design followed Greenberg & Palen, 2021) within an environmental chamber (VEVOR Reptile Incubator) set at the target testing temperature. Prior to serial dehydration, animals were placed within a water bath inside the environmental chamber set at the target temperature for 1 hour to reach full hydration. The environmental chamber remained at the target temperature for the duration of the trials. Initial frog weights were taken following the first set of jumps at full hydration. Dehydration levels were calculated as percent mass lost from their initial mass under the assumption that mass lost would be almost entirely water. Individuals were then placed within their respective tunnels and weighed every five minutes to monitor weight loss until the target dehydration was reached. Serial dehydration, rather than a random, approach reduced the number of times animals were dehydrated, and was a necessary animal welfare consideration (Greenberg & Palen, 2021). There were three occurrences during which frogs were not taken to 70% hydration. The first was on the second day of trials at 15°C when frog A2 had been dehydrating for over 5 hours and was only at 84% hydration. We stopped trials at 75% as we were worried about overly stressing the frog given the long dehydration period. Subsequently, if frogs dehydrated slowly (< 0.01 g every five minutes for over 30 minutes) we added an extra fan to the dehydration tunnel. The second occurrence was when A1 obtained a minor injury and was removed from trials for the day; he was subsequently examined and cleared for a return to trials by a veterinarian. The third occurrence was when frog A6 did not jump during his trial of 24°C at 75% hydration despite provocation and so was not dehydrated to 70% for that temperature.

2.1.4 Jump testing

Once animals reached the target dehydration, they were removed from their tubes with damp gloves and placed into the jumping arena. The arena was a 122cm x 200cm white MDF board

surrounded by an 80 cm high plastic wall (Figure 2.1). A GoPro Hero 11 mini (linear, 4K, 60 fps) was fixed 120 cm above the arena floor. Scale bars 100 cm and 97 cm in length were affixed to the arena floor in the x and y directions. If animals did not jump immediately, they were encouraged to by feigning capture by hand from behind or lightly prodding their urostyle. After a maximum of 6 jumps, they were placed back into their containers and dehydration continued until they had reached the next dehydration target.

Figure 2.1. Jump arena set up. Platform was a 122cm x 200 cm white MDF board surrounded by 80 cm high plastic wall. A GoPro Hero 11 mini (linear, 4K, 60 fps) was fixed 120 cm above the arena floor. Pieces of tape 100 cm and 97 cm in length were affixed to the arena floor in the x and y directions for scale bars respectively. Left image is clear board with a frog placed away from the center. Right image is a screengrab of one trial with labeled trajectories.

2.2 Field Microhabitat Data collection

2.2.1 Study Area and Site Selection

To study the effect of clearcutting and succession on microhabitat quality for gray treefrogs, I used 16 sites split across three areas in the boreal forest transition zone around Thunder Bay, Ontario, Canada: 134 km northwest of the city, near Lac des Milles Lacs/Upsala;

40 km north of the city along Highway 527 and Hazelwood Conservation Area; and up to 120 km southwest of the city between Whitefish, Sandstone, and Sunbeam Lakes (Figure 2.2). All field work was conducted in Northwestern Ontario in the boreal forest transition zone from July to September 2024, during a portion of the active months for gray treefrogs in this region. All sites were within the Pigeon River and Lake Nipigon Ecoregions.

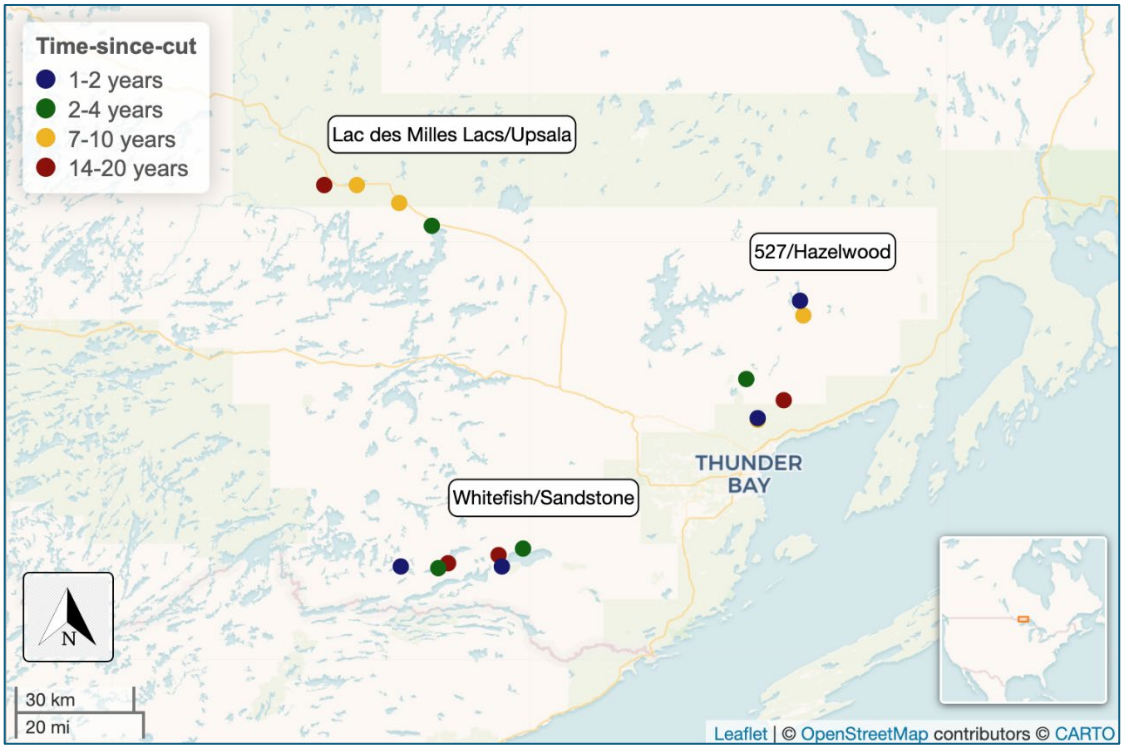

Figure 2.2 All sites used during the summer 2024 field season. There are three main locations with respect to Thunder Bay: Lac des Milles Lacs (northwest) , Whitefish/Sandstone (southwest), and 527/Hazelwood (north of Thunder Bay). Marker colours identify years of succession, i.e. since cutting: 1-2 years (yellow), 2-4 years (green), 7-10 years (red), and 14-18 years (blue).

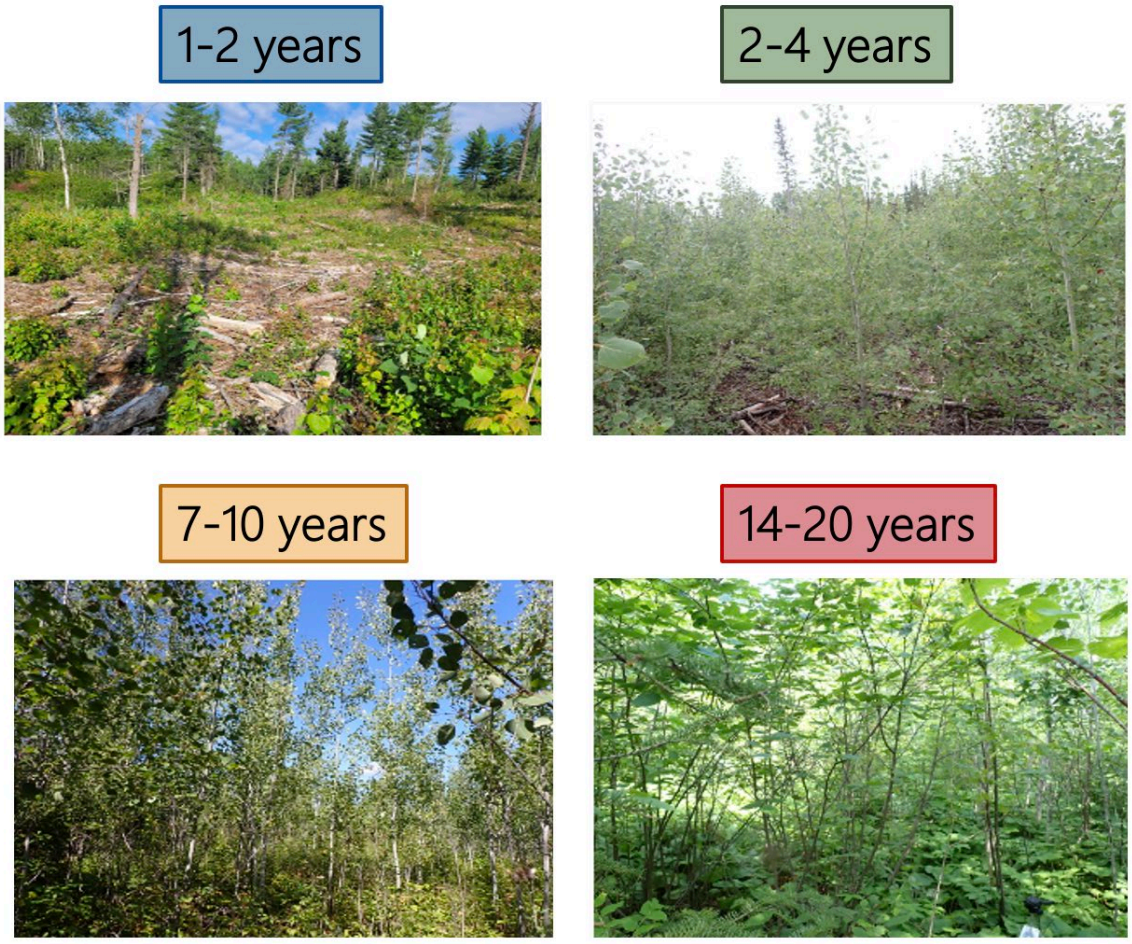

Figure 2.3 Vegetational regrowth across each time-since-cut in all cut sites. All photos were taken from eye height (168cm).

The northwestern Ontario section of the Boreal Shield transition zone consists of mixed-wood and boreal forests, with tree species including black spruce (*Picea mariana*), jack pine (*Pinus banksiana*), white spruce (*Picea glauca*), balsam fir (*Abies balsamea*), trembling aspen (*Populus tremuloides*), white birch (*Betula papyrifera*), and balsam poplar (*Populus balsamifera*) (Brandt et al., 2013). The region is further characterized by numerous lakes, and widespread wetlands such as bogs and fens (Crins et al., 2024). The climate is continental subarctic to humid continental, with long, cold winters and short warm summers. Summer months experience longer

day lengths due to higher latitudes of the boreal zone, experiencing on average 10-12 hours of sunlight (Price, 2013).

I identified all field sites using a combination of LANDSAT data, the Boreal Disturbance Database, and MNRF forest management planning (FMP) maps (Hermosilla et al., 2016; Remmel et al., 2023; Wulder et al., 2024). Sites were controlled for relative size of disturbance and pre-disturbance forest type. Areas that had experienced multiple harvests throughout different years were not used due to lack of available uncut forest for controls and to avoid potential compounding effects from multiple continuous harvests (Anoszko et al., 2022). We restricted our study to seeded clearcuts rather than planted clearcuts because in Ontario planted sites are almost exclusively conifer-dominated, whereas seeded sites regenerate into deciduous stands. Including both would have introduced different regeneration pathways and structural trajectories and increased variation in our clearcut sites. All selected clearcut sites had undergone the same post-harvest regeneration treatments according to the OMNRF harvest inventory plans. However, data on tending, debris removal, and seeding was difficult to obtain for older sites (12+ years). I aimed to minimize differences within sites by identifying areas with similar terrain, slope, and forest type using LANDSAT data and site visits as per recommendations in deMaynadier & Hunter (1995). All cut sites were rapidly colonized by dense stands of aspen (*Populus tremuloides*) and birch (*Betula papyrifera*) all within the same age (Figure 2.3) in contrast to the more compositionally diverse mixed-wood forests that include coniferous species such as balsam fir (*Abies balsamea*) and jack pine (*Pinus banksiana*), alongside native deciduous species.

2.2.2 Study Design

I implemented a crossed hierarchical design in which sites were nested within time-since-cut group and plots were nested within sites. I considered four time-since-cut groups: 1-2 years, 2-4 years, 7-10 years, and 14-20 years. I used 16 sites in total (four time-since-cut group x four replicates); each site was divided into three plots: control (forest not cut recently), edge, and harvested. In each plot, I estimated adult treefrog operative temperatures and evaporative water loss (EWL) using plaster models (Hastings et al., 2023; Peterman et al., 2013; Tracy et al., 2007) in three microhabitats: ground, sheltered trunk, and open trunk (Dodd, 2013; J. R. Johnson et al., 2008). Each site was sampled twice over the season with a minimum of 3 weeks between sample periods (Table 2.1).

Table 2.1 Sites used for sampling with geographic location, sampling dates, region, and time-since-cut groupings. Date ranges indicate that sampling was done over two days for that period to encompass both daytime and evening collection periods.

Site Name	Region	Time-since-cut	Longitude	Latitude	Sampling Dates
A2008	527/Hazelwood	14-20 years	-89.145	48.572	Jul 8-9 and Aug 26, 2024
A2015	527/Hazelwood	7-10 years	-89.075	48.760	Jul 4 and Aug 6-7, 2024
A2022	527/Hazelwood	1-2 years	-89.087	48.791	Jul 3 and Aug 27, 2024
H2016	527/Hazelwood	7-10 years	-89.230	48.526	Jul 27 and Aug 30, 2024
H2020	527/Hazelwood	2-4 years	-89.268	48.618	Jul 5-6 and Aug 28-30, 2024
H2022	527/Hazelwood	1-2 years	-89.230	48.532	Jul 31- Aug 1 and Sep 1, 2024
L2010	Lac des milles Lacs/Upsala	14-20 years	-90.694	49.049	Jul 18-19 and Aug 13, 2024
L2014	Lac des milles Lacs/Upsala	7-10 years	-90.438	49.007	Jul 30-31 and Aug 11, 2024
L2015	Lac des milles Lacs/Upsala	7-10 years	-90.585	49.049	Jul 19-20 and Aug 12, 2024
L2021	Lac des milles Lacs/Upsala	2-4 years	-90.330	48.957	Jul 17 and Aug 10, 2024
W2006	Whitefish/Sandstone	14-20 years	-90.276	48.208	Jul 2-3 and Aug 21, 2024
W2009	Whitefish/Sandstone	14-20 years	-90.104	48.223	Jul 24-25 and Aug 20, 2024
W2020	Whitefish/Sandstone	2-4 years	-90.021	48.241	Jul 23-24 and Aug 15, 2024
W2020B	Whitefish/Sandstone	2-4 years	-90.308	48.195	Aug 4-5 and Aug 22, 2024
W2022	Whitefish/Sandstone	1-2 years	-90.435	48.197	Jul 22-23 and Aug 17, 2024
W2023	Whitefish/Sandstone	1-2 years	-90.091	48.200	Jul 3-4 and Aug 23-24, 2024

2.2.3 Site Preparation

Trees were randomly selected within each cut-block section of the site and then tree species, tree height and diameter at breast height (DBH), and distance between trees was replicated, as closely as possible, in the edge and forested plots. Tree selection was limited by tree availability in harvest plots, as there were generally fewer large standing trees in those environments, particularly in older plots. However, I aimed for two coniferous and two

deciduous in each plot. Edge habitat was considered to be within 30 meters on both sides of the treeline (Boucher et al., 2011; Matlack, 1993). I recorded site-characteristics around each tree including ground, mid-story, and upper story vegetation, canopy cover above replica placement, and leaf litter quantity. I measured heights for each tree whose microhabitats were being measured. I recorded overall macrohabitat weather (temperature, relative humidity, and dewpoint) for each clearcut with a temperature logger (HOBO Onset MX2301A) paired with a radiation shield for each recording period.

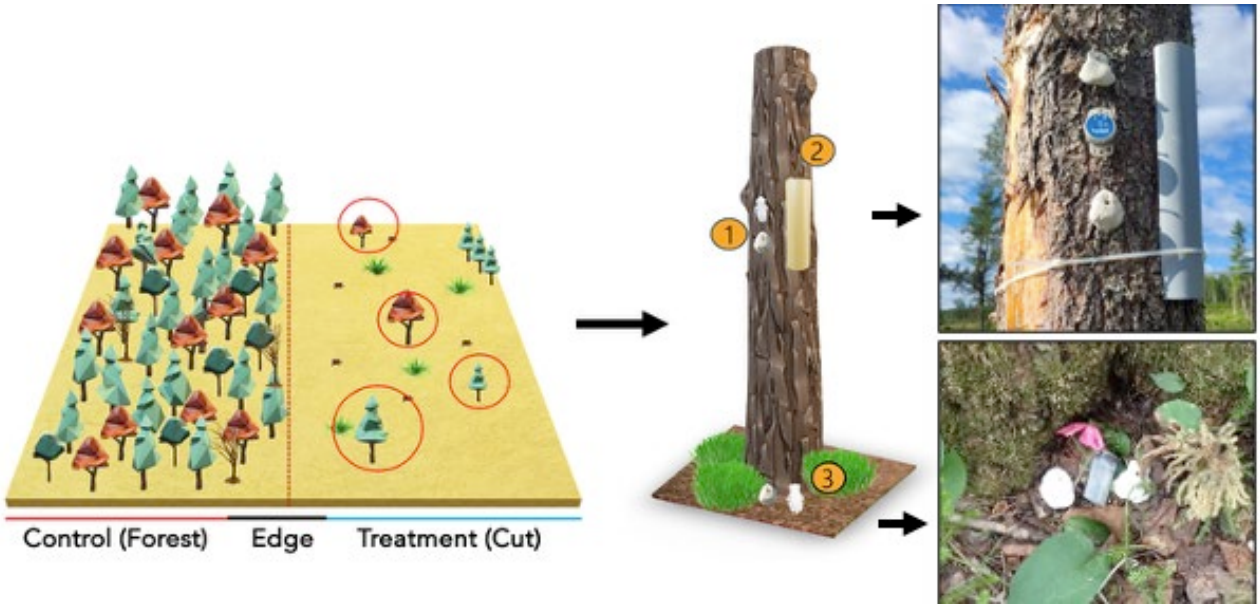

Figure 2.4 Sampling of macro- and micro-habitats at a single site. Left: an idealized site with three macrohabitat plots: Forest, Edge, and Cut. Middle: replica deployment on each tree, with (1) uncovered replicas, (2) replicas covered with pvc pipe, and (3) ground replicas. Right: photos of each microhabitat at a 2022 cut site.

2.2.4 Replica construction and calibration

I used plaster replicas (Hastings et al., 2023; Peterman et al., 2013; Tracy et al., 2007) to measure evaporative water loss (EWL) and surface temperatures in three microhabitats: trunk-covered, trunk-uncovered, and ground. Replicas were based on Tracy et al. (2007). Plaster

replicas were created in two postures that real frogs adopt: water conservation (inactive) and upright (active) (Figure 2.5). Prior to field deployment, I tested whether plaster replicas in upright postures lost more water than those in water conservation. I used five replicas for each posture and tested them over two days. Each of the models were weighed, soaked in water for an hour, re-weighed and then left for four hours at 21°C in front of a fan to simulate the time they will be left in the field. They were then re-weighed to determine water loss as a percentage of original body mass. I found upright models to lose water faster than flat models and thus used both postures for all subsequent work. In total, I built 300 replicas, 150 in each posture.

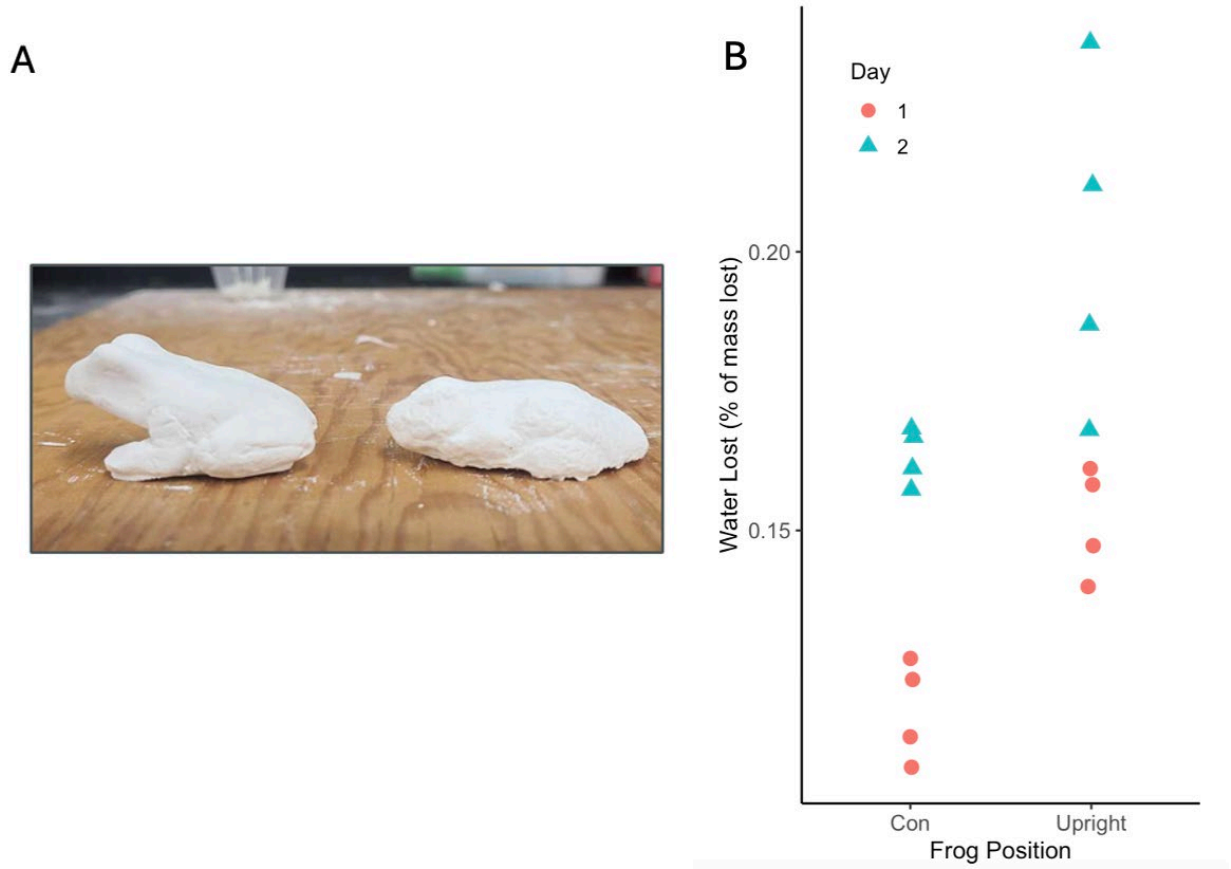

Figure 2.5 Evaporative water loss from plaster replicas in two postures at 22.5 ºC. A: example replicas in upright (left) and water conservation/flat (right) postures. B: Differences in water loss between postures (n=4 replicas in each posture, with water loss measured across 2 days). The plot indicates water loss measurements taken over two days.

To determine if my replicas approximated EWL rates of real frogs, I conducted calibration tests using three of the live frogs captured for the jumping performance tests, three upright replicas, and three flat replicas. These tests were conducted after jump trials had concluded and experimental animals had rested for 2 days. Each frog (real and plaster) was soaked in water for 60 minutes to reach full hydration. They were removed from their water, weighed, brought outside and placed in mesh-covered dishes in direct sunlight. Every five minutes I recorded surface temperatures (using Omega Infrared thermometer), weight, and whether the real frogs were in water conservation. Mass lost every five minutes was calculated by subtracting each weight at five minutes from the initial full hydration weight to get a total weight lost at the end of the 70-minute period. I compared the rate of weight loss between real frogs in upright position with replicas in upright position, and between real frogs in water conservation with replicas in water conservation position (Figure 2.6). I found a significant positive correlation between rates of real frogs and replicas ($r = 0.865$, $p < 0.0001$). I did not perform temperature corrections to match dehydration corrections due to lack of data on internal body temperatures of frogs during correction testing. To calculate the correction between real and replica frog water loss rates, used the following formula:

$$CF = \frac{\beta_1}{\beta_2}$$

Where: CF is the correction factor, β_1 is the slope of linear regression model for treefrog water loss against time; and β_2 is the slope of the linear regression model for replica water loss against time.

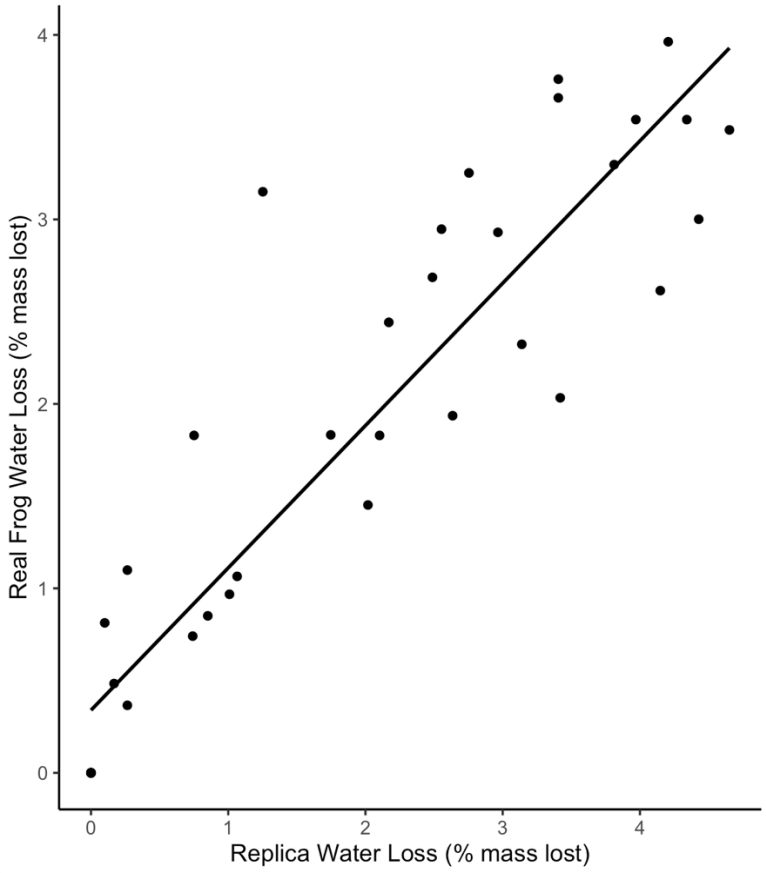

Figure 2.6 Water loss rates of real frogs (n=3) and plaster replicas (n=3) measured every five minutes over 70 minutes in an identical outdoor environment exposed to natural weather conditions (e.g. wind, radiation, humidity, temperature). Black line indicates the linear model for real frog water loss ~ replica water loss.

2.2.5 Field replica deployment

All replicas on tree trunks were placed along the north-facing side of trunks 2 metres from the ground, and ground replicas were placed directly below also on the north-facing side around crevices or under vegetation on the ground. Trunk shelters were made from grey PVC

516 pipe to standardize shelter size and structure. Two replicas of different postures were paired
517 together for each microclimate measurement (Figure 2.5) to estimate conditions at different
518 activity levels in the field. Each pair of replicas was placed as closely together as possible
519 (within 5-6 cm) with a HOBO MX2201 or HOBO pendant temperature datalogger in between
520 them. Out of 16 sites, there were four from the early successional stages at which replicates in
521 the harvest plots were placed on two adjacent trees of the same trunk size and height as single
522 trees were too small to accommodate both models. All other sites had replicas on the same tree.
523 Trunk replica pairs were aligned vertically and ground replica pairs side-by-side (Figure 2.4;
524 right). Vertical positioning of replicas (Figure 2.4) was randomized at each site to account for
525 effects of placement on water loss were.
526 For field deployment, replicas were soaked in water for one hour (time to full saturation),
527 then weighed prior to deployment. I placed replicas at the three microhabitats within each plot
528 (one site x three macrohabitats x three microhabitats x four replicates of each microhabitat = 48
529 replicas at each site). Replicas were left for four hours during the day or 11 hours at night in each
530 plot before being re-weighed to estimate evaporative water loss. Night and day deployment times
531 differed because I assumed that replicas left out for 11 hours during the day would desiccate
532 completely and I would be unable to determine when 100% water loss occurred. I recorded
533 temperature experienced in microhabitats every 30 minutes as closely as possible to each pair of
534 frogs using an unshielded temperature logger (HOBO MX2201 or HOBO pendant) for both day
535 and evening temperatures. Replica surface temperature during the day was recorded manually
536 every 30 minutes using an Omega thermocouple RDXL4SD type T. Data was collected during
537 the day from 10:00 to 14:00, and overnight from 20:00 to 7:30 the next day. Deployment times
538 shifted by 30 minutes near the middle and end of August to match the shift in sunset and sunrise

times. To avoid bias and to minimize differences in deployment and removal times, the order of deployment within each plot was randomized and then maintained for removal to ensure replicas were deployed for equal amounts of time. Since plaster replicas eventually began to deteriorate, they were replaced when their dry mass was reduced to 80% of their original dry mass (Tracy et al., 2007).

2.3 Analysis

All statistical tests were performed using software R version 4.3.1 (R Development Core Team). I used packages nlme (Pinheiro et al., 2025) and glmmTMB (Brooks et al., 2017) for model fitting, DHARMa (Hartig et al., 2024), emmeans (Lenth et al., 2025), performance (Lüdecke et al., 2021), and afex (Singmann et al., 2024) for model checks and post-hoc analysis. I used the interp (Gebhardt et al., 2024) package for bilinear interpolation of performance estimates.

2.3.1 Jump Distance

All videos were analyzed using Kinovea™. I measured the distance from each jump's start to endpoint for each frog and trial combination and used only the maximum jump distance as an estimate of maximal performance (H. John-Alder et al., 1988). If a frog did not jump or move, jump distance was recorded as zero. Jumps were considered distinct from hops as a form of movement and were distinguished by full extension of the frogs' hind limbs (see Mitchell & Bergmann, 2016). Though acceleration is occasionally used as a measure of performance alongside jump distance, (A. Mitchell & Bergmann, 2016; Wilson, 2001) I did not calculate acceleration. Each maximum jump distance was used to fit hydro- and thermal- performance curves in section 2.3.2.

I used a linear mixed effects model to test the effect of the time frogs spent in a trial on jump distance, with fixed effects of time under trial and random effect of frog and date. I conducted this test to isolate potential physiological fatigue from being in trials from the effects of dehydration by comparing control frogs that did not undergo dehydration with test frogs that did undergo dehydration. I found no significant effect of time under trial on control frog jump distance (β =-0.00479, df = 48 , SE = 0.0078, p = 0.541; Figure 2.7).

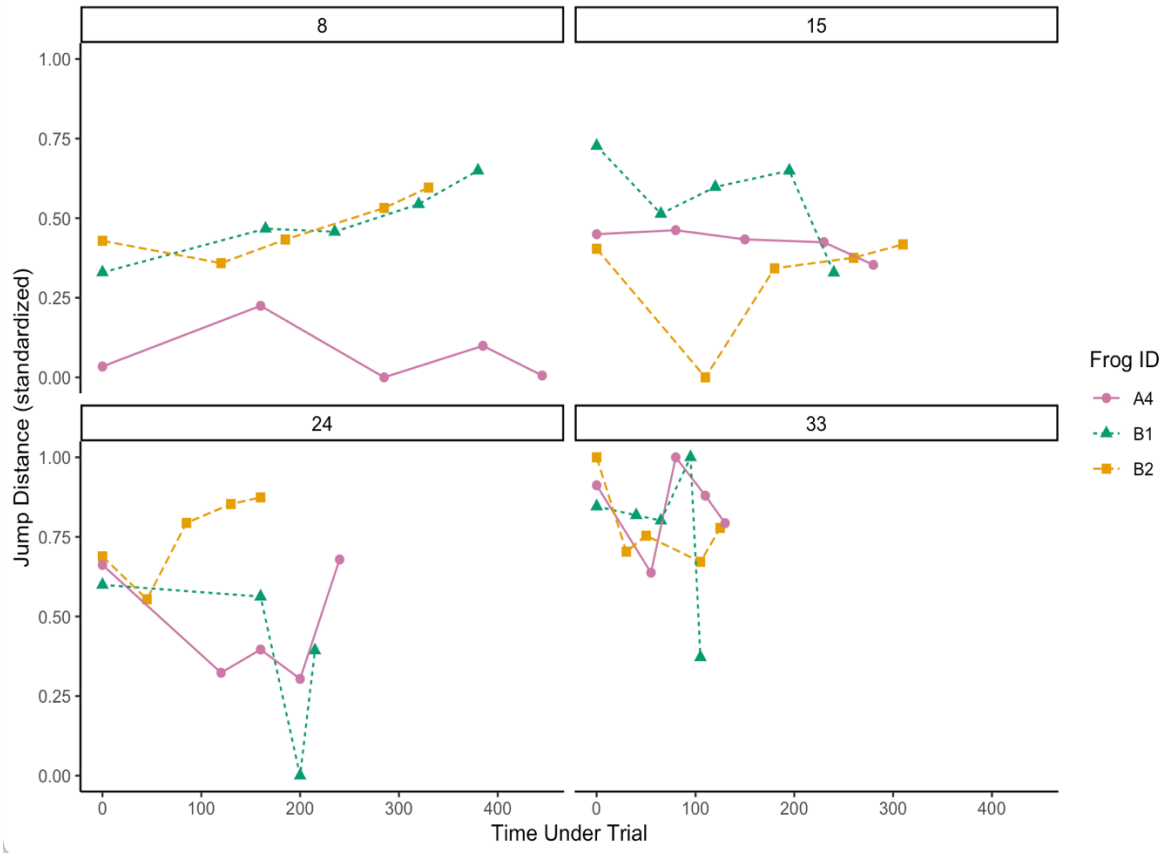

Figure 2.7 The effect of time under trial on jump distances for control frogs. Each plot is grouped by trial temperature. Points indicated normalized jump distances for each of the control frogs.

2.3.2 Hydrothermal Performance Curves

To quantify hydrothermal performance relationships for gray treefrogs, I fit a candidate set of thermal performance functions and dehydration-performance curves to laboratory jumping

data (full list in Appendix B) for each frog separately. To account for uncertainty in model selection, I ranked all fitted candidate models for each frog using Akaike's Information Criterion (AIC), calculated Akaike weights, and generated model-averaged predictions for that individual. This produced one averaged curve for each frog for each axis (temperature or hydration). I modeled thermal and hydric performance relationships separately (univariate fits) because (1) no established functional form exists for a joint temperature–hydration performance curve (Angilletta, 2009; Huey & Stevenson, 1979), and (2) my dataset did not support fitting high-dimensional nonlinear mixed models without convergence failures or biologically unrealistic fits. Fitting models ignoring that each individual was measured multiple times was not an option as it would result in pseudoreplication.

Fitting curves separately for each frog avoided problems with mixed-effects nonlinear model structure and allowed me to retain the shape and scaling of each individual's response (Figure 3.1 and Figure 3.3). Within each frog, I fit candidate functions (adapted Kontopoulos et al., 2024 and Padfield et al., 2021) with nonlinear least squares regression (Appendix B) with either hydration or temperature as a response. I scaled jump distances to 0–1 (where 1 = that frog's maximum distance). I excluded fits if they were multimodal (> three peaks within the observed range), exhibited unrealistic monotonic change across the experimental range, or clearly overfit the data (Angilletta, 2006). I only used frogs that had at least three data points (maximum jump) for each temperature and dehydration combination. This meant that for 70% dehydration, there is no weighted curve for frog A6.

By using a broad candidate set for each univariate relationship and applying model selection and model-averaging, I aimed to reduce selection uncertainty in curve shapes (and therefore parameter estimates) and to ensure that predictions were not unduly influenced by a

single arbitrarily chosen model (mixed models selection: Angilletta, 2006, Dormann et al., 2018; J. B. Johnson & Omland, 2004; Kontopoulos et al., 2024; Rozen-Rechels et al., 2019). Restricting the analysis to a single or small set of functions risks model misspecification, which could bias parameter estimates and predictions (J. B. Johnson & Omland, 2004).

For species-level predictions, I combined curves in two stages:

(1) **Within-frog averaging:** Model-averaged curves were generated using Akaike weights, so the contribution of each candidate function reflected its relative support for that frog's data (Appendix A for model weights).

(2) **Across-frog averaging:** The resulting individual model-averaged curves were then combined into a single population curve by equal-weighting each frog's contribution. This ensured that all individuals contributed equally to the species-level estimate, regardless of the number of candidate functions retained for each frog

I used the population model-averaged curves to build a predictive surface of jumping performance that combines temperature and hydration (Figure 3.5). To estimate field performance, I merged the two univariate surfaces into a bivariate surface by pairing predictions from the corresponding hydration and temperature curves and interpolating across the microhabitat field data (temperatures and hydration states) (**Figure *3.5***). The resulting predicted jump distances served as the response variable in subsequent statistical models comparing potential performance across sites and microhabitats (Section 2.3.3). This approach is analogous to using derived variables, common in species distribution or ecological niche modelling techniques, where predictions are treated as response variables in subsequent analyses (Elith & Leathwick, 2009).

I acknowledge several limitations in the above approach to curve fitting and interpolation. First, treating the curves univariately and later combining them may inflate the effective sample size, since the same individuals contribute to both fits. Second, propagating predictions from two separate models into a single combined surface inevitably carries forward the uncertainties from each fit. Nonetheless, given the current dataset and the study's primary objective of estimating performance consequences under realistic field conditions, this approach represents a compromise between model complexity and data limitations. While this method allows for an integrated link between measured field conditions and laboratory-based performance relationships, it should be interpreted cautiously, as the predictions are subject to the combined errors and assumptions of both datasets.

2.3.3 Hypothesis testing

To examine differences in site conditions between clearcuts, forests, and edges through forest regrowth, I used model-averaged predictions from Section 2.3.2 to estimate expected performance under field conditions, using observed environmental temperature and hydration data. In this section, I tested for differences between macrohabitats (cut, edge, forest), microhabitats (ground, covered, uncovered) across each time-since-cut age. For each hypothesis, I fit mixed effects models with either temperature, water loss, or performance as the response variable. Models were fit for day and night separately. All models included random effects of sites nested within date to account for site variation, weather differences among days, and temporal autocorrelation. I performed all analyses using replica temperatures averaged across the entire period of deployment, corrected water loss levels calculated using the correction factor derived from calibration tests (correction factor ~ 0.7400), and performance estimates derives from jump testing data described above (Section 2.3.2). Sites with a minimum of one rainy day

were removed from the water loss and performance models to allow for proper specification of the nesting structure for date of visit and corresponding sites. For models that demonstrated autocorrelation after including random date effect, I checked for stationarity using Augmented Dickey-Fuller (ADF) tests and used autocorrelation function (ACF) and partial autocorrelation function (PACF) plots to determine p and q values for correlation structures. I checked all final models for assumptions of residual overdispersion, heteroscedasticity, normality, and independence. I performed multiple comparisons of estimated marginal means (with Tukey corrected p-values for multiple comparisons) post hoc tests to analyze interactions and fixed effects of significant in each of the models.

2.3.4 Hypothesis one: macrohabitats through succession

For hypothesis one models with temperature as a response, I fit non-linear mixed effects models (nlme package) with gaussian distributions and autocorrelation specifications (p=1, q=0). For the responses of water loss and performance, I fit generalized linear mixed effects models with a t-family distribution. I fit all models testing hypothesis one with a fixed interaction between macrohabitat (cut, edge, and forest) and age, and main effects of macrohabitat, age, and microhabitat. The random effect was date nested within site (Figure 2.8).

Response: Water loss *or* Temperature *or* Predicted performance

Fixed Effects: Macrohabitat x Age + Microhabitat

Random Effects: (1| site/date)

Figure 2.8 Hypothesis one model structure. Models were fit for each response variable and each period (day or overnight) separately. Models were fit as non-linear mixed effects models with a gaussian distribution and autocorrelation function specifications.

2.3.5 Hypothesis two: microhabitat and posture differences

For all models testing hypothesis two, I fit generalized linear mixed effects models with a t-student distribution (Brooks et al., 2017; glmmTMB package). I included the same fixed effects as for testing hypothesis one but added posture and interaction terms between microhabitat and age, and microhabitat and macrohabitat (Figure 2.9). Effects of posture on temperature could not be determined for overnight data as one temperature measurement was taken for each pair of upright and flat replicas in each microhabitat. I could not directly test the difference between day and night performance effects in the same model due to differences in time intervals for water loss rates. The same procedures and model checks were followed for all models as described above (section 2.3.3).

Response: Water loss *or* Temperature *or* Predicted performance

Fixed Effects: Macrohabitat : Age + Age : Microhabitat + Macrohabitat : Microhabitat + Macrohabitat + Age + Microhabitat + Posture

Random Effects: (1 | site/date)

Figure 2.9 Hypothesis Two Model Structure. Models were fit for each response variable and each period (day or overnight) separately. Models were fit as generalized linear mixed effects models when residual distribution required alternative specification (t-family)

In the above section, my aim was to test for differences in expected performance among habitats and conditions. I therefore used a frequentist approach (linear/mixed-effects models) for hypothesis testing. This is distinct from the statistical method used in Section 2.3.2, wherein I used information-theory to estimate hydrothermal performance curves with no *a priori* hypotheses about general curve shape. These two stages address different questions—curve estimation versus hypothesis testing—and thus employ the statistical framework most appropriate to each objective. Although the second stage is based on predictions from the first, I

treat them as conceptually distinct analyses. Using different statistical paradigms in different parts of an analysis is common in ecological modeling when stages have distinct inferential goals (Burnham & Anderson, 2004; J. B. Johnson & Omland, 2004). In such cases, the choice of framework is guided by the nature of the question being addressed, rather than by strict adherence to a single philosophical approach.

3 RESULTS

3.1 Thermal Performance Curves

Thermal performance curves revealed that both thermal breadth and thermal optima shifted with hydration level (Figure 3.2), with Topt at 100% hydration substantially higher than at other hydration levels. Frogs reached their highest maximum performance at 92% hydration (max = 0.81), and their lowest maximum at 70% hydration (max = 0.26). Thermal performance breadth (defined as the range of temperatures where performance was 90% of maximum) narrowed only slightly; at 100% hydration, it spanned 11 °C while at 70% hydration it spanned 9 °C. However, its position varied greatly, being situated between 28°C and 39.0 °C at 100% hydration and from 22°C – 31 °C at 70%. Individual curves varied in shape and magnitude but consistently showed declines in performance at both high and low thermal extremes when dehydration increased. Individual weighted curves are present in Figure 3.1 demonstrate variation in thermal performance across frogs under different hydration treatments.

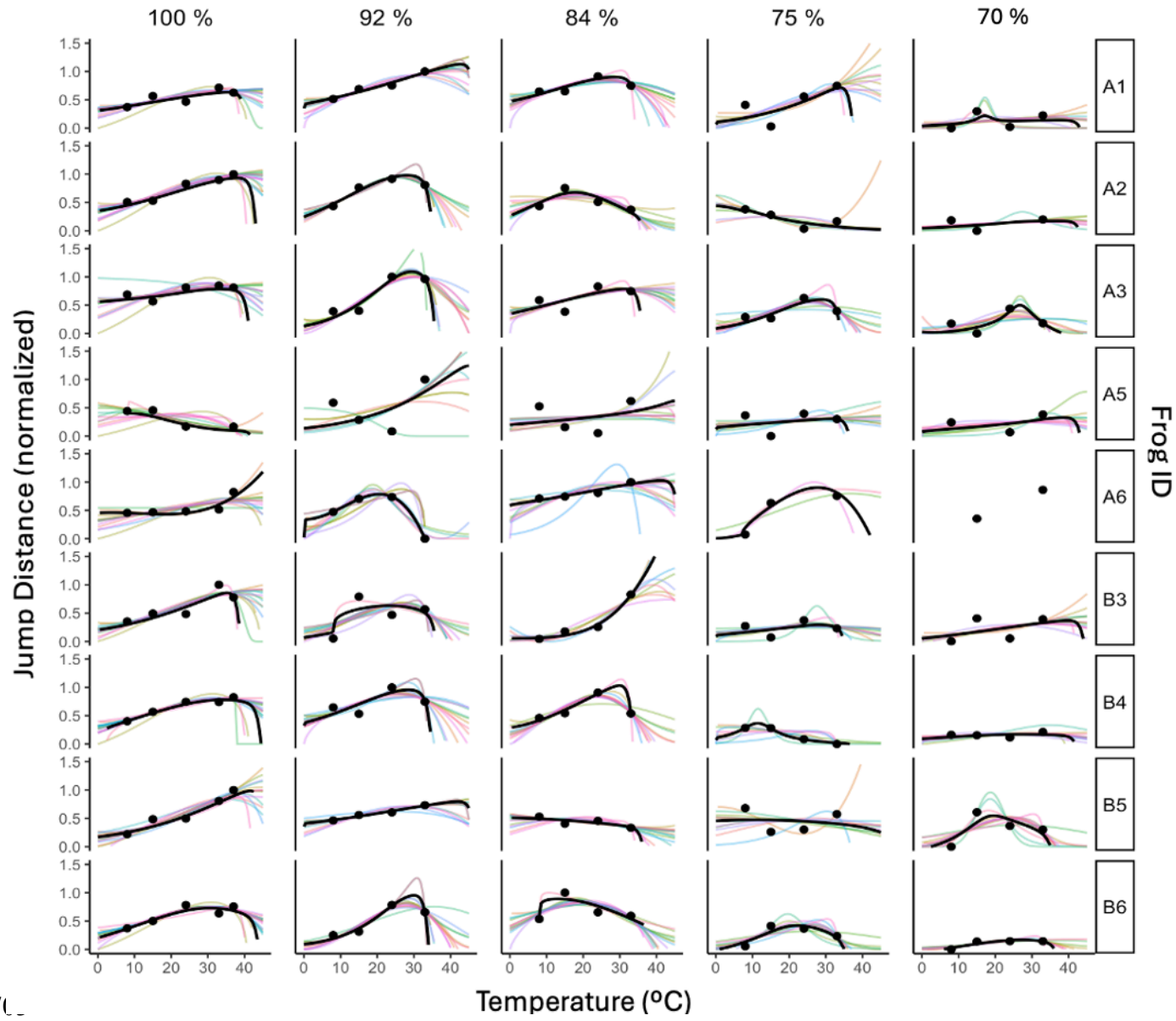

704 **Figure 3.1** Weighted-average thermal performance curves for each frog at each hydration level.
705 Faded coloured lines for each frog (each rectangle) indicate single curves fit from model types.
706 Performance was measured as maximum jump distance, standardized as the proportion of each
707 frog's maximum jump distance across all temperatures. Standardized performance values for each
708 frog are indicated by black points. Temperature was measured from incubation temperatures in
709 which frogs were held during trials. Solid black lines for each plot are results from Akaike
710 weighted average curves for each frog. Not all models were fit for each frog due to parameter (k)
711 restrictions and final curve shapes for each model.

712
713

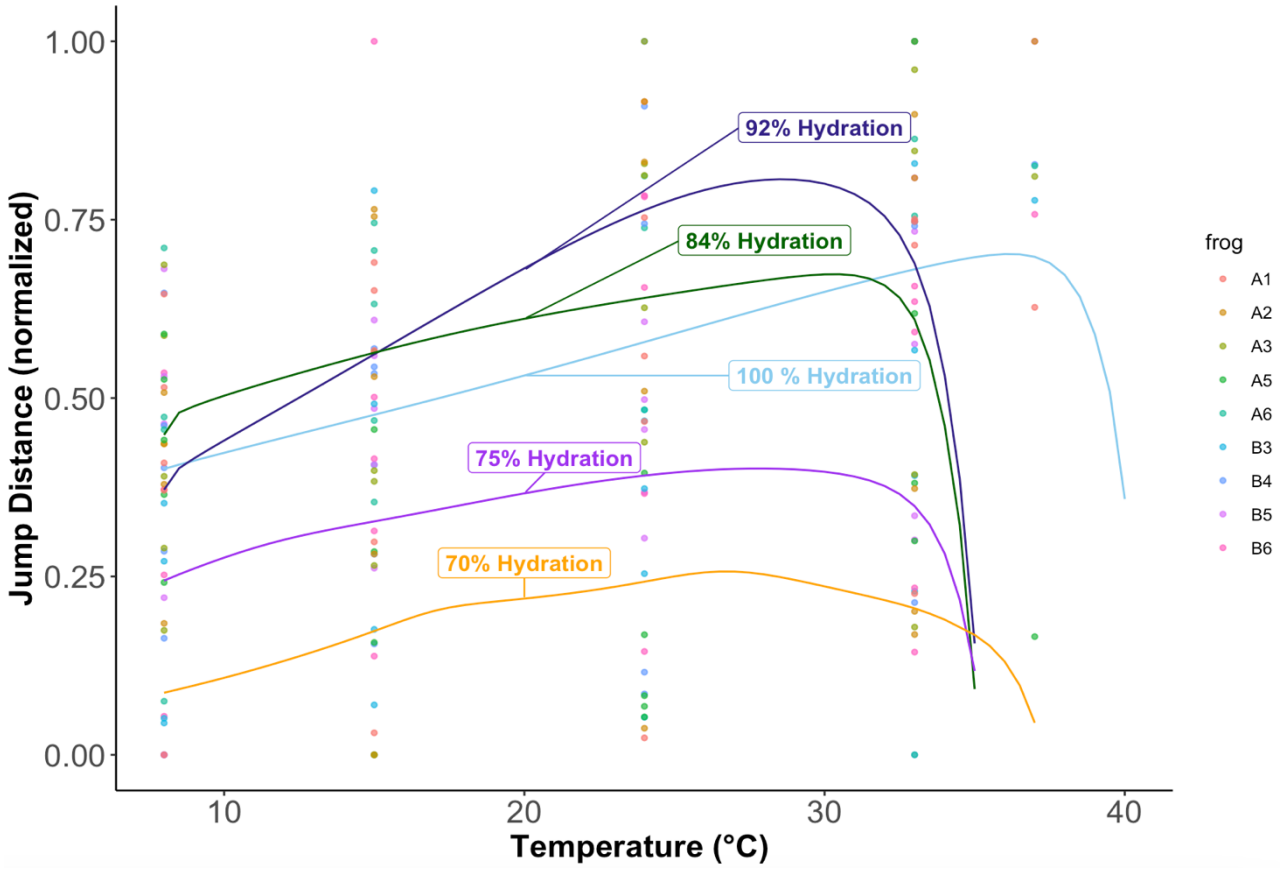

Figure 3.2 Thermal performance curves at five dehydration levels (100%, 92%, 84 %, 75%, 70%). Data for trials was subset for dehydration levels across five temperatures (37°C, 33°C, 24°C, 15°C, 8°C). Frogs were only taken to 37°C at 100% hydration. Performance was measured as jump distance, normalized as the proportion of each frog's maximum jump distance across all temperatures. Temperature was measured from incubation temperatures in which frogs were held during trials. Curves produced are weighted averages from the curves fit to each frog. Coloured points correspond to standardized maximum jump distance for frogs (A1, A2, A3, etc.)

3.2 Hydro-Performance Curves

Hydro-performance curves indicated peak performance between 87%-92% hydration, with the highest optima occurring at 33°C and when frogs were nearly fully hydrated at 98% (Figure 3.4). Across 8, 15, and 24°C, frog performance declined past 10% of their maximum values after reaching 15-20% dehydration. However, at 33°C, this threshold is reached at 10% dehydration. Maximum performance is lowest at the coldest temperature (8°C: max performance = 0.468).

Performance was highest at the warmest temperature (33°C max performance = 0.825) but declined rapidly below 90% hydration (Figure 3.4). Hydro performance curves showed consistent shapes across temperatures, with performance remaining relatively stable until hydration dropped below ~20%, after which all curves declined similarly (Figure 3.4). Individual averaged curves are presented in Figure 3.3, illustrating variation in hydric performance across frogs under different temperature treatments.

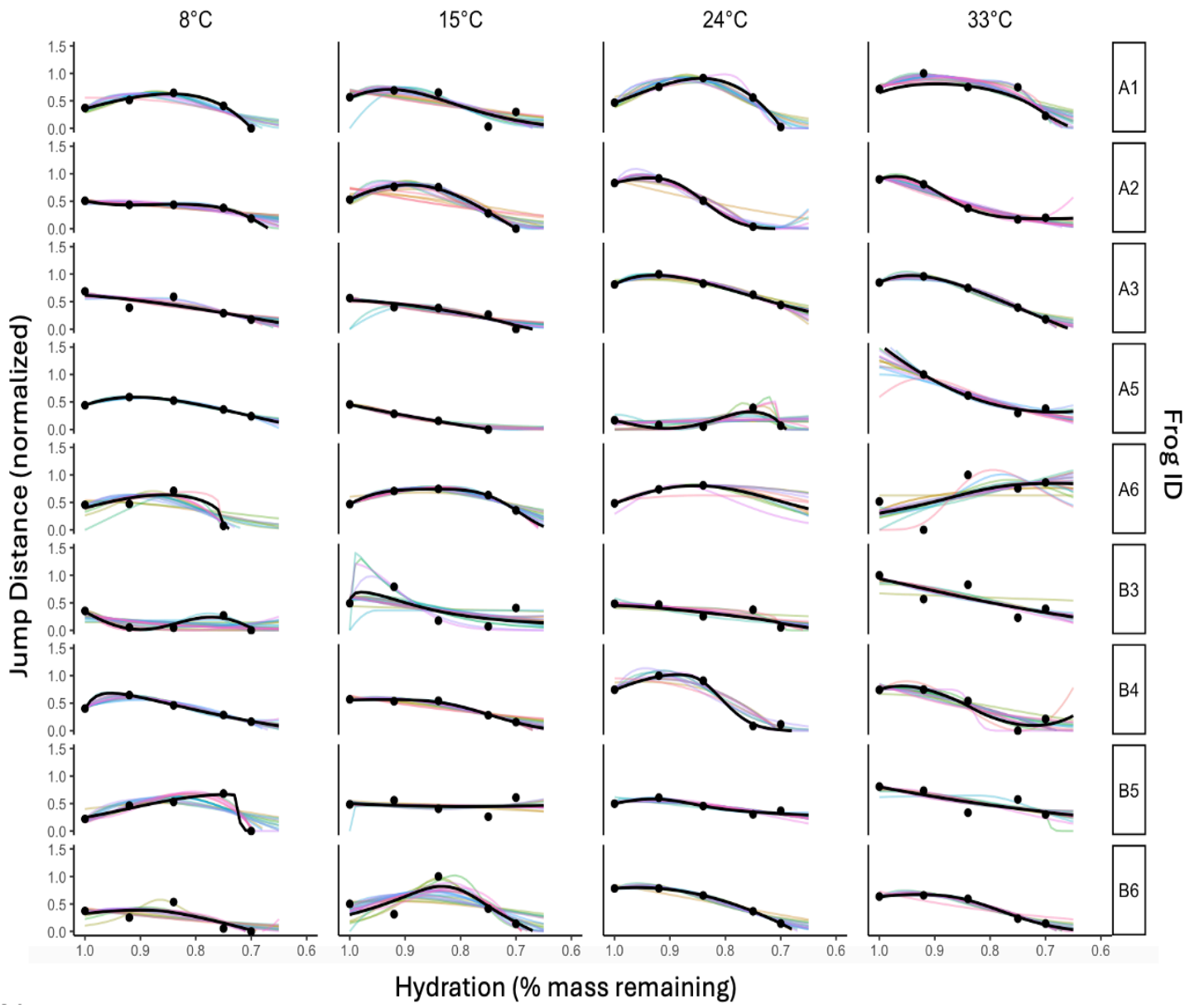

Figure 3.3 Individual weighted-average hydro-performance curves for all frogs and all temperature subsets. Faded coloured lines for each frog (each square) indicate single curves fit from model types (see appendix). Solid black lines for each plot are results from Akaike weighted average curves for each frog. Performance was measured as jump distance, normalized as the proportion of each frog's maximum jump distance across all temperatures. Points indicate these standardized distances for each frog at each hydration level (100, 92, 84, 75, 70 %) Hydration was measured as percentage of fully hydrated mass lost. Not all models were fit for each frog due to parameter (*k*) restrictions and final curve shapes for each model.

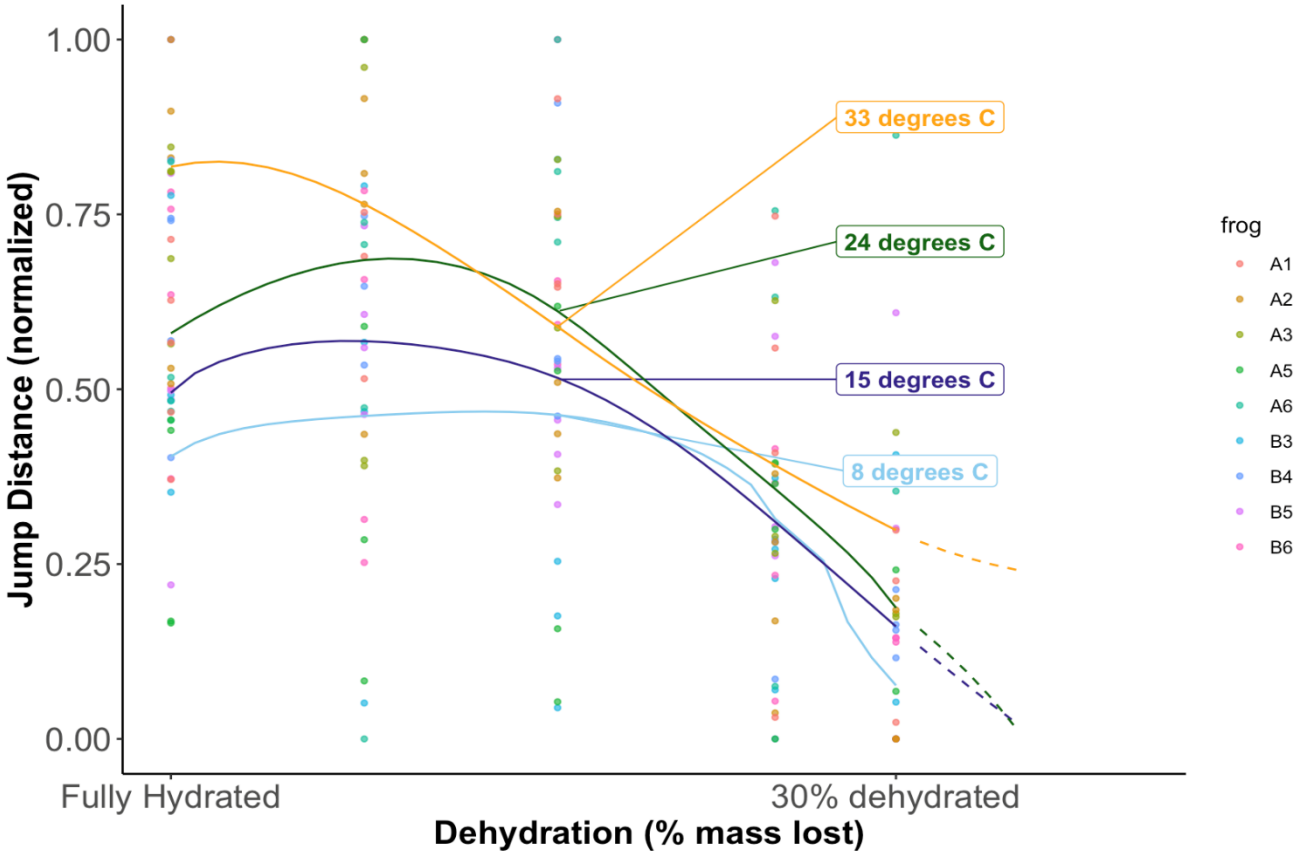

Figure 3.4 Hydro performance curves at four temperatures. Data for trials was subset for water loss rates at each temperature (33°C, 24°C, 15°C, 8°C) across five dehydration levels (100%, 92%, 84 %, 75%, 70%). Performance was measured as jump distance, normalized as the proportion of each frog's maximum jump distance across all temperatures. Hydration was measured as a percentage of fully hydrated mass lost. Curves are averaged from the weighted curves fit to each frog. Coloured points correspond to normalized maximum jump distance for frogs (A1, A2, A3, etc.)

3.3 Hydro-thermal Surface

To estimate the combined effects of temperature and hydration, I constructed a hydrothermal performance surface using the model-averaged curves above. This surface illustrates predicted jump performance across the range of conditions observed in the field (Figure 3.5).

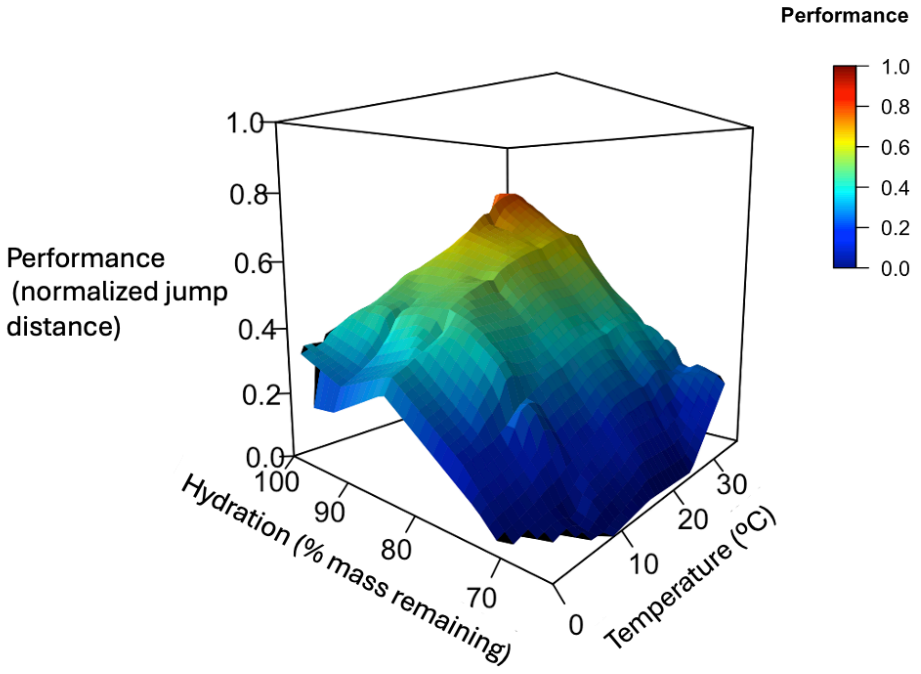

764

765 **Figure 3.5** Hydrothermal performance surface generated from merging the univariate curves for
766 hydro-performance and thermal performance curves and interpolating across a bilinear grid.
767 Performance was measured as jump distance, normalized as the proportion of each frog's
768 maximum jump distance across all temperatures. Hydration was measured as a percentage of
769 fully hydrated mass lost. Temperature was measured from incubation temperatures in which
770 frogs were held during trials.

771 **3.4 H1 - Successional Differences in Macrohabitat**

772

773 For the first hypothesis that forest and cut macrohabitats would be significantly different
774 immediately post-cut and that these differences would persist 20-years post-cut, I tested
775 interaction between macrohabitat (plot) and successional stage with additive effect of
776 microhabitat (Table 3.1 and Table 3.2).

777 *3.4.1 Daytime habitat and age interactions*

778

I found a significant main effect of microhabitat, as well as a significant interaction between plot type and age for all three response variables (temperature, water loss, performance fit for daytime data (Table 3.1).

Table 3.1 Hypothesis one model results for all three response variables during the day. Significant tests used marginal sums of squares for linear mixed effects models. Df indicates the numerator degrees of freedom. For the daytime water loss model, the denominator degrees of freedom (denDF) are: 22262 for plot type, microhabitat, and the plot type × age interaction; and 12 for age. For both the daytime water loss and performance models, the denominator degrees of freedom (denDF) are: 2120 for plot type, microhabitat, and the plot type × age interaction; and 11 for age. Denominator degrees of freedom for linear mixed effects models with lme were calculated using Kenward-Roger approximations. Significant p-values are in bold.

Response	Term	Df	F value	p-value
Temperature	plot type	2	18.52	**<0.001**
	age	3	1.72	0.215
	microhabitat	2	39.71	**<0.001**
	plot type x age	6	16.92	**<0.001**
Hydration	plot type	2	15.34	**<0.001**
	age	3	4.16	**0.034**
	microhabitat	2	452.55	**<0.001**
	plot type x age	6	27.35	**<0.001**
Performance	plot type	2	11.25	**<0.001**
	age	3	2.75	0.093
	microhabitat	2	207.78	**<0.001**
	plot type x age	6	3.65	**0.001**

Post-hoc tests for the interaction between macrohabitat and clearcut age indicated significant differences between habitats for all ages (Figure 3.6). For temperature effects, it was significantly warmer in cut plots than both forest and edge habitats, with the largest difference

between cut and forests 2-4 years old (mean difference = 1.715 ºC, SE = 0.0973, $p < 0.001$). The smallest difference was in cuts 14-20 years old (mean difference = 0.563 ºC, SE = 0.0973, $p < 0.001$). Differences in water loss rates between cut and forests were significant across all ages, with the greatest difference in 1–2-year-old sites (mean difference = 5.15 % weight lost, SE = 0.232, $p < 0.001$) and diminishing over time but remaining significant in our oldest successional stage (14-20-years-old: mean difference = 1.492 % weight lost, SE = 0.269, $p < 0.001$). Estimated performance differences were significant between cut and forests habitats across all ages (Figure 3.6) with the smallest difference occurring in 14-20 year-old cuts (mean difference = 0.024, SE = 0.0052, $p < 0.001$) and the largest differences occurring in our 7-10-year-old and 14-20-year-old successional plots (Figure 3.6).

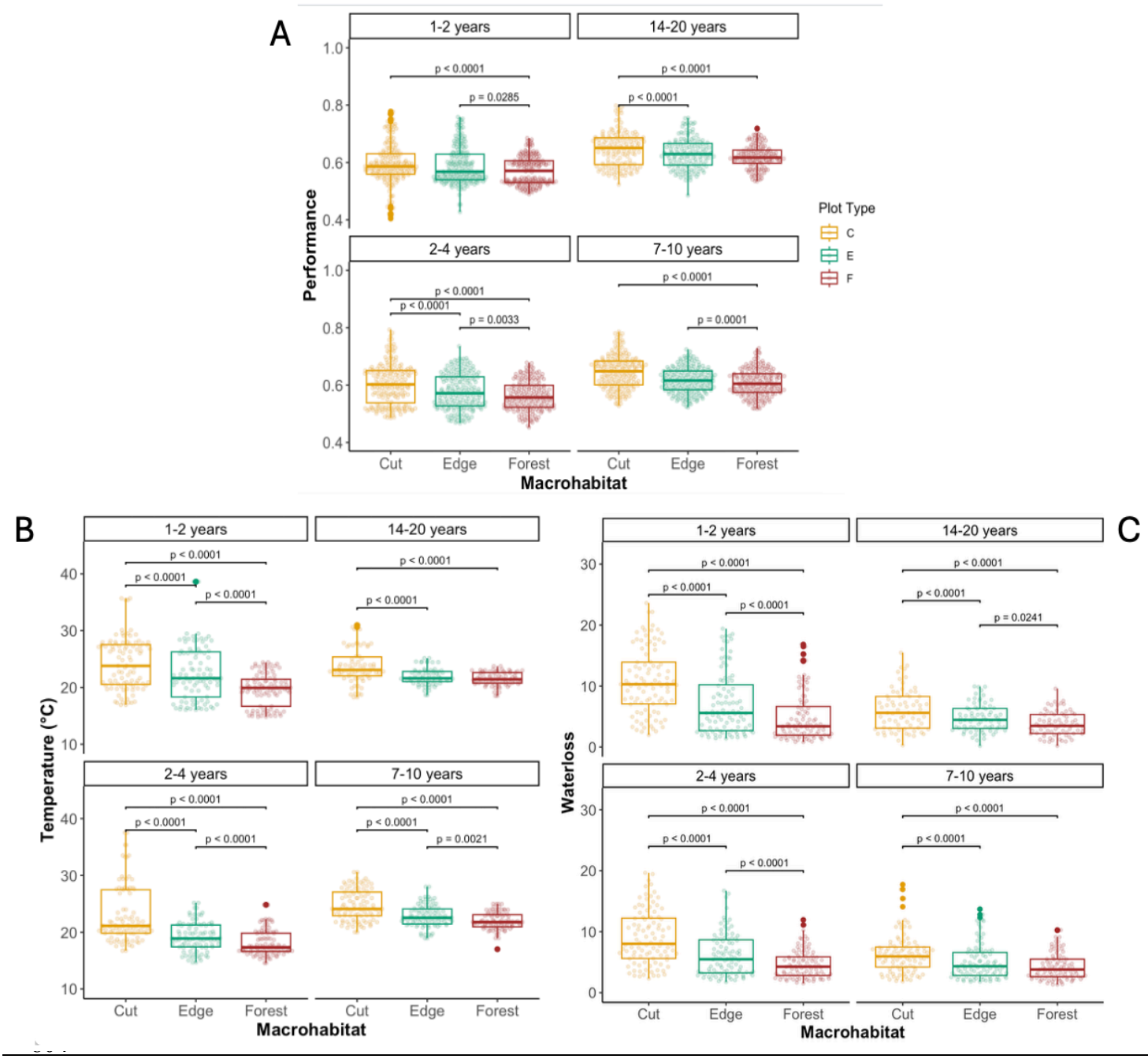

Figure 3.6 Daytime performance (A), temperature (B), and water loss (C) differences between macrohabitats (plot types: cut, edge, and forest). All results are averaged over microhabitat type. Results were generated from mixed effects models with fixed effects of macrohabitat, age, microhabitat, and an interaction term between macrohabitat x age. The model was fit with random effect of date nested within site. Points indicate all raw data. Bars indicate significant differences between pairs of macrohabitats with associated p-values (significant if $p < 0.05$). Comparisons were generated from estimated marginal means of difference between macrohabitats across age groups with Tukey adjusted p-values for multiple comparisons.

3.4.2 Overnight habitat and age interactions

I found a significant main effects of microhabitat, as well as a significant interaction between plot type and age for all three models fit for overnight data (Table 3.2).

Table 3.2 Hypothesis one model results for all three response variables fit for overnight data. Left side table indicates models fit with temperature and performance ANOVA summaries generated using marginal type significance estimates and F-statistics. Right table is the model fit with hydration as a response with summaries generated using likelihood ratio tests with estimated chi squared distributions and model fit with as a glmm. For the overnight performance model, the denominator degrees of freedom (denDF) are: 2069 for plot type, microhabitat, and the plot type × age interaction; and 11 for age. For the overnight temperature model, the denominator degrees of freedom (denDF) are: 2120 for plot type, microhabitat, and the plot type × age interaction; and 11 for age. Denominator degrees of freedom for linear mixed effects models with lme were calculated using Kenward-Roger approximations. Significant effects are indicated by bold p-values.

Response	Term	Df	F value	p-value
Temperature	plot type	2	9.522	**<0.001**
	age	3	1.851	0.1917
	microhabitat	2	241.334	**<0.001**
	plot type x age	6	1.990	0.0643
Performance	plot type	2	21.791	**<0.001**
	age	3	1.349	0.3090
	microhabitat	2	595.230	**<0.001**
	plot type x age	6	7.413	**<0.001**

Response	Term	Df	Chisq	p-value
Hydration	plot type	2	60.518	**<0.001**
	age	3	2.974	0.396
	microhabitat	2	1218.390	**<0.001**
	plot type x age	6	99.297	**<0.001**

Post-hoc tests for the interaction between macrohabitat (plot type) and clearcut age revealed significant differences in performance between habitats for all ages overnight (Figure 3.7 and Table 3.2). For temperature effects, it was significantly warmer in forest plots than both cut and edge habitats in all successional groups except in 1-2 year-since-cut groups, where no significant difference was found (mean difference = 0.213 ºC, SE = 0.1647, $p < 0.399$). The

largest difference between cut and forests occurred in 7–10-year-old sites (mean difference = -0.783 ºC, SE = 0.165, $p < 0.001$), where it was colder in clearcuts than in forests. Water loss was significantly higher in forests than in cuts (Figure 3.7) in almost all age groups except in 2-4 years-since-cut groups (mean difference = -0.117 % weight lost, SE = 0.0895, $p = 0.393$). Water loss was only significantly greater in 2–4-year-old cuts than in forests (mean difference = 0.5213 % weight lost, SE = 0.1070, $p < 0.001$). The largest difference between water loss in cut and forested habitats occurred in 14–20-year-old sites, wherein frogs lost more water in forests (mean difference = -0.737 % weight lost, SE = 0.1234, $p < 0.001$). Resulting performance was significantly higher in forests than in cuts across all ages except in 1-2-year-old sites (Figure 3.7). Performance differences between forest and cuts were largest in 7–10-year-old sites, when forests were significantly higher than cut plots (mean difference = -0.017, SE = 0.0027, $p < 0.001$).

Performance was higher in nearly all time-since-cut groups in forest compared to cut and macrohabitats. This difference was significant in all cut-ages except for 1-2-year-old cuts (Figure 3.7).

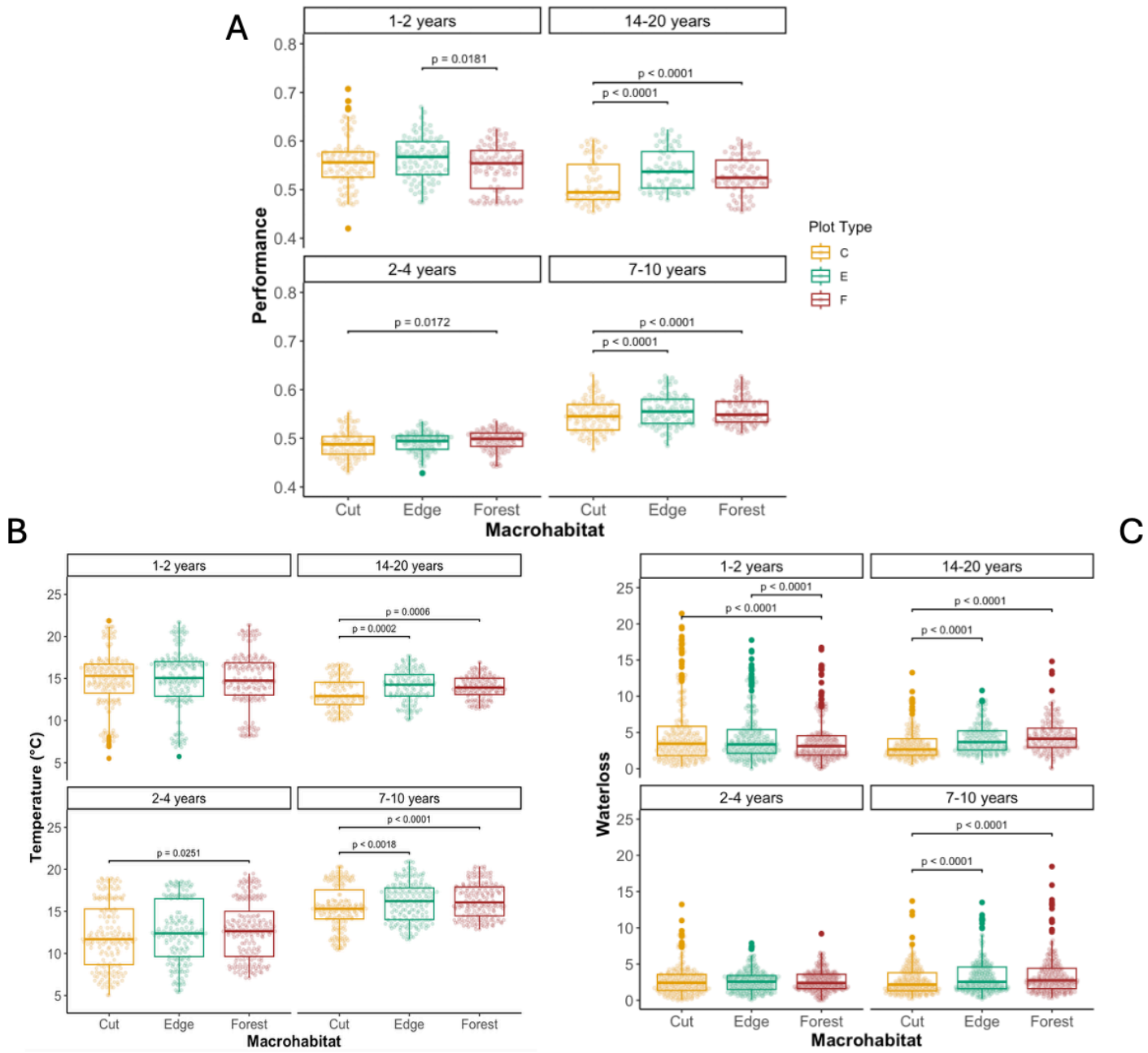

Figure 3.7 Overnight performance (A), temperature (B), and water loss (C) differences between macrohabitats (plot types). Results were generated from mixed effects models with fixed effects of macrohabitat, age, microhabitat, and an interaction term between macrohabitat x age. The model was fit with random effect of date nested within site. Large bold points indicate data outliers, and faded points indicate all raw data. Bars indicate significant differences between pairs of macrohabitats with associated p-values (significant if $p < 0.05$). Comparisons were generated from estimated marginal means of difference between plot types across age groups with Tukey adjusted p-values for multiple comparisons.

3.5 Microhabitat and postural differences across succession in macrohabitats

For the second hypothesis that overnight differences between cut and forests in uncovered microhabitats between would be more pronounced than differences in covered microhabitats during the day, I tested the interactions between macrohabitat (plot), successional stage, and microhabitat (Table 3.3 and Table 3.7).

3.5.1 Daytime microhabitat effects

Models fit for temperature during daytime periods revealed significant interactions between microhabitat and age and plot type with age, but no significant interaction of plot type with microhabitat (Table 3.3). Models for both hydration and temperature revealed significant interactions between all response variables of plot type, microhabitat, and age (Table 3.3).

Table 3.3 Models testing hypothesis two and interactions of plot and age with microhabitat. All estimates were generated from type III significance tests using denominator degrees of freedom (ddf) F tests for p-values. Significant estimates are indicated by bolded p-values. "Df" indicates numerator degrees of freedom for each parameter.

Response	Term	Df	Chisq	p-value
Temperature	plot type	2	53.74	**<0.001**
	microhabitat	2	4.12	0.127
	plot type x age	9	164.96	**<0.001**
	plot type x microhabitat	4	6.67	0.154
	age x microhabitat	6	133.50	**<0.001**
Hydration	plot type	2	8.93	**0.012**
	microhabitat	2	345.91	**<0.001**
	plot type x age	9	206.90	**<0.001**
	plot type x microhabitat	4	110.45	**<0.001**
	age x microhabitat	6	22.64	**0.001**
Performance	plot type	2	22.35	**<0.001**
	microhabitat	2	200.99	**<0.001**
	plot type x age	9	29.64	**0.001**
	plot type x microhabitat	4	10.88	**0.028**
	age x microhabitat	6	269.08	**<0.001**

Post hoc tests for comparisons of temperatures in microhabitats between plots during the day (e.g. uncovered cut vs. uncovered forest) demonstrated significantly higher average temperatures in all cut habitats than in forested habitats in both covered and uncovered microhabitats for all ages (Table 3.4). Differences between temperatures in cut and forests were larger for uncovered microhabitats, and the largest difference by year occurs in 7-10-year-old sites for both covered (mean difference = 1.417 ºC, SE = 0.086, $p < 0.001$) and uncovered (mean difference = 1.4363 ºC, SE = 0.084, $p < 0.001$) microhabitats (Figure 3.8). There were no significant differences between microhabitats within habitat types except between covered and uncovered forest microhabitats in 7–10-year-old sites (Table 3.4).

Table 3.4 Daytime estimated marginal means for microhabitat comparisons within (left) and between (right) macrohabitat types for temperature. Results were generated from Tukey corrected least squares means on the mixed effects models for temperature and hypothesis two. "Age" indicates the time-since-cut group, "contrast" indicates the microhabitat and plot contrasts, with "estimate" as the difference between the estimated marginal means for each term in the pairing going from left to right. Significant contrasts ($p < 0.05$) are indicated in bold.

Contrasts within macrohabitats

Age	Contrast	Estimate	SE	p-value
1-2 years	tree covered C - tree uncovered C	0.060	0.079	0.998
	tree covered F - tree uncovered F	0.079	0.073	0.977
2-4 years	tree covered C - tree uncovered C	0.112	0.081	0.904
	tree covered F - tree uncovered F	0.131	0.072	0.670
7-10 years	tree covered C - tree uncovered C	0.236	0.086	0.132
	tree covered F - tree uncovered F	**0.255**	0.076	0.021
14-20 years	tree covered C - tree uncovered C	0.110	0.080	0.911
	tree covered F - tree uncovered F	0.129	0.075	0.732

Contrasts between macrohabitats

Age	Contrast	Estimate	SE	p-value
1-2 years	tree covered C - tree covered F	**0.854**	0.080	< 0.001
	tree uncovered C - tree uncovered F	**0.873**	0.080	< 0.001
2-4 years	tree covered C - tree covered F	**1.158**	0.082	< 0.001
	tree uncovered C - tree uncovered F	**1.178**	0.079	< 0.001
7-10 years	tree covered C - tree covered F	**1.417**	0.086	< 0.001
	tree uncovered C - tree uncovered F	**1.436**	0.084	< 0.001
14-20 years	tree covered C - tree covered F	**0.393**	0.081	< 0.001
	tree uncovered C - tree uncovered F	**0.412**	0.079	< 0.001

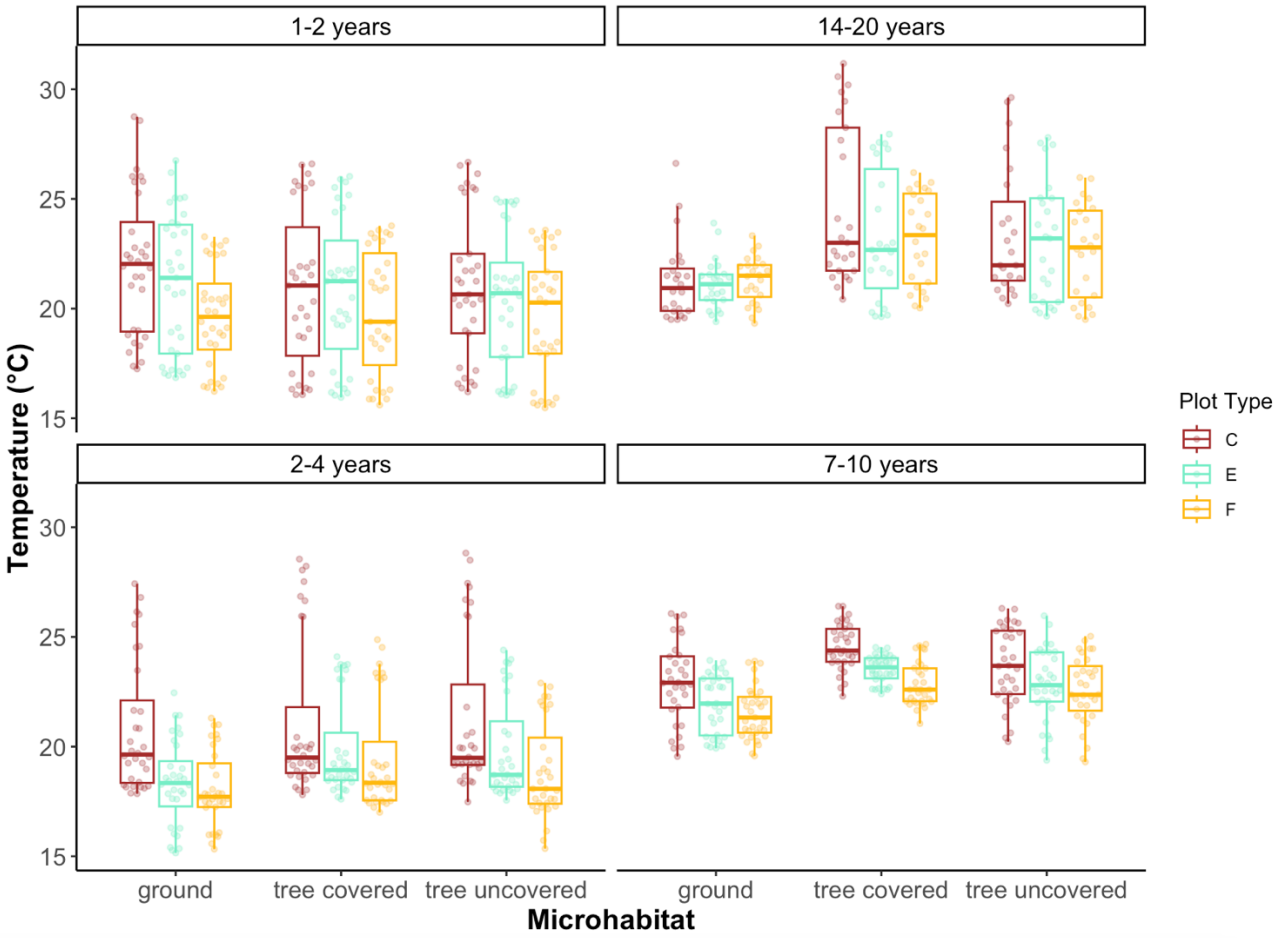

Figure 3.8 Daytime temperature differences between macrohabitats (plot types: cut, edge, and forest). Results were generated from mixed effects models with fixed effects of plot type (macrohabitat), age, microhabitat, and interactions between all three. The model was fit with random effect of date nested within site. Points indicate all raw data. Comparisons were generated from estimated marginal means of difference between microhabitat and macrohabitat interactions across age groups with Tukey adjusted p-values for multiple comparisons.

Post hoc tests for comparisons of water loss rates in microhabitats between plots during the day (e.g. uncovered cut vs. uncovered forest) demonstrated significantly higher water loss rates in cut habitats than in forested habitats in both covered and uncovered microhabitats for all ages (Table 3.5). Differences in water loss rates between cut and forests were larger for uncovered microhabitats, and the largest difference by year occurs in 1-2-year-old sites for both covered (mean difference = 4.9029 % weight lost, SE = 0.242, $p < 0.001$) and uncovered (mean difference = 5.3126 % weight lost, SE = 0.084, $p < 0.001$) microhabitats. Differences between

microhabitats diminished throughout succession but were still significant in our earliest successional stage treatment (14-20-years; Table 3.5). Water loss was significantly higher in uncovered microhabitats within habitat types (e.g. covered cut vs uncovered cut) for all age groups in both forest and clearcut habitats (Table 3.5). Differences between water loss rates in microhabitats was larger in cuts than in forests for all age groups, and differences were greatest in the most recent successional stage (1-2-year-old: mean difference = -1.67 % weight lost, SE = 0.261, $p < 0.001$), with uncovered replicas losing more water (Figure 3.9).

Table 3.5 Daytime estimated marginal means for contrasts in water loss rates for microhabitat comparisons **within** (left) and **between** (right) macrohabitat (plot) types. Results were generated from Tukey corrected least squares means on the mixed effects models for water loss in hypothesis two. "Age" indicates the time-since-cut grouping, "contrast" indicates the microhabitat and plot contrasts and direction, with "estimate" as the difference between the estimated marginal means for each term in the pairing. Significant contrasts ($p < 0.05$) are indicated in bold.

Contrasts within macrohabitats					Contrasts between macrohabitats				
Age	Contrast	Estimate	SE	p-value	Age	Contrast	Estimate	SE	p-value
1-2 years	tree covered C - tree uncovered C	**-1.670**	0.261	< 0.001	**1-2 years**	tree covered C - tree covered F	**4.903**	0.242	< 0.001
	tree covered F - tree uncovered F	**-1.260**	0.218	< 0.001		tree uncovered C - tree uncovered F	**5.313**	0.254	< 0.001
2-4 years	tree covered C - tree uncovered C	**-1.314**	0.251	< 0.001	**2-4 years**	tree covered C - tree covered F	**3.300**	0.234	< 0.001
	tree covered F - tree uncovered F	**-0.905**	0.201	< 0.001		tree uncovered C - tree uncovered F	**3.710**	0.244	< 0.001
7-10 years	tree covered C - tree uncovered C	**-1.517**	0.221	< 0.001	**7-10 years**	tree covered C - tree covered F	**1.901**	0.209	< 0.001
	tree covered F - tree uncovered F	**-1.108**	0.201	< 0.001		tree uncovered C - tree uncovered F	**2.311**	0.213	< 0.001
14-20 years	tree covered C - tree uncovered C	**-1.744**	0.249	< 0.001	**14-20 years**	tree covered C - tree covered F	**1.347**	0.236	< 0.001
	tree covered F - tree uncovered F	**-1.335**	0.231	< 0.001		tree uncovered C - tree uncovered F	**1.757**	0.244	< 0.001

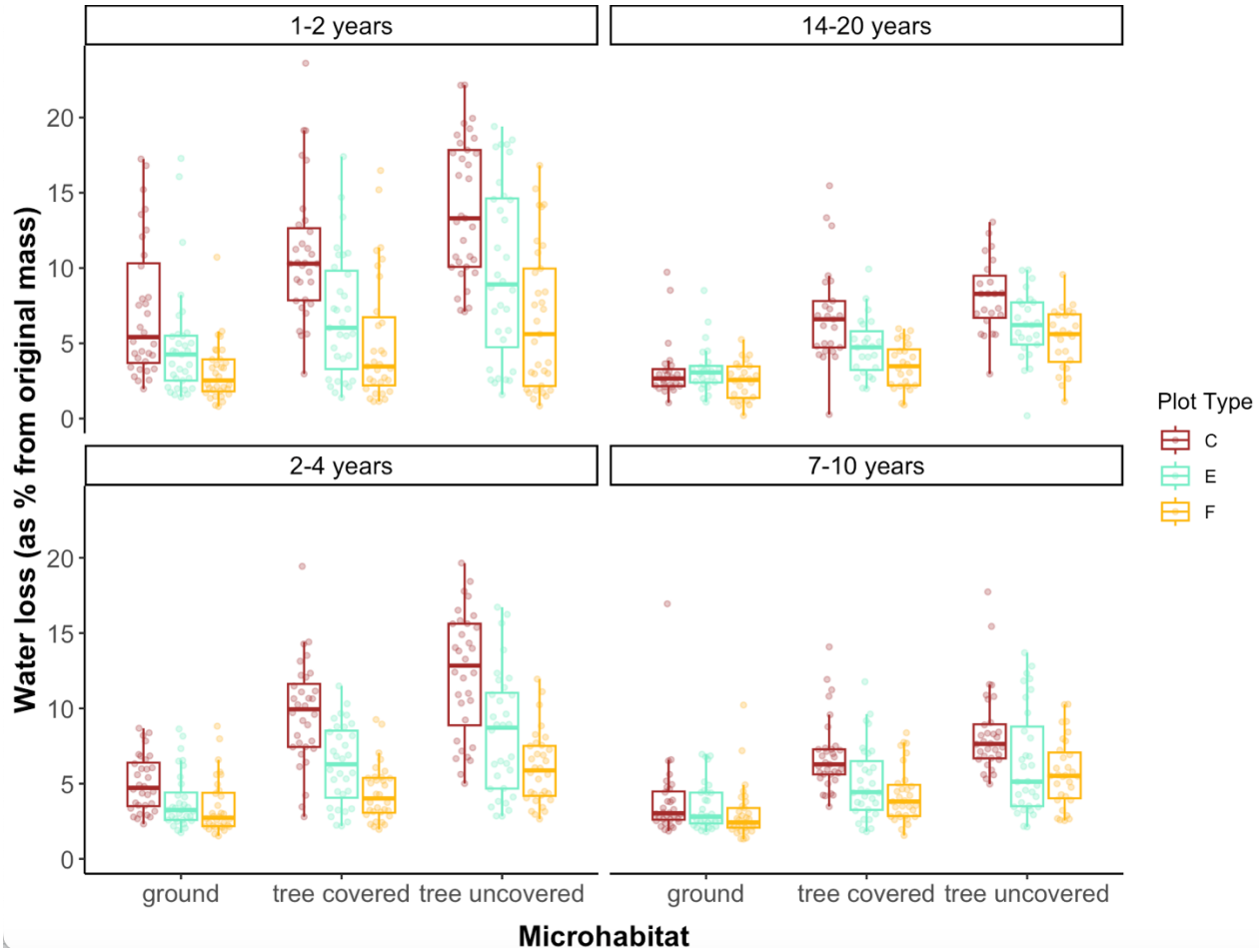

Figure 3.9 Daytime water loss differences between macrohabitats (plot types: cut, edge, and forest). Results were generated from mixed effects models with fixed effects of plot type (macrohabitat), age, microhabitat, and interactions between all three. The model was fit with random effect of date nested within site. Points indicate all raw data. Comparisons were generated from estimated marginal means of difference between microhabitat and macrohabitat interactions across age groups with Tukey adjusted p-values for multiple comparisons.

Post-hoc tests for comparisons of estimated performance in microhabitats between plots during the day (e.g. uncovered cut vs. uncovered forest) indicated significantly higher performance in cut habitats than in forested habitats in both covered and uncovered microhabitats for all ages (Table 3.6). There were no significant differences for performance in cuts between uncovered and covered microhabitats except in the 14-20-year-old cuts (Table 3.6). Between clearcuts and forests, performance was higher in both covered cut and uncovered cuts relative to covered forest and uncovered forest microhabitats (Table 3.6), and the largest

946 difference occurred in 2-4-year-old sites for both covered (mean difference = 0.0451, SE =
947 0.003, $p < 0.001$) and uncovered (mean difference = 0.0367, SE = 0.003, $p < 0.001$)
948 microhabitats. Differences between microhabitats diminished throughout succession but were
949 still significant in our earliest successional stage treatment (14-20-years-old; Table 3.6).
950 Comparisons of estimated performance in uncovered vs. covered microhabitats within
951 plots during the day (e.g. uncovered cut vs. covered cut) indicated significant differences in both
952 forest and clearcut habitats only in our earliest age treatment (14-20-years-old; Table 3.6; Figure
953 3.10). Differences in performance were greater in forests between covered and uncovered
954 microhabitats for the two earliest time-since-cut groups (14-20 years and 7-10 years), with
955 higher estimated performance in uncovered forest microhabitat (Table 3.6; Figure 3.10). There
956 were no significant differences between microhabitats within habitat types 2-4 or 1-2-year-old
957 sites (Table 3.6).
958
959
960
961
962
963
964
965
966
967
968

Table 3.6. Daytime estimated means for contrasts in performance for microhabitat comparisons **within** (left) and **between** (right) macrohabitat (plot) types. Results were generated from Tukey corrected least squares means on the mixed effects models for performance in hypothesis two. "Age" indicates the time-since-cut group, "contrast" indicates the microhabitat and plot contrasts, with "estimate" as the difference between the means for each term in the pairing. Significant contrasts ($p < 0.05$) are indicated in bold.

Contrasts within macrohabitats

Age	Contrast	Estimate	SE	p-value
1-2 years	tree covered C - tree uncovered C	0.0047	0.004	0.955
	tree covered F - tree uncovered F	-0.0037	0.003	0.965
2-4 years	tree covered C - tree uncovered C	0.0004	0.004	1.000
	tree covered F - tree uncovered F	-0.0080	0.003	0.204
7-10 years	tree covered C - tree uncovered C	-0.0106	0.004	0.071
	tree covered F - tree uncovered F	**-0.0190**	0.003	< 0.001
14-20 years	tree covered C - tree uncovered C	**-0.0167**	0.004	< 0.001
	tree covered F - tree uncovered F	**-0.0251**	0.004	< 0.001

Contrasts between macrohabitats

Age	Contrast	Estimate	SE	p-value
1-2 years	tree covered C - tree covered F	**0.0405**	0.004	< 0.001
	tree uncovered C - tree uncovered F	**0.0321**	0.004	< 0.001
2-4 years	tree covered C - tree covered F	**0.0451**	0.003	< 0.001
	tree uncovered C - tree uncovered F	**0.0367**	0.003	< 0.001
7-10 years	tree covered C - tree covered F	**0.0427**	0.003	< 0.001
	tree uncovered C - tree uncovered F	**0.0343**	0.004	< 0.001
14-20 years	tree covered C - tree covered F	**0.0259**	0.004	< 0.001
	tree uncovered C - tree uncovered F	**0.0176**	0.004	< 0.001

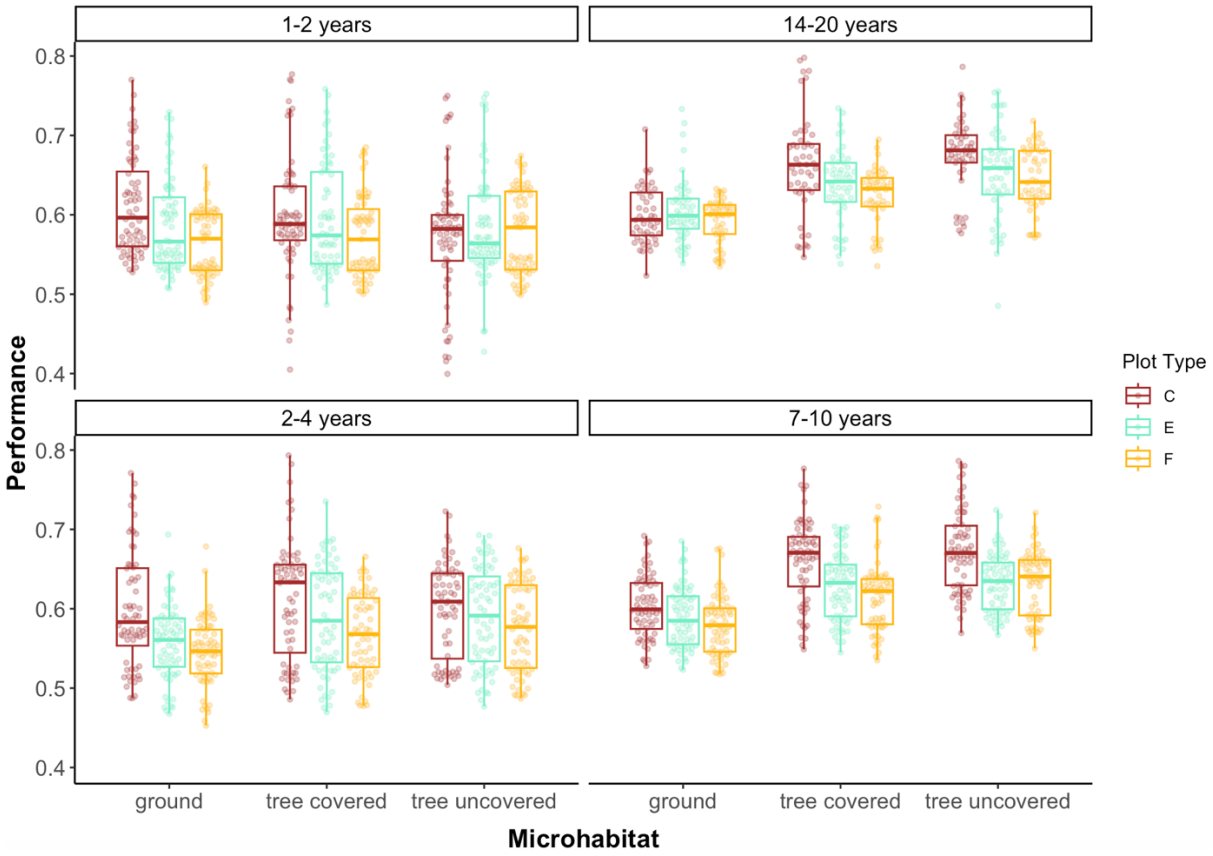

Figure 3.10 Daytime performance differences between macrohabitats (plot types: cut, edge, and forest). Results were generated from mixed effects models with fixed effects of plot type (macrohabitat), age, microhabitat, and interactions between all three. The model was fit with random effect of date nested within site. Points indicate all raw data. Comparisons were generated from estimated marginal means of difference between microhabitat and macrohabitat interactions across age groups with Tukey adjusted p-values for multiple comparisons.

3.5.2 Overnight microhabitat effects

Models fit for temperature during overnight periods revealed significant interactions between microhabitat and age and plot type with age, but no significant interaction of plot type with microhabitat (Table 3.7). Models for hydration indicated significant interactions between all response variables plot type, microhabitat, and age (Table 3.7). Models for performance indicated significant interactions between age with plot, and plot with microhabitat, but no significant interaction between age and microhabitat (Table 3.7).

Table 3.7 Models testing hypothesis two and interactions of plot and age with microhabitat for overnight data. "Df" indicates numerator degrees of freedom for each level. All estimates were generated from likelihood ratio tests and Chi-squared statistics for p-values. Significant contrasts are indicated by bold p-values.

Response	Term	Df	Chisq	p-value
Temperature	plot type	2	18.19	**<0.001**
	microhabitat	2	35.31	**<0.001**
	plot type x age	9	29.56	**0.001**
	plot type x microhabitat	4	7.72	0.102
	age x microhabitat	6	31.30	**<0.001**
Hydration	plot type	2	55.75	**<0.001**
	microhabitat	2	286.97	**<0.001**
	plot type x age	9	97.76	**<0.001**
	plot type x microhabitat	4	35.48	**<0.001**
	age x microhabitat	6	33.11	**<0.001**
Performance	plot type	2	81.63	**<0.001**
	microhabitat	2	177.68	**<0.001**
	plot type x age	9	94.78	**<0.001**
	plot type x microhabitat	4	16.90	**0.002**
	age x microhabitat	6	11.47	0.075

Post hoc tests for comparisons of microhabitat temperatures between plots overnight (e.g. uncovered cut vs. uncovered forest) demonstrated significantly lower average temperatures in cut habitats than in forested habitats in both covered and uncovered microhabitats for all ages except in covered microhabitats in 1-2-year-old sites (mean difference = -0.255 ºC, SE = 0.099, p = 0.194; Table 3.8; Figure 3.11). Differences between temperatures in cut and forests were larger for uncovered microhabitats, and the largest difference occurred in 7-10-year-old sites for both covered (mean difference = -0.713 ºC, SE = 0.119, $p < 0.001$) and uncovered (mean difference = -0.7962 ºC, SE = 0.116, $p < 0.001$) microhabitats (Table 3.8; Figure 3.11). In microhabitats

within plot types (e.g. covered cut vs. uncovered cut), covered microhabitats were significantly warmer than uncovered ones (Table 3.8). Temperature differences between microhabitats within each macrohabitat type were significantly larger in cuts than in forests and were largest in 14-20 and 2-4-year-old sites (Table 3.8; Figure 3.11).

Table 3.8 Overnight estimated marginal means for contrasts in temperature for microhabitat comparisons **within** (left) and **between** (right) macrohabitat (plot) types. Results were generated from Tukey corrected least squares means on the mixed effects models for temperature in hypothesis two. "Age" indicates the time-since-cut group, "contrast" indicates the microhabitat and plot contrasts, with "estimate" as the difference between the estimated means for each term in the pairing going from left to right. Significant contrasts ($p < 0.05$) are indicated in bold.

Contrasts within macrohabitats					Contrasts between macrohabitats				
Age	Contrast	Estimate	SE	p-value	Age	Contrast	Estimate	SE	p-value
1-2 years	tree covered C - tree uncovered C	**0.4174**	0.100	0.001	**1-2 years**	tree covered C - tree covered F	-0.255	0.099	0.194
	tree covered F - tree uncovered F	**0.3342**	0.092	0.009		tree uncovered C - tree uncovered F	**-0.338**	0.097	0.014
2-4 years	tree covered C - tree uncovered C	**0.5729**	0.106	< 0.001	**2-4 years**	tree covered C - tree covered F	**-0.553**	0.103	< 0.001
	tree covered F - tree uncovered F	**0.4897**	0.094	< 0.001		tree uncovered C - tree uncovered F	**-0.636**	0.105	< 0.001
7-10 years	tree covered C - tree uncovered C	**0.4784**	0.116	0.001	**7-10 years**	tree covered C - tree covered F	**-0.713**	0.119	< 0.001
	tree covered F - tree uncovered F	**0.3952**	0.102	0.003		tree uncovered C - tree uncovered F	**-0.796**	0.116	< 0.001
14-20 years	tree covered C - tree uncovered C	**0.5636**	0.107	< 0.001	**14-20 years**	tree covered C - tree covered F	**-0.484**	0.106	< 0.001
	tree covered F - tree uncovered F	**0.4805**	0.099	< 0.001		tree uncovered C - tree uncovered F	**-0.567**	0.104	< 0.001

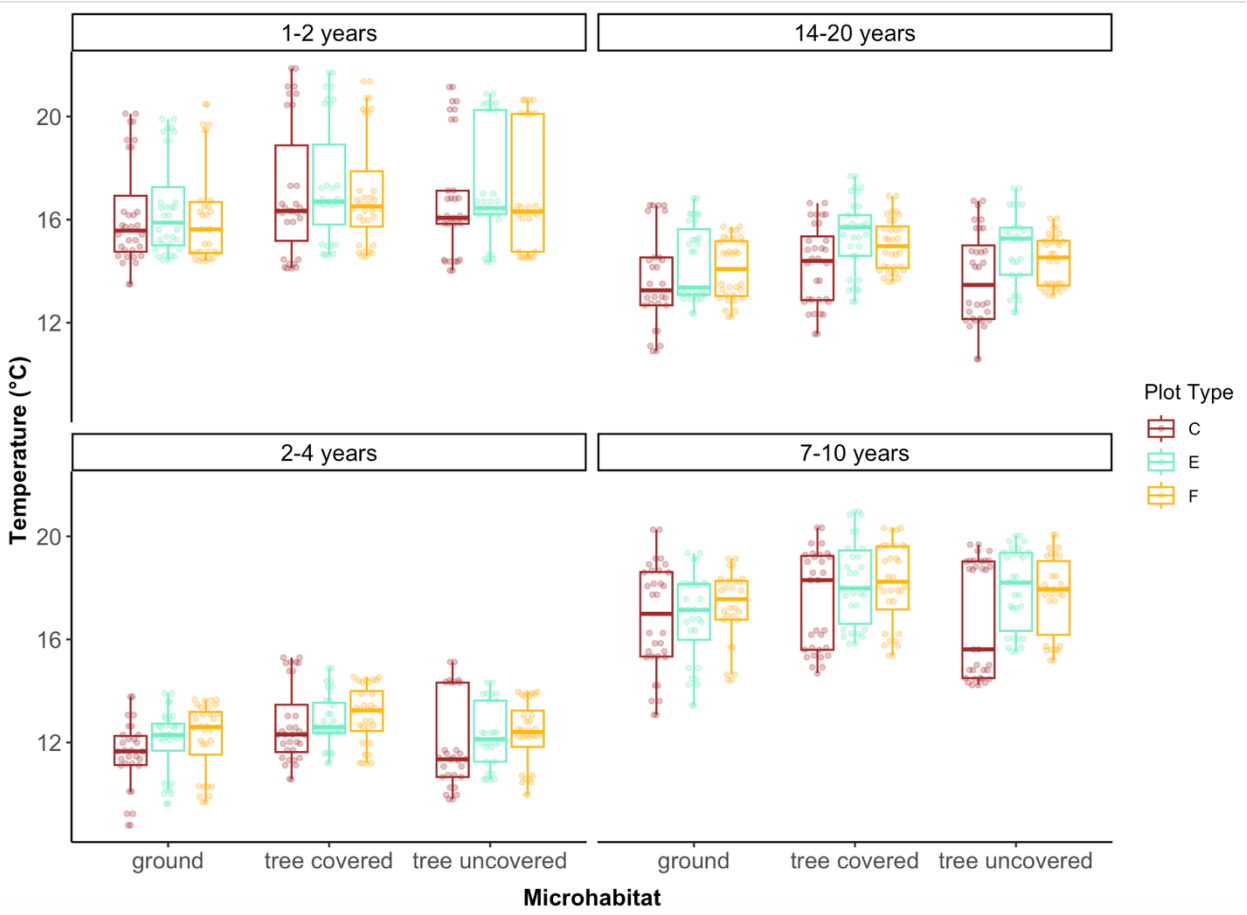

Figure 3.11 Overnight temperature differences between macrohabitats (plot types: cut, edge, and forest). Results were generated from mixed effects models with fixed effects of plot type (macrohabitat), age, microhabitat, and interactions between all three. The model was fit with random effect of date nested within site. Points indicate all raw data. Comparisons were generated from estimated marginal means of difference between microhabitat and macrohabitat interactions across age groups with Tukey adjusted p-values for multiple comparisons.

Post hoc tests for comparisons of water loss rates in microhabitats between plots overnight (e.g. uncovered cut vs. uncovered forest) indicated significantly higher water loss rates in uncovered forested habitats than in uncovered clearcut habitats for all ages except 1-2-year-old sites (Table 3.9; Figure 3.12). Water loss rates in covered cut microhabitats were significantly higher than covered forest microhabitats only in 1-2-year-old-sites (mean difference = 0.941 % weight lost, SE = 0.13, $p < 0.001$; Table 3.9), but were not significant for all other time-since-cut groups. Differences between microhabitats increased throughout succession, with

larger differences clearcut and forest microhabitats overnight in our earliest successional stage (14-20-year-old sites; Table 3.9).

Within macrohabitat types, water loss was significantly higher in uncovered microhabitats (e.g. covered cut vs uncovered cut) for all age groups in only forested habitats but were not significant for clearcuts (Table 3.9; Figure 3.12). Differences between covered and uncovered forest microhabitats were greatest in our earliest successional group, where water loss was higher in uncovered microhabitats (mean difference = -0.8828 % weight lost, SE = 0.148, $p < 0.001$; Table 3.9; Figure 3.12).

Table 3.9. Overnight estimated marginal means for contrasts in water loss for microhabitat comparisons **within** (left) and **between** (right) macrohabitat (plot) types. Results were generated from Tukey corrected least squares means on the mixed effects models for water loss in hypothesis two. "Age" indicates the time-since-cut group, "contrast" indicates the microhabitat and plot contrasts, with "estimate" as the difference between the estimated means for each term in the pairing reading from left to right in the contrast column. Significant contrasts ($p < 0.05$) are indicated in bold.

Contrasts within macrohabitats

Age	Contrast	Estimate	SE	p-value
1-2 years	tree covered C - tree uncovered C	0.1196	0.140	0.995
	tree covered F - tree uncovered F	**-0.6283**	0.129	< 0.001
2-4 years	tree covered C - tree uncovered C	0.2629	0.122	0.438
	tree covered F - tree uncovered F	**-0.4850**	0.115	< 0.001
7-10 years	tree covered C - tree uncovered C	0.2156	0.125	0.734
	tree covered F - tree uncovered F	**-0.5323**	0.124	< 0.001
14-20 years	tree covered C - tree uncovered C	-0.1349	0.153	0.994
	tree covered F - tree uncovered F	**-0.8828**	0.148	< 0.001

Contrasts between macrohabitats

Age	Contrast	Estimate	SE	p-value
1-2 years	tree covered C - tree covered F	**0.9417**	0.130	< 0.001
	tree uncovered C - tree uncovered F	0.1938	0.132	0.868
2-4 years	tree covered C - tree covered F	0.3152	0.117	0.149
	tree uncovered C - tree uncovered F	**-0.4327**	0.116	0.006
7-10 years	tree covered C - tree covered F	-0.1165	0.123	0.990
	tree uncovered C - tree uncovered F	**-0.8644**	0.125	< 0.001
14-20 years	tree covered C - tree covered F	-0.2940	0.149	0.566
	tree uncovered C - tree uncovered F	**-1.0419**	0.146	< 0.001

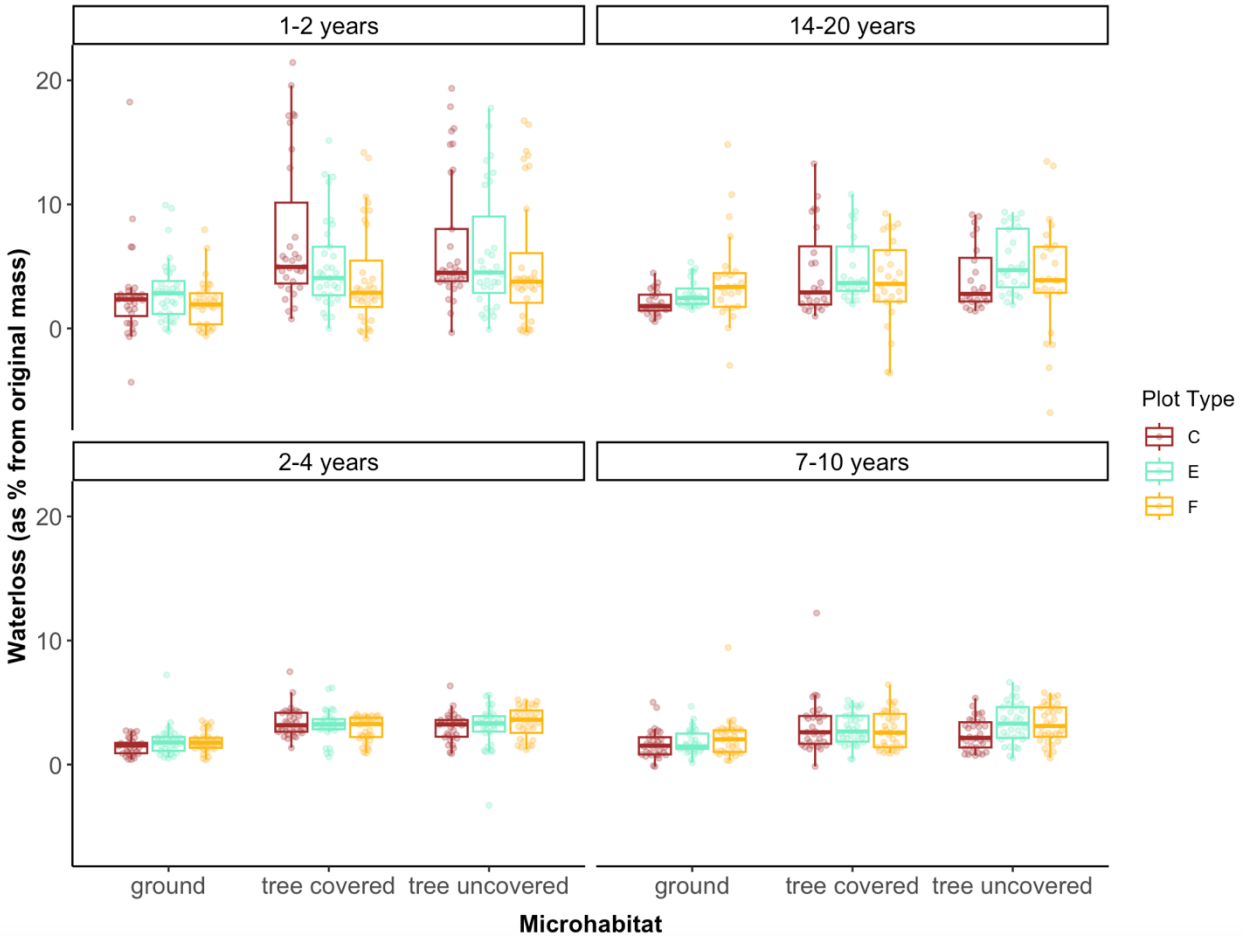

Figure 3.12 Overnight water loss differences between macrohabitats (plot types: cut, edge, and forest). Results were generated from mixed effects models with fixed effects of plot type (macrohabitat), age, microhabitat, and interactions between all three. The model was fit with random effect of date nested within site. Points indicate all raw data. Comparisons were generated from estimated marginal means of difference between microhabitat and macrohabitat interactions across age groups with Tukey adjusted p-values for multiple comparisons.

Post-hoc tests for comparisons of estimated performance in microhabitats between plots overnight (e.g. uncovered cut vs. uncovered forest) indicated significantly higher performance in forested than in clearcut habitats in both covered and uncovered microhabitats for all ages except 2-4 and 1-2-year-old cuts (Table 3.10). Performance was significantly highest in uncovered forest habitats compared with uncovered 7-10-year-old cuts (mean difference = -0.176, SE =

0.002, $p < 0.001$; Table 3.10). Performance was only higher in cuts at covered microhabitats 1-2 years old(mean difference = 0.0085, SE = 0.002, p = 0.007; Table 3.10)

Within microhabitats, performance was higher in covered microhabitats than in uncovered microhabitats for both cuts and forests (Table 3.10). Differences between microhabitats increased throughout succession but were still significant in our earliest successional stage treatment (14-20 years: Table 3.10; Figure 3.13). Differences in performance were only significant between microhabitats in clearcut habitats but not in forest habitats (Table 3.10; Figure 3.13). The largest difference between covered cuts and uncovered cut microhabitats occurred in 14-20-year-old cuts (mean difference = 0.0127, SE = 0.003, $p < 0.001$; Table 3.10).

Table 3.10 Estimated marginal means for contrasts in performance for microhabitat comparisons between habitat types overnight. Results were generated from Tukey corrected least squares means on the mixed effects models for performance in hypothesis two. "Age" indicates the successional group, "contrast" indicates the microhabitat and plot contrasts, with "estimate" as the difference between the estimated means for each term in the pairing. Significant contrasts ($p < 0.05$) are indicated in bold.

Contrasts within macrohabitats

Age	Contrast	Estimate	SE	p-value
1-2 years	tree covered C - tree uncovered C	**0.008**	0.002	0.019
	tree covered F - tree uncovered F	0.001	0.002	0.999
2-4 years	tree covered C - tree uncovered C	**0.011**	0.002	< 0.001
	tree covered F - tree uncovered F	0.005	0.002	0.450
7-10 years	tree covered C - tree uncovered C	**0.008**	0.002	0.029
	tree covered F - tree uncovered F	0.001	0.002	1.000
14-20 years	tree covered C - tree uncovered C	**0.012**	0.003	< 0.001
	tree covered F - tree uncovered F	0.006	0.002	0.340

Contrasts between macrohabitats

Age	Contrast	Estimate	SE	p-value
1-2 years	tree covered C - tree covered F	**0.008**	0.002	0.008
	tree uncovered C - tree uncovered F	0.002	0.002	0.997
2-4 years	tree covered C - tree covered F	-0.004	0.002	0.754
	tree uncovered C - tree uncovered F	**-0.010**	0.002	< 0.001
7-10 years	tree covered C - tree covered F	**-0.012**	0.002	< 0.001
	tree uncovered C - tree uncovered F	**-0.018**	0.002	< 0.001
14-20 years	tree covered C - tree covered F	**-0.009**	0.003	0.007
	tree uncovered C - tree uncovered F	**-0.016**	0.003	< 0.001

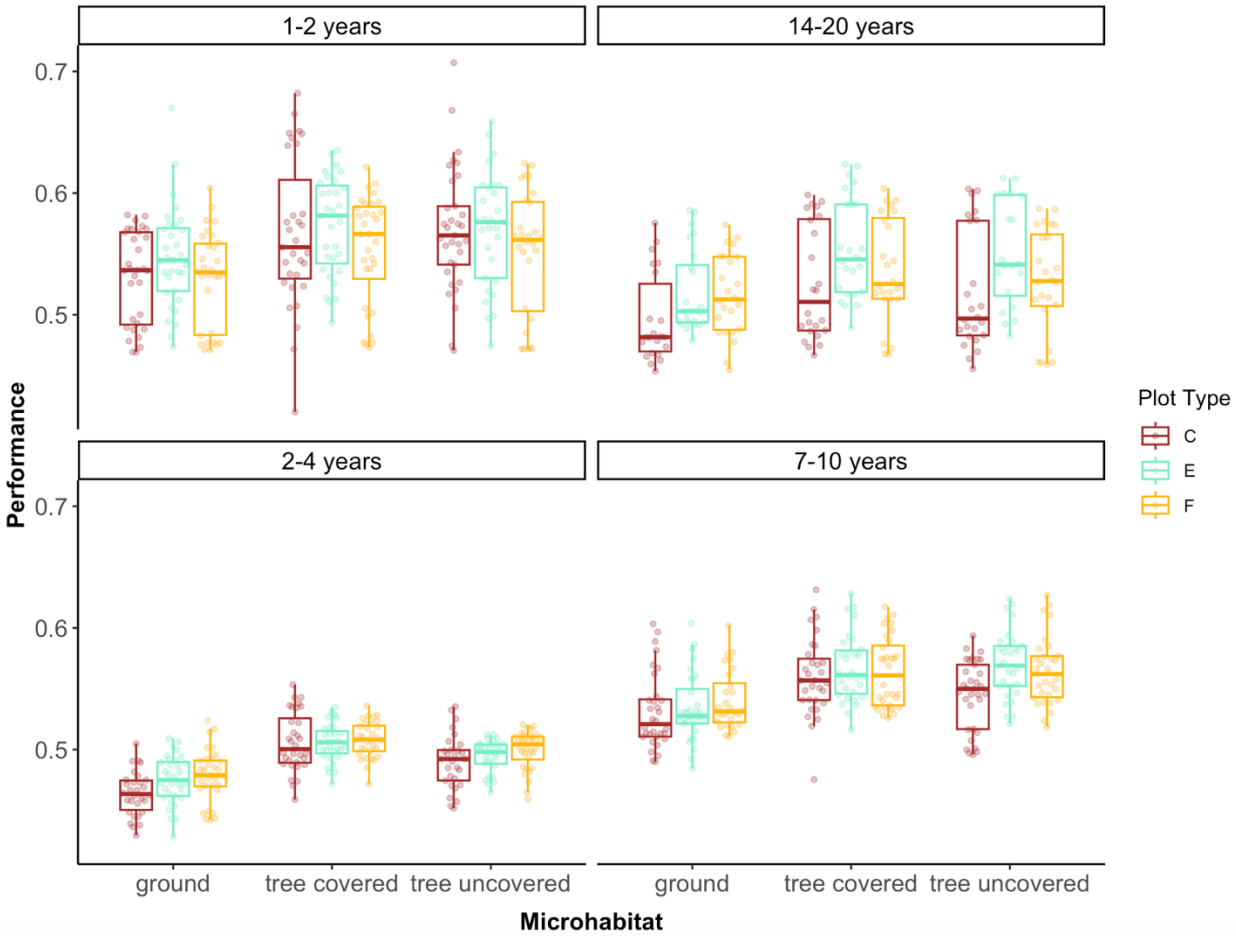

Figure 3.13 Overnight performance differences between macrohabitats (plot types: cut, edge, and forest). Results were generated from mixed effects models with fixed effects of plot type (macrohabitat), age, microhabitat, and interactions between all three. The model was fit with random effect of date nested within site. Points indicate all raw data. Comparisons were generated from estimated marginal means of difference between microhabitat and macrohabitat interactions across age groups with Tukey adjusted p-values for multiple comparisons.

3.5.3 Postural Effects

During the day, upright frogs had significantly higher performance than flat frogs for all time-since-cut groups (mean difference flat-upright = -0.00602, SE = 0.0011, $p < 0.0001$). Upright frogs lost significantly more water than flat frogs during the day across all time-since-cut groups (flat – upright mean difference = -0.00548 % weight lost, SE = 0.0692, $p < .0001$). Differences in temperature across postures were not significantly different (flat – upright mean

difference = 0.00216 ºC, SE =0.0262, p = 0.934). Posture had no significant interactions with plot type, age, or microhabitat for any of the three response variables during the day.

At night, upright frogs had significantly higher performance (flat – upright mean difference = -0.00291, SE = 0.000764, p < .0001) and water loss (flat – upright mean difference = -0.28 % weight lost,, SE = 0.0402, p < .0001) than flat frogs across all ages and plot types and water loss. There were no significant differences in average temperature (flat – upright mean difference = 0.000848 ºC, SE = 0.0252, p = 0.973). Posture had no significant interactions with plot type, age, or microhabitat for any of the three response variables at night.

4 DISCUSSION

4.1 Diminished Performance in Clearcuts Overnight

Clearcuts provide warmer daytime conditions that align with higher gray treefrog performance, but this is offset by reduced structural complexity that accelerates evaporative water loss. However, at night when gray treefrogs are most active, performance is reduced in clearcut microhabitats, while forests maintain more stable overnight environments that support higher physiological performance, a result that is consistent with my second hypothesis. This reflects the colder nighttime temperatures in clearcuts, which approach lower thermal limits (Figure 3.7:C), imposing cold stress that reduces physiological function (M. E. Feder & Hofmann, 1999; Schmidt et al., 2024).

At night, despite greater overstory cover, gray treefrogs in forests actually experience higher water loss than in clearcuts. This increased dehydration likely results from the interaction of temperature, vapor pressure deficit (VPD), and vegetation structure where my replicas were placed (~ 2 m from the ground). Forests retain more heat at night but often have lower relative humidity under the canopy—especially in older-growth stands with large gaps and heightened

exposure to drying winds (De Frenne et al., 2013). Increased airflow in these forests may disrupt boundary layers around frogs and enhance evaporative water loss. In contrast, clearcuts experience radiative cooling, lowering air temperatures and reducing the atmosphere's moisture-holding capacity (Chen et al., 1993). This often brings relative humidity closer to dew point and slows evaporation (De Frenne et al., 2013). Mid-successional clearcuts (10–20 years post-harvest) were observed to have dense shrub and deciduous regrowth, which restricts vertical air movement and traps humid, still air. These conditions promote thicker boundary layers and reduce evaporation, offering some buffer against dehydration despite being more exposed than closed-canopy forests (Peterman et al., 2013; Peterman & Semlitsch, 2014; Rittenhouse et al., 2008).

Although nighttime water loss was greater in forests than clearcuts, performance was estimated to be higher in forests because overall water loss rates were too low to negatively influence performance in either forests or clearcuts. Since water loss rates do not reach critical thresholds overnight, performance is highly dependent on temperature in nighttime microhabitats and the small hydric benefit in clearcuts is offset by lower nighttime temperatures. At colder temperatures, performance may be reduced regardless of hydration state (Figure 3.4; (H. John-Alder et al., 1988; H. B. John-Alder et al., 1989; Navas, 1996). This suggests that although clearcut microhabitats may reduce overnight water loss, the benefit is negligible because frogs are already performance-limited by cold. Impaired performance in clearcuts at night will be enhanced because nighttime (and daytime) performance was lower in uncovered microhabitats and in upright (rather than water conservation) postures. Nocturnal gray treefrogs face a decision during peak activity hours between remaining inactive under thermally favourable cover to reduce physiological stress and emerging into colder, exposed microhabitats to forage and

replenish energy reserves. While amphibians often perform under various hydration and temperature states that do not maximize performance (Anderson & Andrade, 2017; Martin & Huey, 2008; A. Mitchell & Bergmann, 2016; Payne et al., 2015), if environmental temperatures consistently deviate from species' thermal optima, performance capacities such as locomotion, foraging efficiency, predator escape, and reproductive output can decline (Huey et al., 2009; Navas et al., 2016). My results indicate that this decision comes with greater costs in clearcut habitats, where reduced performance will make key activities, like foraging, more costly than in forested environments where overall performance is higher.

4.2 Beneficially heightened daytime temperatures render frogs more vulnerable to desiccation

Water loss, temperature, and performance were all higher in clearcuts than in forests during the day (Table 3.4, Table 3.5, Table 3.6). These results are consistent with previous research demonstrating elevated daytime temperatures and increased evaporative water loss in open-canopy habitats that receive more direct solar radiation (De Frenne et al., 2019; Perez-Navarro et al., 2024; Richard et al., 2021). In contrast to the lower performance observed overnight in clearcuts driven by thermal stress under colder conditions, gray treefrogs may benefit from increased daytime temperatures over relatively short periods of time (4 hours). These performance benefits may be of little ecological relevance since gray treefrogs are predominantly nocturnal and thus most likely to be inactive, in sheltered refuges, during the day. However, even in sheltered refuges, and while adopting water-conservation posture (Anderson & Andrade, 2017; Tracy et al., 2010), inactive frogs will experience greater water loss in clearcuts and thus may need to leave these refuges to rehydrate, incurring costs through increased energy expenditure and increased predation risk that are not present in forested refugia (Rittenhouse et

al., 2009). Moreover, exposure of inactive frogs to higher temperatures in clearcuts while sheltering can elevate metabolic rates and thus induce greater energetic expenditure during inactivity compared to cooler forest refugia, necessitating greater energy acquisition at night (Rollins-Smith & Le Sage, 2023).

It is possible that treefrogs could shift their activity time to take advantage of higher performance in daytime clearcuts, analogous to how some species have altered activity times in response to climate change (Doody et al., 2019; Sinervo et al., 2010). However, the benefits of such a shift may be lower than my results suggest because the full physiological consequences of daytime conditions may not be captured within my four-hour sampling period. The advantage of higher performance depends on dehydration levels not exceeding 15-20%, after which performance declines (Figure 3.4); these thresholds are consistent with those found for other species (Anderson & Andrade, 2017; Greenberg & Palen, 2021). This threshold is likely to be surpassed under continued exposure to elevated clearcut temperatures in high latitude areas with long summer daylight periods, especially because treefrogs may actively increase evaporative water loss to mitigate thermal stress through evaporative cooling when body temperatures rise (Sunday et al., 2014; Tracy et al., 2010, 2014) elevating dehydration risk even in shaded or vegetated microhabitats (Spotila et al., 1992; Tracy, 1976). In the most recent clearcuts (<5 years old), water loss levels reached 20–30% during the four-hour daytime window, resulting in the lowest observed performances in clearcuts across all time-since-cut groups. Therefore, unless gray treefrogs can access sufficient water to rehydrate throughout the day, performance will eventually decline in cuts due to excessive dehydration, rendering them less physiological suitable than forests.

Gray treefrogs may be able to behaviourally buffer negative performance effects of clearcuts by seeking out favourable refugia for hydrothermal regulation. At night, this would mean seeking out covered microhabitats for their warmth, while during the day it would rely on finding water sources for rehydration. At night, covered microhabitats in clearcuts were consistently warmer than uncovered microhabitats across all successional stages (Table 3.8) and therefore provide buffering from decreased temperature stress in exposed clearcuts. This means treefrogs face a decision during peak activity hours between remaining inactive under thermally stable cover to reduce physiological stress or emerging into colder, exposed microhabitats to forage and replenish energy reserves from heightened metabolic activity during the day. A lack of humid, daytime, refugia will render frogs more vulnerable to desiccation if temperatures and water loss levels exceed or near individual limits regardless of their activity levels (Cline & Hunter, 2014; Roznik et al., 2018). The abundance and configuration, i.e. accessibility, of refugia substantially influence the effectiveness, and energetic costs of thermoregulation (Sears et al., 2016; Sears & Angilletta, 2015). While there are no existing data on the availability of hydrothermal refugia in clearcuts, it is well established that they are hotter and drier during the day (Chen et al., 1993; Hocking & Semlitsch, 2008), suggesting that such refugia are likely to be few and far between, a situation that could be heightened by increased periods of drought under ongoing climate change (Soltani et al., 2024; Zhang et al., 2021). Even within clearcuts from 1-14-years-old, refugia may not diminish the thermal stresses of elevated daytime temperatures (Table 3.4). Therefore, frogs may still need to thermoregulate due to temperatures increases within clearcut microhabitats (Scheffers et al., 2013) through evaporative cooling and could be at risk for desiccation despite being covered and inactive.

4.3 Long-term persistence of clearcutting effects

The effects of harvesting on gray treefrog temperature, water loss and performance were still evident after 20 years post-harvest (Figure 3.7; Figure 3.6). The trajectory of post-harvest succession diverges markedly from that of undisturbed forest stands, not only in tree species composition but also in vertical structure and microclimatic buffering (Chen et al., 1993). These differences are particularly relevant given that structural recovery of microhabitats critical for many amphibian species may take over 20 years to establish (Figure 3.7). While some vegetative cover returns rapidly, the transition toward structural and compositional maturity in boreal forests can take between 50-60 years post-clearcut, and full ecological recovery may exceed 60 years depending on disturbance intensity and landscape context (Brassard & and Chen, 2006; Cyr et al., 2009). Given treefrogs relatively short (5-7 year) lifespans compared to microhabitat recovery periods (20+ years), clearcutting could threaten persistence of forest-dwelling biphasic frog populations by causing long-term reductions in the quantity and quality of suitable microhabitat conditions and by reducing landscape connectivity and permeability (Becker et al., 2007; Harper et al., 2008; Semlitsch, 2000) over multiple generations. Long-term effects of clearcutting could lead to reduced amphibian richness and abundance by increasing mortality, promoting evacuation of clearcut habitats, and declines in abundance (deMaynadier & Hunter Jr., 1995; Harper et al., 2015; Semlitsch et al., 2009; Todd et al., 2009; Todd & Rothermel, 2006). Importantly, juvenile dispersal is significantly hindered in early successional or structurally simplified habitats (Patrick et al., 2006). Without immediate recovery of microhabitat spaces, or following years of consecutive dry periods and warmer temperatures, recruitment could be suppressed over multiple generations and shorter-lived species may have no opportunities to recover (Harper et al., 2015).

Additionally, altered habitat quality may lead to overcrowding in smaller forest patches if individuals were unwilling to occupy cleared habitats. This could intensify competition for food and shelter, increase stress and predation risk, and limit energy intake (Veysey Powell & Babbitt, 2015). Energetic constraints could reduce investment in growth, reproduction, and storage, resulting in poorer body condition and smaller adult size across generations (Janin et al., 2011; Veysey Powell & Babbitt, 2015). Collectively, such energetic and demographic constraints can compound population declines in harvested landscapes

The retention of negative performance impacts through succession may also impact metapopulation dynamics by making it more costly to move through the landscape to reach favourable forest patches or edges. Moving through areas where locomotory performance is lower will have greater energetic costs (Harper et al., 2015; Patrick et al., 2006; Rittenhouse et al., 2009; Todd et al., 2009), making dispersal to forest patches more challenging. These effects will be compounded by greater exposure to predation through increased movement frequency, and frogs' own reluctance to cross, more open habitats (Joly et al., 2003; Popescu & Hunter, 2011; Rittenhouse et al., 2009). There is also the potential for synergistic effects where not only may dispersing frogs be more detectable to predators in early successional habitats, but will also have reduced escape ability due to impaired locomotory performance. This increase in landscape resistance may also operate on more micro-scales, increasing the cost of seeking out hydrothermal refugia in successional forest. Together, these constraints may hinder both long-distance dispersal between forest patches and fine-scale movements toward microhabitats offering thermal and hydric refuge, ultimately reducing recolonization rates**,** increasing local extirpation risk, and weakening overall metapopulation connectivity.

Current forest management guidelines in Ontario prioritize connectivity and habitat retention primarily for large mammals like moose and caribou (OMNRF, 2019), often overlooking the fine-scale requirements of smaller taxa with more constrained population ranges. While the OMNRF reports differences of opinion on the importance of landscape pattern versus habitat amount for biodiversity conservation, small-bodied or low-mobility species (like amphibians) are under-represented in the studies cited by OMNRF, even though they may respond differently to landscape pattern due to limited dispersal. Given the vulnerability of even disturbance-resistance amphibians like the gray treefrog to dehydration and thermal extremes (Demaynadier & Hunter, 1998; Harper et al., 2005), maintaining functional corridors of shaded, humid habitat between remnant patches and intact forests is essential for facilitating movement, recolonization, and genetic exchange (see Kuuluvainen, 2009; Kuuluvainen et al., 2021). Therefore, sustainable harvesting practices should consider not only the timing and intensity of silvicultural interventions but also the spatial configuration of harvested and retained areas. Incorporating connectivity planning for a broader range of taxa, especially small vertebrates and invertebrates, will improve the ecological integrity and resilience of regenerating forest landscapes.

4.4 Limitations and assumptions

My results come with several caveats. Firstly, I estimated the performance of gray treefrogs within microhabitats based on measurements of performance in the lab. However, these measures may not accurately capture hydrothermal performance relationships in the field. Additionally conditions that maximize performance may not be preferred conditions in the field (Martin & Huey, 2008; A. Mitchell & Bergmann, 2016). My results demonstrate the *capacity* for performance in relevant microhabitats frogs may encounter in the Boreal Forest transition zone.

However, frogs are subject to various other physiological and ecological considerations that may influence their behaviour and habitat use (Navas et al., 2021). They therefore need to make decisions about conserving energy versus expending energy for activities like foraging, predator avoidance, and hydrothermal-regulation. Frogs in drier and warmer habitats may sacrifice peak locomotor performance (needed for escaping predators or foraging) to reduce dehydration risk (A. Mitchell & Bergmann, 2016). There remains a critical gap in empirical assessments of how and when species prioritize one regulatory mechanism over the other, especially under seasonal or anthropogenically altered conditions where hydrothermal environments are shifting in opposing directions(Gunderson & Stillman, 2015; Navas et al., 2008, 2021). Further, I could not feasibly assess whether acclimation may alter hydrothermal performance curves (Schulte et al., 2011) and thus alter estimates of performance capacity across macro and microhabitats.

My sampling was also restricted in two important ways. First, it largely captures conditions in the mid-story. Most previous research on temperature and water loss has focused on ground-level microhabitats for terrestrial amphibians (Keppel et al., 2017), but for treefrogs conditions in the canopy are likely to be important (Olson et al., 2023)**.** To capture all conditions that gray treefrogs may be facing, future work should explore microclimatic conditions in the mid to upper canopy, where treefrogs may exploit warmer air layers (Johnson et al., 2008; Laughlin et al., 2017; Olson et al., 2023). Measurements taken at a single level likely underestimate the buffering effects of mid-successional vegetation, especially above two meters where boundary layer dynamics and humidity conditions may differ from conditions in the mid to upper canopy layers. It also ignores the potential for vertical movement to allow for hydrothermal buffering (Klinges et al., 2024; Scheffers et al., 2013). Secondly, my sample was entirely male (because of practical limitations on finding females in the field), and past research

indicates that male and female performance may differ under similar physiological conditions due males' smaller body-size, which has been shown to influence metabolic rates, thermal inertia, and performance due to differences in optimal body temperatures (Kingsolver & Huey, 2008; Pottier et al., 2021; Rohr et al., 2018). This underscores the importance of understanding sex specific physiological and behavioral adaptations to predict responses to habitat alterations.

Finally, while my findings show that treefrogs have reduced performance in clearcuts and that these effects are sustained across multiple decades of succession, I do not have evidence that these performance impairments have implications at broader ecological scales, specifically population dynamics. Few studies of thermal vulnerability make this link (Gunderson & Stillman, 2015), but Sinervo et al. 2010 showed that a model in which degradation of thermal environments resulted in individuals behaviorally minimizing exposure to high daytime temperatures by reducing activity, could predict population declines and persistence. The limited research available on physiological costs in clearcut environments have identified reduced amphibian survival and body conditions (Mazerolle et al., 2021; Rittenhouse et al., 2009; Todd et al., 2014; Veysey Powell & Babbitt, 2015), suggesting that the performance costs associated with clearcutting we observed for gray treefrogs in the boreal-transition zone could plausibly influence population abundance and persistence.

5 CONCLUSION

While clearcuts may offer short-term thermal advantages during the day that align with the thermal optima of gray treefrogs, these benefits are counteracted by elevated evaporative water loss due to increased exposure and lack of hydrothermally preferrable refugia. At night, when gray treefrogs are most active, performance capacity is consistently lower in clearcut environments, with forests providing more stable microclimates that better support physiological

function. These microclimatic effects persist even two decades post-harvest, underscoring the long-term physiological costs of clearcutting in forest ecosystems. While climate change alters average conditions over large spatial and temporal scales, habitat modification can produce abrupt and localized microclimatic extremes that directly impact physiological function. These structural changes often go unrecognized in assessments of amphibian vulnerability, despite their potent effects on individual performance and behavioral flexibility. My results highlight the need to incorporate the joint effects of temperature and hydration on microhabitat quality and physiological performance into conservation assessments. Future work should focus on long-term, multi-generational studies of amphibian population recovery in repeatedly disturbed or slowly regenerating forests. While some research has examined amphibian presence across forest age classes (e.g., Patrick et al., 2006; Harper et al., 2015), most have examined abundance immediately post-disturbance, but few have followed population recovery trajectories over time through forest recovery, limiting our understanding of how chronic habitat degradation influences long-term population persistence and dispersal.

6 REFERENCES

Anderson, R. C. O., & Andrade, D. V. (2017). Trading heat and hops for water: Dehydration effects on locomotor performance, thermal limits, and thermoregulatory behavior of a terrestrial toad. *Ecology and Evolution*, *7*(21), 9066–9075. https://doi.org/10.1002/ece3.3219

Angilletta, M. J. (2006). Estimating and comparing thermal performance curves. *Journal of Thermal Biology*, *31*(7), 541–545. https://doi.org/10.1016/j.jtherbio.2006.06.002

Angilletta, M. J. (2009). *Thermal adaptation: A theoretical and empirical synthesis*. Oxford University Press.

Anoszko, E., Frelich, L. E., Rich, R. L., & Reich, P. B. (2022). Wind and fire: Rapid shifts in tree community composition following multiple disturbances in the southern boreal forest. *Ecosphere*, *13*(3), e3952. https://doi.org/10.1002/ecs2.3952

Anyomi, K. A., Neary, B., Chen, J., & Mayor, S. J. (2022). A critical review of successional dynamics in boreal forests of North America. *Environmental Reviews*, *30*(4), 563–594. https://doi.org/10.1139/er-2021-0106

Ashrafi, R., Bruneaux, M., Sundberg, L., Pulkkinen, K., Valkonen, J., & Ketola, T. (2018). Broad thermal tolerance is negatively correlated with virulence in an opportunistic bacterial pathogen. *Evolutionary Applications*, *11*(9), 1700–1714. https://doi.org/10.1111/eva.12673

Becker, C. G., Fonseca, C. R., Haddad, C. F. B., Batista, R. F., & Prado, P. I. (2007). Habitat Split and the Global Decline of Amphibians. *Science*, *318*(5857), 1775–1777. https://doi.org/10.1126/science.1149374

Bennett, A. F. (1978). Activity Metabolism of the Lower Vertebrates. *Annual Review of Physiology*, *40*(Volume 40, 1978), 447–469. https://doi.org/10.1146/annurev.ph.40.030178.002311

Bergeron, Y., & Fenton, N. J. (2012). Boreal forests of eastern Canada revisited: Old growth, nonfire disturbances, forest succession, and biodiversity. *Botany*, *90*(6), 509–523. https://doi.org/10.1139/b2012-034

Bergeron, Y., Harvey, B., Leduc, A., & Gauthier, S. (1999). Forest management guidelines based on natural disturbance dynamics: Stand- and forest-level considerations. *The Forestry Chronicle*, *75*(1), 49–54. https://doi.org/10.5558/tfc75049-1

Biazzo, I., & Quintana-Ascencio, P. (2022). Canopies, the Final Frog-tier: Exploring responses of a specialist treefrog to prescribed fire in a pyrogenic ecosystem. *FIRE ECOLOGY*, *18*(1). https://doi.org/10.1186/s42408-022-00148-1

Boucher, Y., St-Laurent, M.-H., & Grondin, P. (2011). Logging-Induced Edge and Configuration of Old-Growth Forest Remnants in the Eastern North American Boreal Forests. *Natural Areas Journal*, *31*(3), 300–306. https://doi.org/10.3375/043.031.0313

Brandt, J. P., Flannigan, M. D., Maynard, D. G., Thompson, I. D., & Volney, W. J. A. (2013). An introduction to Canada's boreal zone: Ecosystem processes, health, sustainability, and environmental issues. *Environmental Reviews*, *21*(4), 207–226. https://doi.org/10.1139/er-2013-0040

Brassard, B. W., & and Chen, H. Y. H. (2006). Stand Structural Dynamics of North American Boreal Forests. *Critical Reviews in Plant Sciences*, *25*(2), 115–137. https://doi.org/10.1080/07352680500348857

Briere, J.-F., Pracros, P., Le Roux, A.-Y., & Pierre, J.-S. (1999). A Novel Rate Model of Temperature-Dependent Development for Arthropods. *Environmental Entomology*, *28*(1), 22–29. https://doi.org/10.1093/ee/28.1.22

Brooks, M. E., Kristensen, K., Benthem, K. V. J., Magnusson, A., Berg, C. W., Nielsen, A., Skaug, H. J., Maechler, M., & Bolker, B. M. (2017). glmmTMB Balances Speed and Flexibility Among Packages for Zero-inflated Generalized Linear Mixed Modeling. *The R Journal*, *9*(2), 378–400. https://doi.org/10.32614/RJ-2017-066.

Burnham, K. P., & Anderson, D. R. (Eds.). (2004). *Model Selection and Multimodel Inference*. Springer. https://doi.org/10.1007/b97636

Burrow, A. K., McEntire, K. D., & Maerz, J. C. (2023). Estimating the potential drivers of dispersal outcomes for juvenile gopher frogs (Rana capito) using agent-based models. *Frontiers in Ecology and Evolution*, *11*, 1026541. https://doi.org/10.3389/fevo.2023.1026541

Campbell, G. S., & Norman, J. M. (1998). *An introduction to environmental biophysics*. Springer Science and Business Media Inc.

Carleton, T. J., & Maclellan, P. (1994). Woody vegetation responses to fire versus clear-cutting logging: A comparative survey in the central Canadian boreal forest. *Écoscience*, *1*(2), 141–152. https://doi.org/10.1080/11956860.1994.11682238

Chen, J. (1999). Microclimate in Forest Ecosystem and Landscape Ecology. *BioScience*, *49*, 288–297.

Chen, J., Franklin, J. F., & Spies, T. A. (1993). Contrasting microclimates among clearcut,edge, and interior of old-growth Douglas-fir forest. *Agricultural and Forest Meteorology*, *63*, 219–237.

Cline, B. B., & Hunter, M. L. (2014). Different open-canopy vegetation types affect matrix permeability for a dispersing forest amphibian. *Journal of Applied Ecology*, *51*(2), 319–329. https://doi.org/10.1111/1365-2664.12197

Cossins, A. (2012). *Temperature Biology of Animals*. Springer Science & Business Media.

Crins, W. J., Gray, P. A., Uhlig, P. W. C., & Wester, M. C. (2024). *The Ecosystems of Ontario, Part 1: Ecozones and Ecoregions*.

Cyr, D., Gauthier, S., Bergeron, Y., & Carcaillet, C. (2009). Forest management is driving the eastern North American boreal forest outside its natural range of variability. *Frontiers in Ecology and the Environment*, *7*(10), 519–524. https://doi.org/10.1890/080088

Damos, P. T., & Savopoulou-Soultani, M. (2008). Temperature-dependent bionomics and modeling of Anarsia lineatella (Lepidoptera: Gelechiidae) in the laboratory. *Journal of Economic Entomology*, *101*(5), 1557–1567. https://doi.org/10.1603/0022-0493(2008)101[1557:tbamoa]2.0.co;2

Dawe, D. A., Parisien, M.-A., Van Dongen, A., & Whitman, E. (2022). Initial succession after wildfire in dry boreal forests of northwestern North America. *Plant Ecology*, *223*(7), 789–809. https://doi.org/10.1007/s11258-022-01237-6

De Frenne, P., Rodríguez-Sánchez, F., Coomes, D. A., Baeten, L., Verstraeten, G., Vellend, M., Bernhardt-Römermann, M., Brown, C. D., Brunet, J., Cornelis, J., Decocq, G. M., Dierschke, H., Eriksson, O., Gilliam, F. S., Hédl, R., Heinken, T., Hermy, M., Hommel, P., Jenkins, M. A., … Verheyen, K. (2013). Microclimate moderates plant responses to macroclimate warming. *Proceedings of the National Academy of Sciences of the United States of America*, *110*(46), 18561–18565. https://doi.org/10.1073/pnas.1311190110

De Frenne, P., Zellweger, F., Rodríguez-Sánchez, F., Scheffers, B. R., Hylander, K., Luoto, M., Vellend, M., Verheyen, K., & Lenoir, J. (2019). Global buffering of temperatures under forest canopies. *Nature Ecology & Evolution*, *3*(5), 744–749. https://doi.org/10.1038/s41559-019-0842-1

deMaynadier, P. G., & Hunter Jr., M. L. (1995). The relationship between forest management and amphibian ecology: A review of the North American literature. *Environmental Reviews*, *3*(3–4), 230–261. https://doi.org/10.1139/a95-012

Demaynadier, P. G., & Hunter, M. L. (1998). Effects of Silvicultural Edges on the Distribution and Abundance of Amphibians in Maine. *Conservation Biology*, *12*(2), 340–352. https://doi.org/10.1111/j.1523-1739.1998.96412.x

Deutsch, C. A. (2008). Impacts of climate warming on terrestrial ectotherms across latitude. *Proceedings of the National Academy of Sciences, U.S.A*, *105*, 6668–6672.

Dobrowski, S. Z. (2011). A climatic basis for microrefugia: The influence of terrain on climate. *Global Change Biology*, *17*(2), 1022–1035. https://doi.org/10.1111/j.1365-2486.2010.02263.x

Dodd, C. K. (2013). *Frogs of the United States and Canada*.

Doody, J. S., McHenry, C. R., Rhind, D., & Clulow, S. (2019). Novel habitat causes a shift to diurnal activity in a nocturnal species. *Scientific Reports*, *9*(1), 230. https://doi.org/10.1038/s41598-018-36384-2

Dormann, C. F., Calabrese, J. M., Guillera-Arroita, G., Matechou, E., Bahn, V., Bartoń, K., Beale, C. M., Ciuti, S., Elith, J., Gerstner, K., Guelat, J., Keil, P., Lahoz-Monfort, J. J., Pollock, L. J., Reineking, B., Roberts, D. R., Schröder, B., Thuiller, W., Warton, D. I., … Hartig, F. (2018). Model averaging in ecology: A review of Bayesian, information-

theoretic, and tactical approaches for predictive inference. *Ecological Monographs*, *88*(4), 485–504. https://doi.org/10.1002/ecm.1309

Duarte, H., Tejedo, M., Katzenberger, M., Marangoni, F., Baldo, D., Beltrán, J. F., Martí, D. A., Richter-Boix, A., & Gonzalez-Voyer, A. (2012). Can amphibians take the heat? Vulnerability to climate warming in subtropical and temperate larval amphibian communities. *Global Change Biology*, *18*(2), 412–421. https://doi.org/10.1111/j.1365-2486.2011.02518.x

Dupuch, A., & Fortin, D. (2013). The extent of edge effects increases during post-harvesting forest succession. *Biological Conservation*, *162*, 9–16. https://doi.org/10.1016/j.biocon.2013.03.023

Economou, L., & Kontodimas, D. (2004). Comparative Temperature-Dependent Development of Nephus includens (Kirsch) and Nephus bisignatus (Boheman) (Coleoptera: Coccinellidae) Preying on Planococcus citri (Risso) (Homoptera: Pseudococcidae): Evaluation of a Linear and Various Nonlinear Models Using Specific Criteria. *Environmental Entomology*. https://www.academia.edu/20568703/Comparative_Temperature_Dependent_Development_of_Nephus_includens_Kirsch_and_Nephus_bisignatus_Boheman_Coleoptera_Coccinellidae_Preying_on_Planococcus_citri_Risso_Homoptera_Pseudococcidae_Evaluation_of_a_Linear_and_Various_Nonlinear_Models_Using_Specific_Criteria

Elith, J., & Leathwick, J. R. (2009). Species Distribution Models: Ecological Explanation and Prediction Across Space and Time. *Annual Review of Ecology, Evolution, and Systematics*, *40*(Volume 40, 2009), 677–697. https://doi.org/10.1146/annurev.ecolsys.110308.120159

1478 Eubank, W. P., Atmar, J. W., & Ellington, J. J. (1973). The Significance and Thermodynamics of
1479 Fluctuating Versus Static Thermal Environments on Heliothis zea Egg Development
1480 Rates 1. *Environmental Entomology*, *2*(4), 491–496. https://doi.org/10.1093/ee/2.4.491
1481 Feder, M. E., & Hofmann, G. E. (1999). HEAT-SHOCK PROTEINS, MOLECULAR
1482 CHAPERONES, AND THE STRESS RESPONSE: Evolutionary and Ecological
1483 Physiology. *Annual Review of Physiology*, *61*(Volume 61, 1999), 243–282.
1484 https://doi.org/10.1146/annurev.physiol.61.1.243
1485 Fenton, N. J., Simard, M., & Bergeron, Y. (2009). Emulating natural disturbances: The role of
1486 silviculture in creating even-aged and complex structures in the black spruce boreal forest
1487 of eastern North America. *Journal of Forest Research*, *14*(5), 258–267.
1488 https://doi.org/10.1007/s10310-009-0134-8
1489 Franklin, J. F., Spies, T. A., Pelt, R. V., Carey, A. B., Thornburgh, D. A., Berg, D. R.,
1490 Lindenmayer, D. B., Harmon, M. E., Keeton, W. S., Shaw, D. C., Bible, K., & Chen, J.
1491 (2002). Disturbances and structural development of natural forest ecosystems with
1492 silvicultural implications, using Douglas-fir forests as an example. *Forest Ecology and*
1493 *Management*, *155*(1), 399–423. https://doi.org/10.1016/S0378-1127(01)00575-8
1494 Frazier, M. R., Huey, R. B., & Berrigan, D. (2006). Thermodynamics constrains the evolution of
1495 insect population growth rates: "warmer is better." *The American Naturalist*, *168*(4),
1496 512–520. https://doi.org/10.1086/506977
1497 Gardner, T. A., Barlow, J., & Peres, C. A. (2007). Paradox, presumption and pitfalls in
1498 conservation biology: The importance of habitat change for amphibians and reptiles.
1499 *Biological Conservation*, *138*(1–2), 166–179.
1500 https://doi.org/10.1016/j.biocon.2007.04.017

Gatten, R. E. (1987). Activity Metabolism of Anuran Amphibians: Tolerance to Dehydration. *Physiological Zoology*, *60*(5), 576–585. https://doi.org/10.1086/physzool.60.5.30156131

Gatten, R. E., Miller, K., & Full, R. J. (1992). Energetics at Rest and during Locomotion. In M. E. Bicudo & W. W. Burggren (Eds.), *Environmental Physiology of the Amphibians.* (pp. 314–377). University of Chicago Press.

Gebhardt, A., Bivand, R., & library), D. S. (author of the shull. (2024). *interp: Interpolation Methods* (Version 1.1-6) [Computer software]. https://cran.r-project.org/web/packages/interp/index.html

Geiger R., Aron R. H., & Todhunter P. (1965). *The Climate Near the Ground*. Harvard University Press.

Grandpré, L., Gagnon, D., & Bergeron, Y. (1993). Changes in the understory of Canadian southern boreal forest after fire. *Journal of Vegetation Science*, *4*(6), 803–810. https://doi.org/10.2307/3235618

Greenberg, D. A., & Palen, W. J. (2021). Hydrothermal physiology and climate vulnerability in amphibians. *Proceedings of the Royal Society B: Biological Sciences*, *288*(1945), 20202273. https://doi.org/10.1098/rspb.2020.2273

Gunderson, A. R., & Stillman, J. H. (2015). Plasticity in thermal tolerance has limited potential to buffer ectotherms from global warming. *Proceedings of the Royal Society B: Biological Sciences*, *282*(1808), 20150401. https://doi.org/10.1098/rspb.2015.0401

Harper, E. B., Patrick, D. A., & Gibbs, J. P. (2015). Impact of forestry practices at a landscape scale on the dynamics of amphibian populations. *Ecological Applications: A Publication of the Ecological Society of America*, *25*(8), 2271–2284. https://doi.org/10.1890/14-0962.1

1524 Harper, E. B., Rittenhouse, T. a. G., & Semlitsch, R. D. (2008). Demographic Consequences of
1525 Terrestrial Habitat Loss for Pool-Breeding Amphibians: Predicting Extinction Risks
1526 Associated with Inadequate Size of Buffer Zones. *Conservation Biology*, *22*(5), 1205–
1527 1215. https://doi.org/10.1111/j.1523-1739.2008.01015.x
1528 Harper, K. A., Macdonald, S. E., Burton, P. J., Chen, J., Brosofske, K. D., Saunders, S. C.,
1529 Euskirchen, E. S., Roberts, D., Jaiteh, M. S., & Esseen, P. (2005). Edge Influence on
1530 Forest Structure and Composition in Fragmented Landscapes. *Conservation Biology*,
1531 *19*(3), 768–782. https://doi.org/10.1111/j.1523-1739.2005.00045.x
1532 Hartig, F., Lohse, L., & leite, M. de S. (2024). *DHARMa: Residual Diagnostics for Hierarchical*
1533 *(Multi-Level / Mixed) Regression Models* (Version 0.4.7) [Computer software].
1534 https://cran.r-project.org/web/packages/DHARMa/index.html
1535 Hastings, T. P., Hossack, B. R., Fishback, L., & Davenport, J. M. (2023). Using physiological
1536 conditions to assess current and future habitat use of a Subarctic frog. *Integrative*
1537 *Zoology*, *18*(1), 2–14. https://doi.org/10.1111/1749-4877.12649
1538 Hermosilla, T., Wulder, M. A., White, J. C., Coops, N. C., Hobart, G. W., & Campbell, L. B.
1539 (2016). Mass data processing of time series Landsat imagery: Pixels to data products for
1540 forest monitoring. *International Journal of Digital Earth*, *9*(11), 1035–1054.
1541 https://doi.org/10.1080/17538947.2016.1187673
1542 Hillman, S. S. (1978). The roles of oxygen delivery and electrolyte levels in the dehydrational
1543 death ofXenopus laevis. *Journal of Comparative Physiology ? B*, *128*(2), 169–175.
1544 https://doi.org/10.1007/BF00689481

Hillman, S. S., Withers, P. C., Drewes, R. C., & Hillyard, S. D. (2008). *Ecological and Environmental Physiology of Amphibians*. Oxford University Press. https://doi.org/10.1093/acprof:oso/9780198570325.001.0001

Hocking, D. J., & Semlitsch, R. D. (2008). Effects of Experimental Clearcut Logging on Gray Treefrog (Hyla versicolor) Tadpole Performance. *Journal of Herpetology*, *42*(4), 689. https://doi.org/10.1670/07-294R1.1

Hof, C., Araújo, M. B., Jetz, W., & Rahbek, C. (2011). Additive threats from pathogens, climate and land-use change for global amphibian diversity. *Nature*, *480*(7378), 516–519. https://doi.org/10.1038/nature10650

Hossack, B. R., Eby, L. A., Guscio, C. G., & Corn, P. S. (2009). Thermal characteristics of amphibian microhabitats in a fire-disturbed landscape. *Forest Ecology and Management*, *258*(7), 1414–1421. https://doi.org/10.1016/j.foreco.2009.06.043

Hossack, B. R., Lowe, W. H., Honeycutt, R. K., Parks, S. A., & Corn, P. S. (2013). Interactive effects of wildfire, forest management, and isolation on amphibian and parasite abundance. *Ecological Applications*, *23*(2), 479–492. https://doi.org/10.1890/12-0316.1

Huey, R. B., Deutsch, C. A., Tewksbury, J. J., Vitt, L. J., Hertz, P. E., Álvarez Pérez, H. J., & Garland, T. (2009). Why tropical forest lizards are vulnerable to climate warming. *Proceedings of the Royal Society B: Biological Sciences*, *276*(1664), 1939–1948. https://doi.org/10.1098/rspb.2008.1957

Huey, R. B., Kearney, M. R., Krockenberger, A., Holtum, J. A. M., Jess, M., & Williams, S. E. (2012). Predicting organismal vulnerability to climate warming: Roles of behaviour, physiology and adaptation. *Philosophical Transactions of the Royal Society B: Biological Sciences*, *367*(1596), 1665–1679. https://doi.org/10.1098/rstb.2012.0005

Huey, R. B., & Kingsolver, J. G. (1989). Evolution of thermal sensitivity of ectotherm performance. *Trends in Ecology & Evolution*, *4*(5), 131–135. https://doi.org/10.1016/0169-5347(89)90211-5

Huey, R. B., & Stevenson, R. D. (1979). Integrating Thermal Physiology and Ecology of Ectotherms: A Discussion of Approaches. *American Zoologist*, *19*(1), 357–366. https://doi.org/10.1093/icb/19.1.357

Janin, A., Léna, J.-P., & Joly, P. (2011). Beyond occurrence: Body condition and stress hormone as integrative indicators of habitat availability and fragmentation in the common toad. *Biological Conservation*, *144*(3), 1008–1016. https://doi.org/10.1016/j.biocon.2010.12.009

Janisch, E. (1925). Über die Temperaturabhängigkeit biologischer Vorgänge und ihre kurvenmäßige Analyse. *Pflüger's Archiv für die gesamte Physiologie des Menschen und der Tiere*, *209*(1), 414–436. https://doi.org/10.1007/BF01730929

Jõgiste, K., Korjus, H., Stanturf, J. A., Frelich, L. E., Baders, E., Donis, J., Jansons, A., Kangur, A., Köster, K., Laarmann, D., Maaten, T., Marozas, V., Metslaid, M., Nigul, K., Polyachenko, O., Randveer, T., & Vodde, F. (2017). Hemiboreal forest: Natural disturbances and the importance of ecosystem legacies to management. *Ecosphere*, *8*(2), e01706. https://doi.org/10.1002/ecs2.1706

John-Alder, H. B., Barnhart, M. C., & Bennett, A. F. (1989). Thermal Sensitivity of Swimming Performance and Muscle Contraction in Northern and Southern Populations of Tree Frogs (Hyla Crucifer). *Journal of Experimental Biology*, *142*(1), 357–372. https://doi.org/10.1242/jeb.142.1.357

John-Alder, H., Morin, P., & Lawler, S. (1988). Thermal Physiology, Phenology, and Distribution of Tree Frogs. *American Naturalist - AMER NATURALIST*, *132*. https://doi.org/10.1086/284868

Johnson, J. B., & Omland, K. S. (2004). Model selection in ecology and evolution. *Trends in Ecology & Evolution*, *19*(2), 101–108. https://doi.org/10.1016/j.tree.2003.10.013

Johnson, J. R., Mahan, R. D., & Semlitsch, R. D. (2008). Seasonal Terrestrial Microhabitat Use by Gray Treefrogs (Hyla versicolor) in Missouri Oak-hickory Forests. *Herpetologica*, *64*(3), 259–269. https://doi.org/10.1655/07-064.1

Joly, P., Morand, C., & Cohas, A. (2003). Habitat fragmentation and amphibian conservation: Building a tool for assessing landscape matrix connectivity. *Comptes Rendus Biologies*, *326*, 132–139. https://doi.org/10.1016/S1631-0691(03)00050-7

Kamykowski, D. (1985). A survey of protozoan laboratory temperature studies applied to marine dinoflagellate behavior from a field perspective. *Contributions in Marine Science.* https://www.researchgate.net/publication/252320931_A_survey_of_protozoan_laboratory_temperature_studies_applied_to_marine_dinoflagellate_behavior_from_the_viewpoint_of_ecological_implications_Appendix_Kamykowski_D_and_F_G_Giesbrecht_Confidence_limits_

Kearney, M., & Porter, W. P. (2004). MAPPING THE FUNDAMENTAL NICHE: PHYSIOLOGY, CLIMATE, AND THE DISTRIBUTION OF A NOCTURNAL LIZARD. *Ecology*, *85*(11), 3119–3131. https://doi.org/10.1890/03-0820

Kearney, M., & Predavec, M. (2000). DO NOCTURNAL ECTOTHERMS THERMOREGULATE? A STUDY OF THE TEMPERATE GECKO *CHRISTINUS*

MARMORATUS. *Ecology*, *81*(11), 2984–2996. https://doi.org/10.1890/0012-9658(2000)081[2984:DNETAS]2.0.CO;2

Keenan, R. J., & Kimmins, J. P. (1993). The ecological effects of clear-cutting. *Environmental Reviews*, *1*, 121–144.

Keppel, G., Anderson, S., Williams, C., Kleindorfer, S., & O'Connell, C. (2017). Microhabitats and canopy cover moderate high summer temperatures in a fragmented Mediterranean landscape. *PLoS ONE*, *12*(8), e0183106. https://doi.org/10.1371/journal.pone.0183106

Kingsolver, J. G., & Huey, R. B. (2008). Size, temperature, and fitness: Three rules. *Evolutionary Ecology Research*, *10*, 251–268.

Klinges, D. H., Randriambololona, T., Lange, Z. K., Laterza-Barbosa, J., Randrianandrasana, H., & Scheffers, B. R. (2024). Vertical and diel niches modulate thermal selection by rainforest frogs. *Proceedings of the Royal Society B: Biological Sciences*, *291*(2034), 20241497. https://doi.org/10.1098/rspb.2024.1497

Köhler, A., Sadowska, J., Olszewska, J., Trzeciak, P., Berger-Tal, O., & Tracy, C. R. (2011). Staying warm or moist? Operative temperature and thermal preferences of common frogs (Rana temporaria. *Herpetological Journal*, *21*, 17–26.

Kontopoulos, D.-G., Sentis, A., Daufresne, M., Glazman, N., Dell, A. I., & Pawar, S. (2024). No universal mathematical model for thermal performance curves across traits and taxonomic groups. *Nature Communications*, *15*(1), 8855. https://doi.org/10.1038/s41467-024-53046-2

Krenek, S., Berendonk, T. U., & Petzoldt, T. (2011). Thermal performance curves of *Paramecium caudatum*: A model selection approach. *European Journal of Protistology*, *47*(2), 124–137. https://doi.org/10.1016/j.ejop.2010.12.001

Kuuluvainen, T. (2009). Forest Management and Biodiversity Conservation Based on Natural Ecosystem Dynamics in Northern Europe: The Complexity Challenge. *AMBIO: A Journal of the Human Environment*, *38*(6), 309–315. https://doi.org/10.1579/08-A-490.1

Kuuluvainen, T., Angelstam, P., Frelich, L., Jõgiste, K., Koivula, M., Kubota, Y., Lafleur, B., & Macdonald, E. (2021). Natural Disturbance-Based Forest Management: Moving Beyond Retention and Continuous-Cover Forestry. *Frontiers in Forests and Global Change*, *4*. https://doi.org/10.3389/ffgc.2021.629020

Lactin, D. J., Holliday, N. J., Johnson, D. L., & Craigen, R. (1995). Improved rate model of temperature-dependent development by arthropods. *Environmental Entomology 24: 68-75.*

Larocque, G. R., Bell, F. W., Searle, E. B., Mayor, S. J., Schiks, T., & Kalantari, P. (2024). Simulating the Long-Term Response of Forest Succession to Climate Change in the Boreal Forest of Northern Ontario, Canada. *Forests*, *15*(8), Article 8. https://doi.org/10.3390/f15081417

Laughlin, M. M., Olson, E. R., & Martin, J. G. (2017). Arboreal camera trapping expands *Hyla versicolor* complex (Hylidae) canopy use to new heights. *Ecology*, *98*(8), 2221–2223. https://doi.org/10.1002/ecy.1843

Lenth, R. V., Banfai, B., Bolker, B., Buerkner, P., Giné-Vázquez, I., Herve, M., Jung, M., Love, J., Miguez, F., Piaskowski, J., Riebl, H., & Singmann, H. (2025). *emmeans: Estimated Marginal Means, aka Least-Squares Means* (Version 1.11.2) [Computer software]. https://cran.r-project.org/web/packages/emmeans/index.html

Lertzman-Lepofsky, G. F., Kissel, A. M., Sinervo, B., & Palen, W. J. (2020). Water loss and temperature interact to compound amphibian vulnerability to climate change. *Glob. Change Biol*, *26*, 4868–4879.

Lindenmayer, D. B., Kooyman, R. M., Taylor, C., Ward, M., & Watson, J. E. M. (2020). Recent Australian wildfires made worse by logging and associated forest management. *Nature Ecology & Evolution*, *4*(7), 898–900. https://doi.org/10.1038/s41559-020-1195-5

Logan, J. A., Wollkind, D. J., Hoyt, S. C., & Tanigoshi, L. K. (1976). An Analytic Model for Description of Temperature Dependent Rate Phenomena in Arthropods 1. *Environmental Entomology*, *5*(6), 1133–1140. https://doi.org/10.1093/ee/5.6.1133

Lüdecke, D., Ben-Shachar, M. S., Patil, I., Waggoner, P., & Makowski, D. (2021). performance: An R Package for Assessment, Comparison and Testing of Statistical Models. *Journal of Open Source Software*, *6*(60), 3139. https://doi.org/10.21105/joss.03139

Luedtke, J. A., Chanson, J., Neam, K., Hobin, L., Maciel, A. O., Catenazzi, A., Borzée, A., Hamidy, A., Aowphol, A., Jean, A., Sosa-Bartuano, Á., Fong G., A., de Silva, A., Fouquet, A., Angulo, A., Kidov, A. A., Muñoz Saravia, A., Diesmos, A. C., Tominaga, A., … Stuart, S. N. (2023). Ongoing declines for the world's amphibians in the face of emerging threats. *Nature*, *622*(7982), 308–314. https://doi.org/10.1038/s41586-023-06578-4

Lundmark, H., Josefsson, T., & Östlund, L. (2017). The introduction of modern forest management and clear-cutting in Sweden: Ridö State Forest 1832–2014. *European Journal of Forest Research*, *136*(2), 269–285. https://doi.org/10.1007/s10342-017-1027-6

Máliš, F., Ujházy, K., Hederová, L., Ujházyová, M., Csölleová, L., Coomes, D. A., & Zellweger, F. (2023). Microclimate variation and recovery time in managed and old-growth

temperate forests. *Agricultural and Forest Meteorology*, *342*, 109722. https://doi.org/10.1016/j.agrformet.2023.109722

Martin, T. L., & Huey, R. B. (2008). Why "Suboptimal" Is Optimal: Jensen's Inequality and Ectotherm Thermal Preferences. *The American Naturalist*, *171*(3), E102–E118. https://doi.org/10.1086/527502

Matlack, G. R. (1993). Microenvironment variation within and among forest edge sites in the eastern United States. *Biological Conservation*, *66*(3), 185–194. https://doi.org/10.1016/0006-3207(93)90004-K

Mazerolle, M. J., Lapointe, M. S. P., Imbeau, L., & Joanisse, G. (2021). Woodland salamander population structure and body condition under irregular shelterwood systems. *Canadian Journal of Forest Research*, *51*(9), 1281–1291. https://doi.org/10.1139/cjfr-2020-0405

Mitchell, A., & Bergmann, P. J. (2016). Thermal and moisture habitat preferences do not maximize jumping performance in frogs. *Functional Ecology*, *30*(5), 733–742. https://doi.org/10.1111/1365-2435.12535

Mitchell, W. A., & Angilletta Jr, M. J. (2009). Thermal games: Frequency-dependent models of thermal adaptation. *Functional Ecology*, *23*(3), 510–520. https://doi.org/10.1111/j.1365-2435.2009.01542.x

Moore, F. R., & Gatten Jr, R. E. (1989). Locomotor performance of hydrated, dehydrated, and osmotically stressed anuran amphibians. *Herpetologica*, *1*, 101–110.

Murcia, C. (1995). Edge effects in fragmented forests: Implications for conservation. *Trends in Ecology & Evolution*, *10*(2), 58–62. https://doi.org/10.1016/S0169-5347(00)88977-6

Natural Resources, O. M. & Forestry. (2001). *Forest management guide for natural disturbance pattern emulation, Version 3.1*. Ontario Ministry of Natural Resources. Queen's Printer for Ontario, Toronto.

Natural Resources, O. M. & Forestry. (2023). *Forest Management Guide for Boreal Landscapes in Ontario*.

Navas, C. A. (1996). Metabolic Physiology, Locomotor Performance, and Thermal Niche Breadth in Neotropical Anurans. *Physiological Zoology*, *69*(6), 1481–1501. https://doi.org/10.1086/physzool.69.6.30164271

Navas, C. A., Gomes, F. R., & Carvalho, J. E. (2008). Thermal relationships and exercise physiology in anuran amphibians: Integration and evolutionary implications. *Comparative Biochemistry and Physiology Part A: Molecular & Integrative Physiology*, *151*(3), 344–362. https://doi.org/10.1016/j.cbpa.2007.07.003

Navas, C. A., Gomes, F. R., & De Domenico, E. A. (2016). Physiological ecology and conservation of anuran amphibians. In D. V. Andrade, C. R. Bevier, & J. E. Carvalho (Eds.), *Amphibian and Reptile Adaptations to the Environment: Interplay Between Physiology and Behavior.* (pp. 155–188). CRC Press.

Navas, C. A., Gouveia, S. F., Solano-Iguarán, J. J., Vidal, M. A., & Bacigalupe, L. D. (2021). Amphibian responses in experimental thermal gradients: Concepts and limits for inference. *Comparative Biochemistry and Physiology Part B: Biochemistry and Molecular Biology*, *254*, 110576. https://doi.org/10.1016/j.cbpb.2021.110576

Neel, L. K., & McBrayer, L. D. (2018). Habitat management alters thermal opportunity. *Functional Ecology*, *32*(8), 2029–2039. https://doi.org/10.1111/1365-2435.13123

Nowakowski, A. J., Watling, J. I., Thompson, M. E., Brusch, G. A., Catenazzi, A., Whitfield, S. M., Kurz, D. J., Suárez-Mayorga, Á., Aponte-Gutiérrez, A., Donnelly, M. A., & Todd, B. D. (2018). Thermal biology mediates responses of amphibians and reptiles to habitat modification. *Ecology Letters*, *21*(3), 345–355. https://doi.org/10.1111/ele.12901

Olson, E. R., Laughlin, M. M., & Martin, J. G. (2023). Reaching New Heights: Arboreal Camera Trapping Provides New Insights on the Ecology of Gray Treefrogs (Hyla versicolor). *Journal of Herpetology*, *57*(3), 281–289. https://doi.org/10.1670/22-060

Padfield, D., O'Sullivan, H., & Pawar, S. (2021). rTPC and nls.multstart: A new pipeline to fit thermal performance curves in r. *Methods in Ecology and Evolution*, *12*(6), 1138–1143. https://doi.org/10.1111/2041-210X.13585

Patrick, D. A., Hunter, M. L., & Calhoun, A. J. K. (2006). Effects of experimental forestry treatments on a Maine amphibian community. *Forest Ecology and Management*, *234*(1), 323–332. https://doi.org/10.1016/j.foreco.2006.07.015

Payne, N. L., Smith, J. A., Meulen, D. E., Taylor, M. D., Watanabe, Y. Y., Takahashi, A., Marzullo, T. A., Gray, C. A., Cadiou, G., & Suthers, I. M. (2015). Temperature dependence of fish performance in the wild: Links with species biogeography and physiological thermal tolerance. *Functional Ecology*, *30*(6), 903–912. https://doi.org/10.1111/1365-2435.12618

Perez-Navarro, M. A., Lloret, F., Molina-Venegas, R., Alcántara, J. M., & Verdú, M. (2024). Plant canopies promote climatic disequilibrium in Mediterranean recruit communities. *Ecology Letters*, *27*(2), e14391. https://doi.org/10.1111/ele.14391

Peterman, W. E., Locke, J. L., & Semlitsch, R. D. (2013). Spatial and temporal patterns of water loss in heterogeneous landscapes: Using plaster models as amphibian analogues. *Canadian Journal of Zoology*, *91*(3), 135–140. https://doi.org/10.1139/cjz-2012-0229

Peterman, W. E., & Semlitsch, R. D. (2014). Spatial variation in water loss predicts terrestrial salamander distribution and population dynamics. *Oecologia*, *176*(2), 357–369. https://doi.org/10.1007/s00442-014-3041-4

Pinheiro, J. P., Bates, D., DebRoy, S., Sarkar, D., Heisterkamp, S., Van Willigen, B., Ranke, J., & R Core Team. (2025). *nlme: Linear and Nonlinear Mixed Effects Models* (Version 3.1-168) [Computer software]. https://cran.r-project.org/web/packages/nlme/index.html

Popescu, V. D., & Hunter, M. L. (2011). Clear-cutting affects habitat connectivity for a forest amphibian by decreasing permeability to juvenile movements. *Ecological Applications*, *21*(4), 1283–1295. https://doi.org/10.1890/10-0658.1

Pottier, P., Burke, S., Drobniak, S. M., Lagisz, M., & Nakagawa, S. (2021). Sexual (in)equality? A meta-analysis of sex differences in thermal acclimation capacity across ectotherms. *Functional Ecology*, *35*(12), 2663–2678. https://doi.org/10.1111/1365-2435.13899

Pottier, P., Kearney, M. R., Wu, N. C., Gunderson, A. R., Rej, J. E., Rivera-Villanueva, A. N., Pollo, P., Burke, S., Drobniak, S. M., & Nakagawa, S. (2025). Vulnerability of amphibians to global warming. *Nature*, *639*(8056), 954–961. https://doi.org/10.1038/s41586-025-08665-0

Pough, F. H., Taigen, T. L., Stewart, M. M., & Brussard, P. F. (1983). Behavioral Modification of Evaporative Water Loss by a Puerto Rican Frog. *Ecology*, *64*(2), 244–252. https://doi.org/10.2307/1937072

1765 Prates, I., & Navas, C. A. (2009). Cutaneous Resistance to Evaporative Water Loss in Brazilian
1766 Rhinella (Anura: Bufonidae) from Contrasting Environments. *Copeia*, *2009*(3), 618–622.
1767 https://doi.org/10.1643/CP-08-128
1768 Preest, M. R., & Pough, F. H. (1989). Interaction of Temperature and Hydration on Locomotion
1769 of Toads. *Functional Ecology*, *3*(6), 693. https://doi.org/10.2307/2389501
1770 Price, D. T. (2013). Anticipating the consequences of climate change for Canada's boreal forest
1771 ecosystems. *Environmental Reviews*, *21*, 322–365.
1772 Ratkowsky, D. A., Lowry, R. K., McMeekin, T. A., Stokes, A. N., & Chandler, R. E. (1983).
1773 Model for bacterial culture growth rate throughout the entire biokinetic temperature
1774 range. *Journal of Bacteriology*, *154*(3), 1222–1226.
1775 https://doi.org/10.1128/jb.154.3.1222-1226.1983
1776 Remmel, T. K., Ouellette, M., & Wu, W. J. (2023). A boreal wildfire and harvesting database
1777 with ensemble confidence attributes for Ontario (1972–2021+). *International Journal of*
1778 *Applied Earth Observation and Geoinformation*, *117*, 103199.
1779 https://doi.org/10.1016/j.jag.2023.103199
1780 Rezende, E. L., & Bozinovic, F. (2019). Thermal performance across levels of biological
1781 organization. *Philosophical Transactions of the Royal Society of London. Series B,*
1782 *Biological Sciences*, *374*(1778), 20180549. https://doi.org/10.1098/rstb.2018.0549
1783 Richard, B., Dupouey, J.-L., Corcket, E., Alard, D., Archaux, F., Aubert, M., Boulanger, V.,
1784 Gillet, F., Langlois, E., Macé, S., Montpied, P., Beaufils, T., Begeot, C., Behr, P.,
1785 Boissier, J.-M., Camaret, S., Chevalier, R., Decocq, G., Dumas, Y., … Lenoir, J. (2021).
1786 The climatic debt is growing in the understorey of temperate forests: Stand characteristics

matter. *Global Ecology and Biogeography*, *30*(7), 1474–1487. https://doi.org/10.1111/geb.13312

Rittenhouse, T. A. G., Harper, E. B., Rehard, L. R., & Semlitsch, R. D. (2008). The Role of Microhabitats in the Desiccation and Survival of Anurans in Recently Harvested Oak–Hickory Forest. *Copeia*, *2008*(4), 807–814. https://doi.org/10.1643/CH-07-176

Rittenhouse, T. A. G., Semlitsch, R. D., & Thompson, F. R. I. (2009). Survival costs associated with wood frog breeding migrations: Effects of timber harvest and drought. *Ecology. 90(6): 1620-1630.*, *90*, 1620–1630. https://doi.org/10.1890/08-0326.1

Robinson, M., Nielsen, S. E., Eaton, B., & Paszkowski, C. (2023). Effect of variable retention forestry on wood frogs (*Lithobates sylvaticus*) in early successional boreal mixedwood forests. *Canadian Journal of Zoology*, *101*(3), 172–188. https://doi.org/10.1139/cjz-2022-0062

Rogowitz, G. L., Cortés-Rivera, M., & Nieves-Puigdoller, K. (1999). Water loss, cutaneous resistance, and effects of dehydration on locomotion of Eleutherodactylus frogs. *Journal of Comparative Physiology B: Biochemical, Systemic, and Environmental Physiology*, *169*(3), 179–186. https://doi.org/10.1007/s003600050209

Rohr, J. R., Civitello, D. J., Cohen, J. M., Roznik, E. A., Sinervo, B., & Dell, A. I. (2018). The complex drivers of thermal acclimation and breadth in ectotherms. *Ecology Letters*, *21*(9), 1425–1439. https://doi.org/10.1111/ele.13107

Rollins-Smith, L. A., & Le Sage, E. H. (2023). Heat stress and amphibian immunity in a time of climate change. *Philosophical Transactions of the Royal Society B: Biological Sciences*, *378*(1882), 20220132. https://doi.org/10.1098/rstb.2022.0132

Rome, L. C., Stevens, E. D., & John-Alder, H. B. (1992). Influence of Temperature and Thermal Acclimation on Physiological Function. In M. E. Bicudo & W. W. Burggren (Eds.), *Environmental Physiology of the Amphibians*. The University of Chicago Press.

Rozen-Rechels, D., Dupoué, A., Lourdais, O., Chamaillé-Jammes, S., Meylan, S., Clobert, J., & Le Galliard, J.-F. (2019). When water interacts with temperature: Ecological and evolutionary implications of thermo-hydroregulation in terrestrial ectotherms. *Ecology and Evolution*, *9*(17), 10029–10043. https://doi.org/10.1002/ece3.5440

Roznik, E. A., Rodriguez-Barbosa, C. A., & Johnson, S. A. (2018). Hydric Balance and Locomotor Performance of Native and Invasive Frogs. *Frontiers in Ecology and Evolution*, *6*, 159. https://doi.org/10.3389/fevo.2018.00159

Ruiz, T., Koussoroplis, A.-M., Danger, M., Aguer, J.-P., Morel-Desrosiers, N., & Bec, A. (2019). *The Threshold Elemental Ratio of an ectotherm decreases then increases with rising temperature* (p. 681239). bioRxiv. https://doi.org/10.1101/681239

Rutschmann, A., Perry, C., Le Galliard, J.-F., Dupoué, A., Lourdais, O., Guillon, M., Brusch IV, G., Cote, J., Richard, M., Clobert, J., & Miles, D. B. (2024). Ecological responses of squamate reptiles to nocturnal warming. *Biological Reviews*, *99*(2), 598–621. https://doi.org/10.1111/brv.13037

Scheffers, B. R., Brunner, R. M., Ramirez, S. D., Shoo, L. P., Diesmos, A., & Williams, S. E. (2013). Thermal Buffering of Microhabitats is a Critical Factor Mediating Warming Vulnerability of Frogs in the Philippine Biodiversity Hotspot. *Biotropica*, *45*(5), 628–635. https://doi.org/10.1111/btp.12042

Schmidt, R., Zummach, C., Sinai, N., Sabino-Pinto, J., Künzel, S., Dausmann, K. H., & Ruthsatz, K. (2024). Physiological responses to a changing winter climate in an early

spring-breeding amphibian. *Ecology and Evolution*, *14*(7), e70042. https://doi.org/10.1002/ece3.70042

Schulte, P. M., Healy, T. M., & Fangue, N. A. (2011). Thermal Performance Curves, Phenotypic Plasticity, and the Time Scales of Temperature Exposure. *Integrative and Comparative Biology*, *51*(5), 691–702. https://doi.org/10.1093/icb/icr097

Sears, M. W., & Angilletta, M. J. (2015). Costs and benefits of thermoregulation revisited: Both the heterogeneity and spatial structure of temperature drive energetic costs. *The American Naturalist*, *185:E94–E102*.

Sears, M. W., Angilletta, M. J., Schuler, M. S., Borchert, J., Dilliplane, K. F., & Stegman, M. (2016). Configuration of the thermal landscape determines thermoregulatory performance of ectotherms. *Proceedings of the National Academy of Sciences of the United States of America*, *113*, 10595–10600.

Semlitsch, R. (2000). Principles for Management of Aquatic-Breeding Amphibians. *The Journal of Wildlife Management*, *64*, 615. https://doi.org/10.2307/3802732

Semlitsch, R. D., Todd, B. D., Blomquist, S. M., Calhoun, A. J. K., Gibbons, J. W., Gibbs, J. P., Graeter, G. J., Harper, E. B., Hocking, D. J., Hunter, M. L., Jr., Patrick, D. A., Rittenhouse, T. A. G., & Rothermel, B. B. (2009). Effects of Timber Harvest on Amphibian Populations: Understanding Mechanisms from Forest Experiments. *BioScience*, *59*(10), 853–862. https://doi.org/10.1525/bio.2009.59.10.7

Senzano, L. M., & Andrade, D. V. (2018). Temperature and dehydration effects on metabolism, water uptake, and the partitioning between respiratory and cutaneous evaporative water loss in a terrestrial toad. *Journal of Experimental Biology*, jeb.188482. https://doi.org/10.1242/jeb.188482

Shi, P., & Ge, F. (2010). A comparison of different thermal performance functions describing temperature-dependent development rates. *Journal of Thermal Biology*, *35*(5), 225–231. https://doi.org/10.1016/j.jtherbio.2010.05.005

Shoemaker, V. H., Hillman, S. S., Hillyard, S. D., Jackson, D. C., Mcclanahan, L. L., Withers, P., & Wygoda, M. (1992). Exchange of water, ions and respiratory gases in terrestrial amphibians. In M. Feder & W. Burggren (Eds.), *Environmental Physiology of the Amphibians* (pp. 125–150). The University of Chicago Press.

Shoemaker, V. H., & Nagy, K. A. (1977). Osmoregulation in amphibians and reptiles. *Annual Review of Physiology*, *39*, 449–471. https://doi.org/10.1146/annurev.ph.39.030177.002313

Sinervo, B., Méndez-de-la-Cruz, F., Miles, D. B., Heulin, B., Bastiaans, E., Villagrán-Santa Cruz, M., Lara-Resendiz, R., Martínez-Méndez, N., Calderón-Espinosa, M. L., Meza-Lázaro, R. N., Gadsden, H., Avila, L. J., Morando, M., De la Riva, I. J., Sepulveda, P. V., Rocha, C. F. D., Ibargüengoytía, N., Puntriano, C. A., Massot, M., … Sites, J. W. (2010). Erosion of Lizard Diversity by Climate Change and Altered Thermal Niches. *Science*, *328*(5980), 894–899. https://doi.org/10.1126/science.1184695

Singmann, H., Bolker, B., Westfall, J., Aust, F., Ben-Shachar, M. S., Højsgaard, S., Fox, J., Lawrence, M. A., Mertens, U., Love, J., Lenth, R., & Christensen, R. H. B. (2024). *afex: Analysis of Factorial Experiments* (Version 1.4-1) [Computer software]. https://cran.r-project.org/web/packages/afex/index.html

Soltani, K., Amiri, A., Ebtehaj, I., Cheshmehghasabani, H., Fazeli, S., Gumiere, S. J., & Bonakdari, H. (2024). Advanced Forecasting of Drought Zones in Canada Using Deep

Learning and CMIP6 Projections. *Climate*, *12*(8), Article 8. https://doi.org/10.3390/cli12080119

Spotila, J. R., O'Connor, M. P., & Bakken, G. S. (1992). Biophysics of heat and mass transfer. Pages 59-81 in M.E. In Bicudo & W. W. Burggren (Eds.), *Environmental Physiology of the Amphibians*. The University of Chicago Press.

Stuart, S. N., Chanson, J. S., Cox, N. A., Young, B. E., Rodrigues, A. S. L., Fischman, D. L., & Waller, R. W. (2004). Status and Trends of Amphibian Declines and Extinctions Worldwide. *Science*, *306*(5702), 1783–1786. https://doi.org/10.1126/science.1103538

Sunday, J. M., Bates, A. E., Kearney, M. R., Colwell, R. K., Dulvy, N. K., Longino, J. T., & Huey, R. B. (2014). Thermal-safety margins and the necessity of thermoregulatory behavior across latitude and elevation. *Proceedings of the National Academy of Sciences*, *111*(15), 5610–5615. https://doi.org/10.1073/pnas.1316145111

Taylor, S. E., & Sexton, O. J. (1972). Some Implications of Leaf Tearing in Musaceae. *Ecology*, *53*(1), 143–149. https://doi.org/10.2307/1935720

Thomas, M. K., Kremer, C. T., Klausmeier, C. A., & Litchman, E. (2012). A global pattern of thermal adaptation in marine phytoplankton. *Science (New York, N.Y.)*, *338*(6110), 1085–1088. https://doi.org/10.1126/science.1224836

Todd, B. D., Blomquist, S. M., Harper, E. B., & Osbourn, M. S. (2014). Effects of timber harvesting on terrestrial survival of pond-breeding amphibians. *Forest Ecology and Management*, *313*, 123–131. https://doi.org/10.1016/j.foreco.2013.11.011

Todd, B. D., Luhring, T. M., Rothermel, B. B., & Gibbons, J. W. (2009). Effects of forest removal on amphibian migrations: Implications for habitat and landscape connectivity.

Journal of Applied Ecology, *46*(3), 554–561. https://doi.org/10.1111/j.1365-2664.2009.01645.x

Todd, B. D., & Rothermel, B. B. (2006). Assessing quality of clearcut habitats for amphibians: Effects on abundances versus vital rates in the southern toad (*Bufo terrestris*). *Biological Conservation*, *133*(2), 178–185. https://doi.org/10.1016/j.biocon.2006.06.003

Toledo, R. C., & Jared, C. (1993). Cutaneous adaptations to water balance in amphibians. *Comparative Biochemistry and Physiology Part A: Physiology*, *105*(4), 593–608. https://doi.org/10.1016/0300-9629(93)90259-7

Tomlinson, S., & Phillips, R. D. (2015). Differences in metabolic rate and evaporative water loss associated with sexual dimorphism in thynnine wasps. *Journal of Insect Physiology*, *78*, 62–68. https://doi.org/10.1016/j.jinsphys.2015.04.011

Tracy, C. R. (1976). A Model of the Dynamic Exchanges of Water and Energy between a Terrestrial Amphibian and Its Environment. *Ecological Monographs*, *46*(3), 293–326. https://doi.org/10.2307/1942256

Tracy, C. R., Betts, G., Richard Tracy, C., & Christian, K. A. (2007). Plaster Models to Measure Operative Temperature and Evaporative Water Loss of Amphibians. *Journal of Herpetology*, *41*(4), 597–603. https://doi.org/10.1670/07-006.1

Tracy, C. R., Christian, K. A., & Tracy, C. R. (2010). Not just small, wet, and cold: Effects of body size and skin resistance on thermoregulation and arboreality of frogs. *Ecology*, *91*(5), 1477–1484. https://doi.org/10.1890/09-0839.1

Tracy, C. R., Tixier, T., Le Nöene, C., & Christian, K. A. (2014). Field Hydration State Varies among Tropical Frog Species with Different Habitat Use. *Physiological and Biochemical Zoology*, *87*(2), 197–202. https://doi.org/10.1086/674537

Tuff, K. T., Tuff, T., & Davies, K. F. (2016). A framework for integrating thermal biology into fragmentation research. *Ecology Letters*, *19*(4), 361–374. https://doi.org/10.1111/ele.12579

Urban, M. C., Tewksbury, J. J., & Sheldon, K. S. (2012). On a collision course: Competition and dispersal differences create no-analogue communities and cause extinctions during climate change. *Proceedings. Biological Sciences*, *279*(1735), 2072–2080. https://doi.org/10.1098/rspb.2011.2367

Veysey Powell, J. S., & Babbitt, K. J. (2015). Despite Buffers, Experimental Forest Clearcuts Impact Amphibian Body Size and Biomass. *PLoS ONE*, *10*(11), e0143505. https://doi.org/10.1371/journal.pone.0143505

Weber, M. G., & Flannigan, M. D. (1997). Canadian boreal forest ecosystem structure and function in a changing climate: Impact on fire regimes. *Environmental Reviews*, *5*(3–4), 145–166. https://doi.org/10.1139/a97-008

Wells, K. D. (2010). *The Ecology and Behavior of Amphibians*. University of Chicago Press. https://press.uchicago.edu/ucp/books/book/chicago/E/bo5298950.html

Wilson, R. S. (2001). Geographic variation in thermal sensitivity of jumping performance in the frog Limnodynastes peronii. *Journal of Experimental Biology*, *204*(24), 4227–4236. https://doi.org/10.1242/jeb.204.24.4227

Wolf, K. D., Higuera, P. E., Davis, K. T., & Dobrowski, S. Z. (2021). Wildfire impacts on forest microclimate vary with biophysical context. *Ecosphere*, *12*(5), e03467. https://doi.org/10.1002/ecs2.3467

Wulder, M. A., Hermosilla, T., White, J. C., Bater, C. W., Hobart, G., & Bronson, S. C. (2024). Development and implementation of a stand-level satellite-based forest inventory for

Canada. *Forestry: An International Journal of Forest Research*, *97*(4), 546–563. https://doi.org/10.1093/forestry/cpad065

Young, J. E., Christian, K. A., Donnellan, S., Tracy, C. R., & Parry, D. (2005). Comparative Analysis of Cutaneous Evaporative Water Loss in Frogs Demonstrates Correlation with Ecological Habits. *Physiological and Biochemical Zoology*, *78*(5), 847–856. https://doi.org/10.1086/432152

Zhang, F., Biederman, J. A., Dannenberg, M. P., Yan, D., Reed, S. C., & Smith, W. K. (2021). Five Decades of Observed Daily Precipitation Reveal Longer and More Variable Drought Events Across Much of the Western United States. *Geophysical Research Letters*, *48*(7), e2020GL092293. https://doi.org/10.1029/2020GL092293

7 APPENDIX A

7.1 Weighted average results for individual thermal performance curves

Table 7.1 Delta AIC values for each model and frog included in the final thermal performance curve at 100% hydration. Model name indicates all models fit for each frog. NAs in column values indicates that the specified model did not fit for the corresponding frog. Models with lower delta AIC were given higher weights towards the final curves for each frog.

	Δ AIC								
Model Name	**A1**	**A2**	**A3**	**A5**	**A6**	**B3**	**B4**	**B5**	**B6**
Analytis K I	2.13	5.76	4.77	7.83	9.05	5.08	1.69	6.07	0.30
Ashrafi I	1.10	0.00	0.70	0.01	0.00	3.68	2.55	NA	1.03
Atkin	0.90	0.78	1.53	2.12	5.05	3.87	0.37	0.00	0.23
Briere I	2.94	2.17	2.16	0.91	7.21	5.35	3.93	3.94	3.33
Briere I no int	7.30	11.20	12.34	14.03	12.16	5.51	12.77	4.01	5.95
Eubank	0.93	0.56	1.46	0.00	5.77	3.38	1.67	0.21	0.38
Gaussian	0.91	1.05	1.64	2.17	6.51	3.98	0.00	2.73	0.00
Gaussian Gomp	2.80	2.85	7.63	4.10	11.23	5.76	2.27	NA	2.00
Janisch I	0.92	0.65	1.50	1.40	5.98	3.68	1.01	0.81	0.19
Lactin I	1.34	2.08	2.45	4.73	NA	3.51	2.38	2.47	1.51
Lactin II	2.87	2.74	2.92	NA	NA	6.82	4.38	10.45	3.57
Logan I	2.86	2.74	NA	NA	9.28	5.61	4.24	NA	3.50
Ratkowsky	4.98	7.02	8.07	NA	NA	NA	5.63	NA	NA
Rezende	2.87	2.26	2.79	NA	11.71	5.51	3.59	6.62	3.11
Ruiz	2.90	2.05	0.00	NA	NA	NA	2.00	3.15	2.00
Simplified Beta	NA	NA	NA	NA	NA	NA	NA	NA	0.08
Taylor S	2.45	3.27	5.98	8.79	8.63	4.06	1.42	2.64	0.48
Tomlinson P	0.00	1.65	0.82	6.91	NA	0.00	5.62	4.39	3.66
Weibull	2.06	2.87	2.84	2.05	8.36	NA	0.33	3.98	1.75

Table 7.2. Delta AIC values for individually fit thermal performance curves at 92% hydration. Model name indicates all models fit for each frog. NAs in column values indicates that the specified model did not fit for the corresponding frog. Models with lower delta AIC were given higher weights towards the final curves for each frog.

	Δ AIC								
Model Name	**A1**	**A2**	**A3**	**A5**	**A6**	**B3**	**B4**	**B5**	**B6**
Analytis K I	5.67	0.65	3.78	1.34	3.43	4.13	2.34	8.49	6.55
Ashrafi	1.03	5.18	2.78	NA	0.00	4.57	1.34	1.53	5.64
Atkin	NA	2.57	2.49	0.00	NA	4.39	2.22	NA	4.23
Briere I	3.35	6.30	3.95	2.40	26.27	6.43	2.44	3.49	6.14
Briere II	12.19	0.00	4.78	2.94	10.33	5.36	5.75	17.12	6.08
Eubank	0.18	4.96	0.00	NA	22.91	4.64	1.82	0.34	0.26
Gaussian	1.92	0.32	3.05	0.76	28.75	4.16	2.43	2.31	5.40
Gaussian Gomp	14.63	2.32	NA	3.21	NA	6.10	4.55	3.71	10.82
Janisch I	0.84	3.52	1.48	0.15	22.13	4.47	2.09	1.13	2.78
Lactin I	3.15	6.09	1.16	0.42	NA	4.79	1.30	5.60	2.07
Lactin II	2.77	8.17	NA	NA	10.23	6.86	1.35	3.20	NA
Logan I	NA	NA	NA	NA	NA	NA	4.76	15.38	NA
Mitchell angilletta	7.87	NA	3.87	NA	18.85	NA	NA	6.93	6.88
Rezende	NA	NA	3.33	NA	28.03	8.17	3.46	NA	4.30
Simplified Beta	2.46	NA	4.25	NA	10.39	3.81	3.04	NA	6.47
Taylor S	5.34	2.12	3.44	NA	NA	4.30	2.18	10.35	5.90
Tomlinson P	0.00	8.51	NA	0.00	14.95	5.11	0.00	0.00	0.00
Weibull	4.04	NA	4.47	2.53	17.87	0.00	3.99	4.04	5.67

Table 7.3. Delta AIC values for individually fit thermal performance curves at 84% hydration. Model name indicates all models fit for each frog. NAs in column values indicates that the specified model did not fit for the corresponding frog. Models with lower delta AIC were given higher weights towards the final curves for each frog.

	Δ AIC								
Model Name	**A1**	**A2**	**A3**	**A5**	**A6**	**B3**	**B4**	**B5**	**B6**
Analytis K I	3.88	3.45	1.07	0.87	9.11	7.66	7.87	5.55	5.74
Ashrafi	1.98	4.35	0.32	NA	NA	0.84	5.91	0.34	6.45
Atkin	3.79	2.73	0.74	0.10	NA	0.00	7.22	0.00	5.41
Briere I	1.79	7.92	1.91	NA	1.08	9.32	3.63	2.33	NA
Eubank	3.44	0.00	0.60	0.00	NA	NA	6.22	0.31	4.47
Gaussian	4.06	4.19	1.13	0.95	9.43	6.47	11.38	2.43	5.80
Gaussian Gomp	6.37	3.80	2.68	2.44	12.47	NA	NA	2.02	6.94
Janisch I	3.69	0.90	0.68	0.36	2.27	NA	7.28	4.68	4.71
Janisch II	6.89	NA	2.55	2.10	6.55	NA	NA	1.72	NA
Lactin II	2.50	6.20	NA	NA	4.86	NA	NA	2.65	8.31
Logan I	6.84	NA	2.63	2.54	11.99	NA	NA	2.09	8.26
Mitchell A	NA	2.14	NA	NA	7.06	5.75	NA	3.51	5.02
Rezende Bozinovic	4.77	NA	2.67	NA	20.88	2.82	6.34	NA	NA
Ruiz	NA	NA	NA	0.67	NA	2.48	NA	NA	NA
Simplified Beta	5.06	2.21	1.14	NA	4.89	NA	9.06	0.00	4.80
Simplified Briere	3.94	3.86	0.95	0.49	5.39	10.28	8.26	3.09	5.92
Taylor S	4.22	3.96	1.16	0.69	10.57	NA	7.21	6.87	6.15
Tomlinson P	0.00	5.26	0.00	0.10	0.00	NA	0.00	0.78	NA
Weibull	5.44	NA	2.73	2.26	5.09	4.96	8.56	2.00	0.00

Table 7.4. Delta AIC values for individually fit thermal performance curves at 75% hydration. Model name indicates all models fit for each frog. NAs in column values indicates that the specified model did not fit for the corresponding frog. Models with lower delta AIC were given higher weights towards the final curves for each frog.

	Δ AIC								
Model Name	**A1**	**A2**	**A3**	**A5**	**A6**	**B3**	**B4**	**B5**	**B6**
Analytis K I	1.59	5.37	4.07	0.40	NA	0.90	11.17	1.95	0.78
Ashrafi I	0.00	NA	3.10	0.00	NA	0.57	4.66	NA	1.45
Atkin I	0.48	0.24	3.20	0.10	NA	0.86	NA	0.00	1.42
Briere I	2.43	NA	3.23	1.99	NA	2.13	NA	NA	3.62
Eubank	0.37	0.00	1.67	0.11	NA	0.65	0.00	0.59	1.02
Gaussian	0.84	1.52	5.48	0.43	4.78	0.92	10.31	1.52	4.19
Gaussian Gomp	NA	2.79	NA	2.16	NA	3.05	NA	2.21	2.05
Janisch I	0.51	1.56	2.96	1.01	NA	2.79	7.35	0.99	2.30
Lactin II	NA	NA	NA	NA	NA	NA	NA	NA	4.80
Logan I	NA	NA	9.22	2.10	NA	2.80	NA	2.08	NA
Rezende	2.98	NA	3.68	2.83	NA	2.58	20.77	6.57	6.25
Simplified Beta	2.12	NA	4.54	0.70	NA	1.29	5.33	NA	0.45
Simplified Briere	1.85	4.90	4.57	0.25	NA	0.88	14.96	1.06	0.00
Simplified Briere II	3.32	2.97	NA	NA	NA	NA	NA	2.90	NA
Taylor S	NA	NA	3.65	NA	0.62	NA	NA	NA	2.59
Tomlinson P	0.47	NA	0.00	0.05	NA	0.00	13.21	NA	3.40
Weibull	2.66	2.24	4.80	2.16	0.00	2.81	NA	2.00	NA

Table 7.5. Delta AIC values for individually fit thermal performance curves at 70% hydration. Model name indicates all models fit for each frog. NAs in column values indicates that the specified model did not fit for the corresponding frog. Models with lower delta AIC were given higher weights towards the final curves for each frog.

	Δ AIC							
Model Name	**A1**	**A2**	**A3**	**A5**	**B3**	**B4**	**B5**	**B6**
Analytis K I	0.85	0.56	2.70	0.85	0.17	3.65	1.50	2.42
Ashrafi	0.86	NA	3.55	NA	0.02	NA	1.89	2.72
Ashrafi II	0.81	NA	4.40	NA	0.04	NA	0.34	0.00
Atkin	0.83	0.00	2.40	0.01	0.00	1.00	1.77	3.57
Briere I	1.04	0.84	2.91	1.23	0.19	7.04	1.94	3.08
Eubank	0.00	0.07	0.00	0.00	0.04	4.33	NA	4.52
Gaussian	0.88	0.47	4.55	0.88	0.16	3.65	2.81	5.00
Gaussian Gomp	NA	NA	6.58	NA	NA	3.71	2.97	5.01
Janisch I	0.23	1.23	0.61	0.90	0.24	9.80	0.43	NA
Lactin I	0.85	NA	NA	0.28	0.05	NA	NA	NA
Lactin II	NA	NA	NA	NA	NA	NA	NA	6.44
Logan I	NA	NA	6.66	NA	NA	4.55	NA	NA
Mitchell A	NA	NA	NA	NA	NA	0.00	NA	NA
Simplified Beta	1.44	1.93	4.26	1.14	0.56	5.74	1.26	9.72
Simplified Briere	NA	0.55	4.22	0.70	0.06	2.67	1.08	0.57
Taylor S	0.85	0.44	NA	0.77	0.16	4.23	1.76	2.88
Tomlinson phil	0.83	0.00	NA	0.01	0.00	1.01	2.88	4.80
Weibull	2.20	2.29	5.64	2.36	1.68	3.40	0.00	3.04

7.2 Weighted average results for individual hydro-performance curves.

Table 7.6 Delta AIC values for individually fit hydro-performance curves at 33 ºC. Model name indicates all models fit for each frog. NAs in column values indicates that the specified model did not fit for the corresponding frog. Models with lower delta AIC were given higher weights towards the final curves for each frog.

	Δ AIC								
Model Name	**A1**	**A2**	**A3**	**A5**	**A6**	**B3**	**B4**	**B5**	**B6**
2nd Polynomial	0.96	15.48	29.71	0.00	0.44	0.00	4.74	0.02	7.04
3rd Order Polynomial	2.78	6.54	16.20	NA	NA	1.94	NA	1.91	6.79
Analytis K I	1.94	15.06	14.25	5.73	0.38	0.00	0.00	0.23	4.81
Ashrafi I	1.04	15.66	28.92	NA	0.41	0.00	NA	0.00	6.78
Ashrafi II	1.02	15.52	29.18	NA	0.43	0.00	4.69	0.01	6.83
Briere I	1.67	15.56	14.23	6.37	1.24	0.00	4.14	0.25	5.75
Briere II	2.64	17.61	34.76	8.64	5.91	2.01	6.70	2.28	NA
Eubank	3.14	12.13	32.89	3.82	2.55	0.55	4.78	0.78	10.63
Gaussian	2.41	NA	21.00	NA	0.24	4.12	NA	0.14	4.83
Gaussian Gomp	7.55	NA	NA	NA	4.27	4.73	11.44	5.36	NA
Janisch I	2.88	11.50	28.83	5.28	0.00	0.53	4.03	1.03	8.41
Janisch II	2.12	11.00	25.77	6.36	NA	1.97	3.32	1.75	0.61
Kamykowski	2.74	NA	NA	NA	4.39	4.04	7.84	4.42	9.71
Lactin I	2.78	13.30	32.11	4.05	0.63	0.04	3.52	0.10	10.43
Lactin II	3.56	17.28	0.00	3.22	2.07	2.00	5.80	2.00	7.52
Logan I	NA	17.65	NA	NA	3.95	2.00	7.47	2.14	NA
Mitchell A	1.99	NA	19.65	NA	NA	0.62	NA	1.51	3.77
Modified Deutsch	4.25	NA	NA	NA	NA	NA	NA	5.63	0.00
Modified Gauss	0.00	14.86	32.81	9.24	2.21	2.02	NA	2.08	5.58
Ratkowsky	3.81	16.16	17.05	7.73	2.41	2.01	NA	2.23	5.93
Ruiz	4.41	0.00	23.02	9.70	1.26	2.03	3.49	NA	6.83
Simplified Beta	2.53	11.99	29.23	4.73	0.45	0.01	6.10	0.21	8.97
Simplified Briere	1.19	16.29	25.47	7.56	0.68	0.05	4.65	0.43	6.21
Skew Normal	1.95	14.48	22.51	6.21	NA	2.02	3.42	2.11	2.78
Taylor Sexton	2.10	14.78	16.96	6.31	0.34	0.51	2.57	2.12	5.64
Thomas 2012	2.57	13.46	7.52	6.20	2.19	2.00	NA	2.12	7.23
Tomlinson P	NA	16.95	NA	4.05	0.48	0.03	6.50	0.10	17.47
Weibull	1.34	12.95	19.89	9.82	2.00	2.49	4.10	2.94	5.75

Table 7.7 Delta AIC values for individually fit hydro-performance curves at 24 ºC. Model name indicates all models fit for each frog. NAs in column values indicates that the specified model did not fit for the corresponding frog. Models with lower delta AIC were given higher weights towards the final curves for each frog.

	Δ AIC								
Model Name	**A1**	**A2**	**A3**	**A5**	**A6**	**B3**	**B4**	**B5**	**B6**
2nd Polynomial	23.36	274.03	6.60	8.03	13.88	0.00	9.13	7.68	43.78
3rd Order Polynomial	4.00	NA	3.81	NA	NA	1.06	NA	NA	0.00
Analytis K I	30.86	251.50	2.91	4.02	0.00	0.32	NA	6.98	56.01
Ashrafi I	24.50	NA	6.09	7.97	5.50	0.01	8.88	7.65	19.86
Ashrafi II	24.01	273.82	6.27	NA	13.88	0.03	8.97	7.60	32.49
Briere I	NA	283.79	9.09	8.39	189.85	0.56	NA	6.62	81.49
Briere II	25.31	277.58	11.24	5.91	NA	1.93	12.54	9.83	62.14
Eubank	31.54	NA	2.81	8.23	NA	0.62	NA	5.82	77.13
Gaussian	29.56	269.29	4.26	8.23	0.00	0.45	4.40	6.93	70.81
Gaussian Gomp	NA	NA	14.35	NA	NA	5.34	NA	8.73	NA
Janisch I	30.80	NA	3.15	4.02	0.00	0.54	NA	6.30	74.92
Janisch II	NA	NA	3.15	5.56	NA	0.51	NA	6.81	65.54
Kamykowski	13.63	NA	0.95	10.20	NA	3.36	NA	9.29	12.61
Lactin I	NA	NA	0.22	8.06	25.49	0.50	NA	5.26	76.34
Lactin II	31.34	NA	0.39	9.77	NA	2.14	8.87	8.01	63.72
Logan I	NA	NA	NA	NA	NA	4.54	NA	12.35	NA
Mitchell A	28.12	235.10	5.00	3.54	0.00	0.36	NA	7.23	66.33
Modified Deutsch	NA	271.86	0.82	8.83	NA	NA	0.45	7.48	68.88
Modified Gauss	24.01	NA	2.05	9.68	NA	NA	NA	9.23	63.79
Ratkowsky	29.63	9.25	1.68	10.05	NA	2.28	NA	7.72	65.98
Ruiz	31.92	272.96	5.64	NA	NA	2.45	6.42	0.00	72.82
Simplified Beta	NA	NA	0.00	8.05	0.00	0.46	8.46	6.15	74.64
Simplified Briere	29.49	272.09	3.62	8.07	6.33	0.06	8.04	7.34	54.00
Skew Normal	12.69	0.00	NA	6.03	212.96	NA	0.00	7.10	64.96
Taylor S	5.50	263.63	4.94	0.00	NA	0.37	NA	8.86	69.91
Thomas 2012	10.46	6.64	1.60	9.78	NA	1.86	NA	7.27	7.41
Tomlinson P	NA	NA	NA	8.06	NA	1.04	NA	NA	NA
Weibull	0.00	6.18	2.95	5.71	213.61	0.34	12.82	7.93	41.77

Table 7.8 Delta AIC values for individually fit hydro-performance curves at 15 ºC. Model name indicates all models fit for each frog. NAs in column values indicates that the specified model did not fit for the corresponding frog. Models with lower delta AIC were given higher weights towards the final curves for each frog.

	Δ AIC								
Model Name	**A1**	**A2**	**A3**	**A5**	**A6**	**B3**	**B4**	**B5**	**B6**
2nd Polynomial	2.07	0.00	0.29	NA	8.18	1.51	4.49	0.00	2.71
3rd Order polynomial	NA	0.29	NA	NA	6.91	NA	6.10	NA	2.29
Analytis K I	0.76	4.31	0.00	0.00	5.03	NA	6.83	0.84	3.68
Ashrafi I	3.47	19.41	3.62	5.65	NA	1.54	14.95	0.10	NA
Ashrafi II	2.42	17.05	0.50	0.07	NA	1.53	8.98	0.09	4.60
Briere I	2.92	18.31	3.68	NA	16.67	1.62	12.60	1.42	4.39
Briere II	4.34	10.11	1.81	2.38	22.05	3.62	6.21	3.46	4.61
Eubank	0.16	12.03	4.23	13.46	14.43	1.04	10.73	0.93	0.00
Gaussian	0.13	6.64	2.93	NA	12.02	2.81	7.26	0.84	2.34
Gaussian Gomp	4.73	NA	9.24	15.44	NA	3.60	17.12	NA	6.67
Janisch I	0.00	10.10	3.70	11.55	13.60	1.17	9.44	0.93	1.04
Janisch II	1.61	4.80	5.57	10.86	13.19	1.18	2.18	2.84	0.62
Kamykowski	5.04	2.59	2.64	NA	NA	5.47	8.24	4.85	5.79
Lactin I	0.57	13.52	3.65	15.79	17.49	0.65	10.83	0.84	4.57
Lactin II	2.91	3.36	3.13	NA	15.50	3.52	7.99	2.26	5.59
Logan I	5.15	NA	17.39	NA	NA	NA	NA	NA	8.91
Mitchell A	NA	2.35	2.26	6.81	10.89	NA	5.90	0.93	NA
Modified Deutsch	2.00	2.88	5.18	NA	7.22	NA	0.00	NA	3.45
Modified Gauss	3.30	NA	NA	NA	0.00	3.36	3.00	2.81	5.26
Ratkowsky	2.51	2.54	3.91	8.01	12.45	3.31	7.43	2.84	4.73
Ruiz	1.40	9.60	4.97	12.93	14.02	3.64	9.27	1.91	4.61
Simplified Beta	0.44	12.48	4.01	13.56	16.21	0.00	9.69	0.87	4.30
Simplified Briere	1.73	1.61	0.66	3.94	13.54	1.69	5.50	0.85	3.70
Skew Normal	2.11	1.42	4.27	11.22	11.51	2.19	2.08	2.84	2.17
Taylor S	0.59	8.27	2.45	5.53	5.45	NA	4.18	0.90	1.66
Thomas 2012	2.50	0.51	1.58	NA	6.28	NA	5.49	2.90	3.80
Tomlinson P	3.60	19.60	4.41	14.47	NA	1.62	15.21	0.85	NA
Weibull	3.89	15.50	0.69	12.81	8.48	3.22	6.13	2.93	3.34

Table 7.9 Delta AIC values for individually fit hydro-performance curves at 8 ºC. Model name indicates all models fit for each frog. NAs in column values indicates that the specified model did not fit for the corresponding frog. Models with lower delta AIC were given higher weights towards the final curves for each frog.

	Δ AIC								
Model Name	**A1**	**A2**	**A3**	**A5**	**A6**	**B3**	**B4**	**B5**	**B6**
2nd Polynomial	8.83	14.29	0.05	15.50	4.75	8.90	18.73	13.15	0.19
3rd Order Polynomial	NA	0.00	NA	5.62	NA	2.00	13.04	10.57	1.83
Analytis K I	1.92	15.51	0.00	4.42	3.11	0.00	14.11	10.59	0.00
Ashrafi I	NA	17.78	0.69	NA	NA	8.84	NA	NA	3.16
Ashrafi II	NA	14.45	0.07	NA	8.47	8.91	NA	NA	1.39
Briere I	NA	15.71	0.38	NA	NA	9.71	NA	15.79	2.97
Briere II	5.38	15.27	2.00	NA	5.32	11.73	NA	16.62	2.06
Eubank	15.25	16.71	1.17	11.06	6.94	9.18	10.05	14.91	1.65
Gaussian	13.63	15.73	0.54	10.20	6.25	10.98	15.25	14.20	1.16
Gaussian Gomp	NA	19.90	2.59	NA	10.84	11.37	NA	NA	4.91
Janisch I	14.66	16.36	0.98	9.71	6.79	9.60	12.46	14.65	1.86
Janisch II	NA	4.63	1.32	11.32	NA	11.37	7.39	NA	NA
Kamykowski	0.00	12.96	3.84	NA	14.56	13.85	11.05	8.36	4.06
Lactin I	17.48	16.68	0.73	14.47	NA	9.99	4.18	15.84	3.45
Lactin II	14.96	17.25	2.24	0.00	8.59	9.88	0.00	16.54	2.63
Logan I	NA	NA	2.40	NA	13.90	NA	NA	18.84	8.39
Mitchell A	12.50	15.29	0.51	11.74	NA	0.77	16.58	13.90	NA
Modified Deutsch	NA	14.70	2.08	5.47	NA	11.74	NA	NA	NA
Ruiz	15.71	17.73	2.54	11.88	8.34	11.82	13.89	16.20	3.24
Simplified Beta	16.85	16.16	0.56	9.94	7.79	9.40	5.80	15.57	2.28
Simplified Briere	13.17	14.87	0.11	6.48	6.16	9.85	15.79	14.77	0.67
Skew Normal	NA	11.79	2.01	8.76	NA	11.27	4.54	0.00	NA
Taylor Sexton	15.24	17.83	0.76	2.27	2.54	9.55	12.35	9.52	1.49
Thomas 2012	0.31	15.01	1.94	1.73	4.77	11.23	6.15	12.22	1.28
Tomlinson P	NA	17.85	0.78	NA	NA	9.21	NA	NA	3.38
Weibull	18.76	9.90	2.18	NA	0.00	11.61	NA	8.18	NA

8 APPENDIX B

8.1 Mathematical Models Tested

To describe the effect of temperature (ºC) and dehydration on performance, I used a candidate set of 31 non-linear models to generate performance curves (Table 8.1).

Table 8.1 Functions for all models used to fit the final thermal and hydric performance curves. P(z) indicates performance, and *z* is the parameter describing the fixed effect of either water loss or temperature for all models. Parameter definitions are described in the parameter column.

Model Name	Fixed Response Variable (z)	Model Function	Parameters
2nd Order Polynomial (2024)	Water loss or Temperature	$P(z) = az^2 + bz + c$	***a:*** shape parameter that defines the rate at 0 ***b* and *c***: shape parameters with no biological meaning.
3rd Order Polynomial (2024)	Water loss or Temperature	$P(z) = az^3 + bz^2 + cz + d$	***a, b, c,* and *d***: shape parameters with no biological meaning.
Analytis Kontodimas I (2004)	Water loss or Temperature	$P(z) = a(z - T_{min})^2(T_{\max - z})$	***a:*** scale parameter defining curve height **T_{min}:** low temperature (T) or hydration (H) at which the rate becomes negative **T_{max}:** high T or H at which rate becomes negative

Ashrafi I (2018)	Water loss or Temperature	$P(z) = a+b(z)^2 * \log(z) + cz^3$	***a, b* and *c***: shape parameters with no biological meaning.
Ashrafi II (2018)	Water loss or Temperature	$P(z) = a + b * d(z)^{\frac{3}{2}} + d * z^2$	***a, b, c,* and *d***: shape parameters with no biological meaning.
Biere I (1999)	Water loss or Temperature	$P(z) = a * z * (z - T_{min}) * \sqrt{((T_{\max}) - z)}$	***a:*** scale parameter defining maximum height of the curve **T_{min}:** as above **T_{max}:** as above ***z*:** temperature or hydration - fixed
Briere II (1999)	Water loss or Temperature	$P(z) = a * z * (z - T_{min}) * (T_{max} - z)^{\frac{1}{m}}$	***a:*** as in *Briere I* **T_{min}:** as above **T_{max}:** as above ***m**:* shape parameter to adjust curve asymmetry
Biere I (added intercept)	Water loss or Temperature	$P(z) = a * z * (z - T_{min}) * \sqrt{((T_{\max}) - z)} + d$	***a:*** as in *Briere I* **T_{min}:** as above **T_{max}:** as above ***m and d**:* shape parameters to adjust curve asymmetry and starting point.
Eubank (1973)	Water loss or Temperature	$P(z) = a\left((z - T_{pk})^2 + b\right)$	***a:*** scale parameter defining curve height. **T_{pk}:** optimum T or H ***b**:* shape parameter

Gaussian (2006)	Water loss or Temperature	$P(z) = P_{opt} * \exp\left(-0.5 * \left(\frac{abs(z - T_{pk})}{a} \right)^2 \right)$	***a:*** defines curve width $\mathbf{T_{pk}}$**:** optimum T or H $\mathbf{P_{opt}}$**:** maximum performance at $\mathbf{T_{pk}}$
Gaussian-Gompertz (2006)	Water loss or Temperature	$P(z) = d * \exp\left(-\exp(b * (z - T_{pk}) - \theta) - a * (z - T_{pk})^2 \right)$	***m****:* scale parameter defining curve height ***a***: shape parameter $\mathbf{T_{pk}}$: optimum T or H
Janisch I (1925)	Water loss or Temperature	$P(z) = \left(\frac{1}{\left(\left(\frac{m}{2} \right) * (a^{z - T_{pk}} + a^{-(z - T_{pk})}) \right)} \right)$	***m****:* scale parameter defining curve height ***a***: shape parameter $\mathbf{T_{pk}}$: optimum T or H
Janisch II (1925)	Water loss or Temperature	$P(z) = \left(\frac{1}{\left(\left(\frac{m}{2} \right) * (a^{z - T_{pk}} + b^{-(z - T_{pk})}) \right)} \right)$	***m****:* scale parameter defining curve height ***a***: shape parameter for curve incline ***b***: shape parameter for curve decline $\mathbf{T_{pk}}$: optimum T or H
Kamykowski (1985)	Temperature	$P(z) = a * (1 - exp^{(-b * (z - T_{min}))}) * (1 - \exp^{-c * (T_{max} - z)})$	***a, b*** and ***c***: shape parameters with no biological meaning
Lactin I (1995)	Water loss or Temperature	$P(z) = exp(\rho * z) - exp(\rho * T_{max} - \left(\frac{(T_{max} - z)}{DT} \right)$	$\boldsymbol{\rho}$: shape constant determining steepness of curve incline $\mathbf{T_{max}}$: T or H at which the curve begins to decelerate (maximum) ***DT***: thermal or hydric safety margin

Lactin II (1995)	Water loss or Temperature	$P(z) = \exp(\rho * z) - \exp\left(\rho * T_{\max} - \left(\frac{(T_{\max} - z)}{DT}\right)\right) + \lambda$	$\boldsymbol{\rho}$: shape constant determining steepness of curve incline $\boldsymbol{\lambda}$: shape constant for curve height $\mathbf{T_{max}}$: T or H at which the curve begins to decelerate (maximum) $\boldsymbol{DT}$: thermal or hydric safety margin
Logan I (1976)	Water loss	$P(z) = psi * (\exp(\rho * z) - \exp(\rho * T_{max} - \left(\frac{(T_{max} - z)}{DT}\right))$	$\boldsymbol{\rho}$: shape constant determining rate of curve incline $\boldsymbol{psi}$**:** shape constant determining rate of incline after lower threshold $\mathbf{T_{max}}$: T or H at which the curve begins to decelerate (maximum) $\boldsymbol{DT}$: thermal or hydric safety margin
Mitchell-Angilletta (2009)	Water loss or Temperature	$P(z) = \left(\frac{1}{2 * b}\right) * \left(1 + \cos\left(\left(\frac{(z - T_{pk})}{b}\right) * pi\right)\right) * a$	$\mathbf{T_{pk}}$: optimum T or H ***a:*** scale parameter ***b:*** scale parameter for performance breadth
Modified Deutsch (2008; 2011)	Water loss	$P(z) =$ $if\ z \leq T_{pk}:\ P_{opt} * \exp\left(-\left(\frac{z - T_{pk}}{2\sigma}\right)^2\right)$ $if\ z > T_{pk}: P_{opt} - P_{opt} * \left[1 - \left(\frac{z - T_{pk}}{T_{pk} - T_{max}}\right)^2\right]$	$\mathbf{P_{opt}}$**:** maximum performance at $\mathbf{T_{pk}}$ $\mathbf{T_{pk}}$: optimum T or H **σ** = shape parameter defining steepness of curve decline $\mathbf{T_{max}}$: T or H at which the curve begins to decelerate (maximum)

Modified Gaussian (2006)	Water loss	$P(z) = P_{opt} * \exp\left(-0.5 * \left(\frac{abs(z - T_{pk})}{a} \right)^{b} \right)$	$\mathbf{T_{pk}}$: optimum T or H; ***a:*** shape parameter for curve width ***b:*** scale parameter for curve asymmetry $\mathbf{P_{opt}}$**:** maximum performance at $\mathbf{T_{pk}}$
Ratkowsky (modified) (1983)	Water loss or Temperature	$P(z) = \left(a * (z - T_{min}) * \left(1 - \exp(b * (z - T_{max})) \right) \right)^{2}$	***a:*** defined as sqrt(P(z)/z- $\mathbf{T_{min}}$) $\mathbf{T_{min}}$**:** low T or H at which rate becomes negative $\mathbf{T_{max}}$**:** high T or H at which rate becomes negative ***b****:* parameter for fitting data beyond optimum
Ruiz (2019)	Water loss or Temperature	$P(z) = B_0 + DB_{\max} * \exp\left(-a * \left(z - T_{pk} \right)^{2} \right)$	$\boldsymbol{B_0}$***:*** parameter describing shifts in rate (or minimum performance level) $\boldsymbol{DB_{max}}$: parameter controlling the height of the curve above baseline B_0. ***a****:* scale parameter defining curve decline rate after T_{pk}. $\boldsymbol{T_{pk}}$**:** optimum T or H

Rezende-Bosinovic (2019)	Temperature	$P(z) =$ $if\ z \leq T_{th}$: $\quad B_0 * \exp\left(\frac{\log(Q_{\{10\}})}{\frac{10}{z}}\right)$ $if\ z > T_{th}$: $\quad B_0 * \exp\left(\frac{\log(Q_{\{10\}})}{\frac{10}{z}}\right) * (1 - d * (b - z)^2)$	**Q_{10}:** the fold change in performance as a result of increasing the temperature by 10 ºC ***B_0:*** parameter describing shifts in rate (or minimum performance level) ***b*:** parameter threshold T or H beyond which the curve declines ***d*:** parameter controlling the rate of decline beyond the threshold temperature, T_{th}
Simplified Beta (2008)	Water loss or Temperature	$P(z) = \left(rho * \left(alpha - \left(\frac{z}{10}\right)\right)\right) * \left(\frac{z}{10}\right)^{beta}$	***rho, beta,*** and ***alpha***: shape parameters with no biological meaning.
Simplified Briere (1999)	Water loss or Temperature	$P(z) = \left(a * (z - T_{\min}) * \sqrt{(T_{max} - z)}\right)$	***a:*** scale parameter for maximum rate of curve **T_{min}:** low T or H at which rate becomes negative **T_{max}:** high T or H at which rate becomes negative
Simplified Briere II (1999)	Water loss or Temperature	$P(z) = \left(a * (z - T_{\min}) * (T_{max} - z)^{\frac{1}{m}}\right)$	***a:*** scale parameter for maximum rate of curve **T_{min}:** low T or H at which rate becomes negative **T_{max}:** high T or H at which rate becomes negative

			m: shape parameter to adjust curve asymmetry
Skew Normal (2012)	Water loss or Temperature	$P(z) = \left(a * \left(\exp\left(\frac{(-(z - b)^2)}{(sigma^2)} \right) \right) * \left(1 + \text{erf}\left(\frac{(-\lambda * (z - b))}{sigma} \right) \right) \right)$	***a:*** scale constant determining maximum height of the curve ***b:*** scale parameter controlling the T or H at which performance is optimized ***sigma:*** parameter controlling curve breadth (width) ***λ*:** parameter controlling curve asymmetry
Taylor Sexton (1972)	Water loss or Temperature	$P(z) = P_{opt} * \frac{\left[-(z - T_{min})^4 + 2(z - T_{min})^2 * \left(T_{pk} - T_{min} \right)^2 \right]}{\left(T_{pk} - T_{min} \right)^4}$	***a:*** defines curve width **T_{min}:** low T or H at which rates become negative **T_{pk}:** optimum T or H **P_{opt}:** maximum performance at **T_{pk}**
Thomas (2012)	Water loss or Temperature	$P(z) = a * exp^{b*z} \left(1 - \left(\left(\frac{z - T_{opt}}{\frac{c}{2}} \right) \right)^2 \right)$	***a:*** shape constant with no biological meaning ***b:*** shape constant with no biological meaning **T_{opt}:** location of the maximum height of the curve ***c*:** range of T or H over which the performance rate is positive

Tomlinson-Phillips (2015)	Water loss or Temperature	$P(z) = B_0 * \left(exp(a * z) - exp(z - b) \right)$	$\boldsymbol{B_0}$**:** scale parameter for performance rate at T_{min} ***a:*** shape constant indicating upwards slope of the curve ***b:*** parameter controlling peak height of the curve.
Weibull (2024; 2010)	Water loss or Temperature	$P(z) = P_{opt} * \left(\left(\frac{c-1}{c} \right)^{\frac{1-c}{c}} \right) * \left(\left(\left(\frac{z - T_{pk}}{d} \right) + \left(\frac{c-1}{c} \right)^{\frac{1}{c}} \right)^{(c-1)} \right) * \exp\left(- \left(\left(\frac{(z - T_{pk})}{d} \right) + \left(\frac{c-1}{c} \right)^{\frac{1}{c}} \right)^{c} + \left(\frac{c-1}{c} \right) \right)$	$\boldsymbol{P_{opt}}$**:** maximum performance value T_{pk}: T or H at which performance is optimized ***d:*** parameter describing the curve breadth ***c:*** parameter defining the overall curve shape